Title
Jump Conditions for Green-Naghdi Theory and Some Applications

Author
Zhang, Xinyu

Publication Date
2000

Peer reviewed

INFORMATION TO USERS

This manuscript has been reproduced from the microfilm master. UMI films the text directly from the original or copy submitted. Thus, some thesis and dissertation copies are in typewriter face, while others may be from any type of computer printer.

The quality of this reproduction is dependent upon the quality of the copy submitted. Broken or indistinct print, colored or poor quality illustrations and photographs, print bleedthrough, substandard margins, and improper alignment can adversely affect reproduction.

In the unlikely event that the author did not send UMI a complete manuscript and there are missing pages, these will be noted. Also, if unauthorized copyright material had to be removed, a note will indicate the deletion.

Oversize materials (e.g., maps, drawings, charts) are reproduced by sectioning the original, beginning at the upper left-hand corner and continuing from left to right in equal sections with small overlaps.

Photographs included in the original manuscript have been reproduced xerographically in this copy. Higher quality 6" x 9" black and white photographic prints are available for any photographs or illustrations appearing in this copy for an additional charge. Contact UMI directly to order.

Bell & Howell Information and Learning
300 North Zeeb Road, Ann Arbor, MI 48106-1346 USA
800-521-0600

Jump Conditions for Green-Naghdi Theory and Some Applications

by

Xinyu Zhang

B.E. (Harbin Shipbuilding Engineering Institute) 1993
M.S. (Institute of Mechanics, Chinese Academy of Sciences) 1996

A dissertation submitted in partial satisfaction of the
requirement of the degree of

Doctor of Philosophy

in

Engineering-Naval Architecture and Offshore Engineering

in the

GRADUATE DIVISION

of the

UNIVERSITY OF CALIFORNIA, BERKELEY

Committee in charge:

Professor William C. Webster, Chair
Professor Rodney J. Sobey
Professor Ronald W. Yeung

Fall 2000

Bell & Howell Information and Learning Company
300 North Zeeb Road
P.O. Box 1346
Ann Arbor, MI 48106-1346

Jump Conditions for Green-Naghdi Theory and Some Applications

by

Xinyu Zhang

Table of Contents

List of Figures iii
List of Symbols vi

1.0 Introduction 1

§1.1 Motivation 1
§1.2 Perturbation method & Green-Naghdi method 7
§1.3 Application of Green-Naghdi Methods to Breaking Waves 11

2.0 Green-Naghdi theory 21

§2.1 Derivation of the general Green-Naghdi equations 22
§2.2 Governing equations for shallow water 30
§2.3 Green-Naghdi Level I theory 33
§2.4 Green-Naghdi Level II theory 36

3.0 Jump conditions for Green-Naghdi theory 40

§3.1 General formula of jump conditions for steady two-dimensional flows 42
§3.2 Jump conditions for Green-Naghdi Level I theory 48

4.0 Steady inviscid free waterfall 61

§4.1 General solution of free waterfalls through Green-Naghdi Level-I theory 64
4.1.1 Governing equations for region I (flow over a smooth bottom) 64
4.1.2 Discussion of the restricted theory 68
4.1.3 Governing equations for region III (free waterfall) 70
4.1.4 Boundary conditions 72
4.1.5 Jump conditions 76
§4.2 Free waterfall over a flat bottom 79
4.2.1 Solution of the problem 80
4.2.2 Results and discussion 84
§4.3 Free waterfall over an arbitrary, smooth bottom 89
4.3.1 Solution of the problem 89
4.3.2 Results and discussion 94
§4.4 Free waterfall over a non-smooth bottom 104
4.4.1 Formulation of the problem 105
4.4.2 Application of jump conditions 109
4.4.3 Results and discussion 116

5.0 Steady inviscid flow under a sluice gate 126

§5.1 Flow under a vertical sluice gate 127
5.1.1 Governing equations for region I and II 129
5.1.2 Jump conditions 131
5.1.3 Solutions 134
§5.2 Flow departing from confined parallel flat surfaces 138
5.2.1 Governing equations for region I 139
5.2.2 Governing equations for region II 142
5.2.3 Jump conditions 144
5.2.4 Results and discussions 146
§5.3 Flow departing from confined non-smooth top surface 152
5.3.1 Governing equations for three regions 153
5.3.2 Boundary conditions and jump conditions 157
5.3.3 Results and discussions 162

6.0 Steady inviscid flow over a weir 169

§6.1 Thin weirs 170
6.1.1 Formulation of the problem 171
6.1.2 Jump conditions 173
6.1.3 Solutions 176
6.1.4 Results and discussions 180
§6.2 Broad crested weirs 188
6.2.1 Formulation of the problem 189
6.2.2 Jump conditions 191
6.2.3 Solutions 194
6.2.4 Results and discussions 197

7.0 Summary and Conclusions 204

References 207

Appendix A 212

List of Figures

Fig. 1.1	Schematic of division of plunging breaker into two parts	13
Fig. 1.2	Schematic of plunging breaker and weir flow and sluice flow	19
Fig. 2.1	Sketch of a fluid body bounded by two material surfaces	23
Fig. 2.2	Sketch of the velocity profile for Green-Naghdi Level-I theory	34
Fig. 2.3	Sketch of the velocity profile for Green-Naghdi Level-II theory	37
Fig. 4.1.1	Illustration of waterfall over a flat bottom	62
Fig. 4.2.1	A plot of the solution exhibiting profiles of the fluid sheet for an upstream height $H_1 = 1$m and for three values of the Froude number Fr, that is, Fr = 1.25, 2.0 and 4.0	86
Fig. 4.2.2	Comparison between present solution, experimental results of Rouse (1936) and the solution of Southwell & Raisey (1946) for Fr = 1 and $H_1 = 1$ m	87
Fig. 4.2.3	The integral pressure throughout the flow region for different values of Fr	87
Fig. 4.2.4	The bottom pressure in the upstream for different values of Fr	88
Fig. 4.3.1	Schematic of waterfall over a smooth bottom	89
Fig. 4.3.2	A plot of the solution exhibiting profiles of the fluid sheet for an upstream height $H_1 = 1$m and the bottom surface $\alpha = 0$ when $x < -3$, and $\alpha = 0.0037x^3 + 0.033x^2 + 0.1x + 0.1$ when $-3 \le x \le 0$ for different Froude numbers, Fr = 1.25, 2.0 and 4.0	96
Fig. 4.3.3	Close look near the junction x = 0 for Fig. 4.3.2	97
Fig. 4.3.4	Plot of waterfall over different smooth bottom at Fr = 2.0	97
Fig. 4.3.5	Plot of the horizontal velocity u_0 for different bottoms	98
Fig. 4.3.6	Local Froude number for different non-flat smooth bottoms	98
Fig. 4.3.7	Local Froude number when the Froude number upstream is minimum	101
Fig. 4.3.8	Vertical velocity on the top and bottom in region I when the Froude number upstream is minimum	102
Fig. 4.3.9	The distribution of the bottom pressure when the Froude number Fr = 1.282, and the bottom $\alpha(x) = 0.0111x^3 + 0.1x^2 + 0.3x + 0.3$ for $-3 \le x \le 0$, and $\alpha = 0$ for $x < -3$	102
Fig. 4.3.10	The distribution of the integral pressure when the Froude number Fr = 1.282, and the bottom $\alpha(x) = 0.0111x^3 + 0.1x^2 + 0.3x + 0.3$ for $-3 \le x \le 0$, and $\alpha = 0$ for $x < -3$	103
Fig. 4.4.1	Schematic of waterfall over a non-smooth bottom	105
Fig. 4.4.2	Numerical results for flow over an inclined bottom for different Fr	120
Fig. 4.4.3	Distribution of local Froude number under different Fr far upstream	120
Fig. 4.4.4	Plot of the integral pressure P_0 in the whole region	121
Fig. 4.4.5	Plot of the pressure on the bottom in region I (K=0.1, Fr=1.365)	121
Fig. 4.4.6	Plot of local Froude number for the minimum Fr (K=0.05, a=3m)	122

Fig. 4.4.7	Minimum upstream Froude number for different slopes of bottom K	122
Fig. 4.4.8	Plot of the top and bottom surfaces for K=0.25	123
Fig. 4.4.9	Plot of the top and bottom surfaces for K=0.50	123
Fig. 4.4.10	Plot of the top and bottom surfaces for K=0.95	124
Fig. 4.4.11	Plot of the local Froude numbers for different K	124
Fig. 4.4.12	The elevation of the free surface over the top of the inclined weir as a function of the slope of bottom K	125
Fig. 5.1.1	Schematic of flow under a vertical sluice gate	128
Fig. 5.1.2	Profile of the water surface below a vertical gate, comparison of present solution, numerical results of Isaacs and the experimental results of Smetana (1948)	137
Fig. 5.2.1	Schematic of the flow departing from confined parallel flat surfaces	139
Fig. 5.2.2	Plot of the free surface in the downstream when $\hat{p}_0 > 0$	148
Fig. 5.2.3	Plot of the free surface in the downstream when $\hat{p}_0 < 0$	149
Fig. 5.2.4	Steady, two-dimensional flow past a semi-infinite flat-bottomed body in finite-depth water	150
Fig. 5.3.1	Schematic of the flow departing form a non-smooth top surface	152
Fig. 5.3.2	Plot of waves in region III for different Froude numbers	163
Fig. 5.3.3	Plot of the wave height in region III as a function of Froude number	163
Fig. 5.3.4	Plot of waves in region III for different top pressures far upstream	164
Fig. 5.3.5	Plot of the wave length in region III as a function of the slope K of the top surface	165
Fig. 5.3.6	Plot of the wave height in region III for different slopes K of the top surface	165
Fig. 5.3.7	Illustration of a solution of region III when far downstream is uniform	168
Fig. 5.3.8	Plot of the free surface in region III for different Froude numbers	168
Fig. 6.1.1	Schematic of flow over a thin weir	171
Fig. 6.1.2	Computed free surface profile for the flow over a thin weir, here the Froude number Fr = 0.1, and the thickness of fluid far upstream $H_1 = 1.0$m	182
Fig. 6.1.3	Computed free surface profile at Fr = 0.2	182
Fig. 6.1.4	Computed free surface profile at Fr = 0.3	183
Fig. 6.1.5	Computed free surface profile at Fr = 0.4	183
Fig. 6.1.6	Plot of the ratio H/W as a function of the Froude number	184
Fig. 6.1.7	The distribution of the integral pressure P_0 in the downstream when Fr = 0.1 and $H_1 = 1$m	184
Fig. 6.2.1	Schematic of the flow over a broad crested weir	189
Fig. 6.2.2	Illustration of the supercritical flow over a broad crested weir	197
Fig. 6.2.3	Plot of solutions for different Froude numbers for W=0.1m	199
Fig. 6.2.4	Plot of solutions for different heights of the weir at Fr = 2.0	199
Fig. 6.2.5	Plot of H_3 as a function of the weir height W at Fr = 2.0 and $H_1 = 1.0$m	200

Fig. 6.2.6	Plot of H_4 as a function of the weir height W at Fr = 2.0 and H_1 = 1.0m	200
Fig. 6.2.7	Plot of u_0 at infinity as a function of the weir height W	201
Fig. A.1	Schematic for derivation of the jump condition associated With the energy equation at x=-a	212

List of Symbols

A, B, C, D	constants used to determine the profile of fluid jet in the downstream
a	horizontal distance of the inclined bottom
d	the opening of a sluice gate
$\mathbf{e}_i$	base vectors of the Cartesian coordinates in Eulerian space. and $\mathbf{e}_3$ is oriented vertically upward
F_1	horizontal force between the sides of $x = x_0$. $F_1 = \lim_{\delta \to 0} \int_{x=x_0-\delta}^{x=x_0+\delta} (\hat{p}\,\beta_x - \bar{p}\,\alpha_x)dx$
F_3	vertical force between the sides of $x = x_0$. $F_3 = \lim_{\delta \to 0} \int_{x_0-\delta}^{x_0+\delta} [-\hat{p} + \bar{p} - \rho g \varphi]dx$
Fr	Froude number. $Fr = \frac{u}{\sqrt{g H_1}}$
g	acceleration due to gravity: $g = 9.81\ m/s^2$
H_1	the thickness of fluid sheet far upstream
H_3	the thickness of fluid sheet at the departure point
H_4	the thickness of fluid sheet far downstream
H_b	elevation of the top of the inclined bottom
H_n	$H_n = \int_\alpha^\beta \zeta^n d\zeta = \frac{1}{n+1}(\beta^{n+1} - \alpha^{n+1})$
h_0	total head of fluid
K	index of the level of Green-Naghdi theory
K	slope of the thickness of fluid sheet at a joint point
K	constant slope of the inclined bottom
K_0	slope of thickness of the fluid sheet at the departure point of an inclined bottom
K_b	slope of the bottom surface at a joint point
L	moment on the face of the weir and bottom of the channel. $L = \lim_{\delta \to 0} \int_{-\delta}^{+\delta} [P_0 - \rho g \varphi \psi - \hat{p}\beta + \bar{p}\alpha]dx$
L	length of a broad crested weir
P_n	n^{th} integrated pressure, $P_n = \int_\alpha^\beta p\lambda_n d\zeta$, or $P_n = \int_\alpha^\beta p\zeta^n d\zeta$ for shallow water problems

P'_n	n^{th} integrated pressures, that is, $P'_n = \int_\alpha^\beta p\lambda_n' d\zeta$, here the prime denotes the derivative with regard to ζ
p	fluid pressure
$\hat{p}$	pressure on the top surface β
$\bar{p}$	pressure on the bottom surface α
Q	volume flow flux of fluid
R_1, R_2, R_3	constants of integration
S_1, S_2, S_3	constants of integration
t	time
U_1	uniform horizontal velocity far upstream
U_4	uniform horizontal velocity far downstream
u	horizontal velocity in two-dimensional system
u_n	n^{th} order component of horizontal velocity u, n = 0, 1, ...
$\mathbf{v}(\mathbf{x}, t)$	velocity vector at a point **x** and time t
v	vertical velocity in two-dimensional system
v_n	n^{th} order component of vertical velocity v, n = 0, 1, ...
W	height of a weir
$W_n^i(x_1, x_2, t)$	n^{th} order component of the velocity v_i, $v_i(x_1, x_2, \zeta, t) = \sum_{n=0}^{K} W_n^i(x_1, x_2, t)\lambda_n(\zeta)$, i = 1, 2, 3.
$\mathbf{x}$	distance vector of a point in Eulerian space
x_1, x_2, x_3	Cartesian coordinates, and x_3 vertically upward
$\tilde{x}$	non-dimensionalized horizontal coordinate $\tilde{x} = \frac{x}{H_1}$
y_{mn}	integral of shape functions: $y_{mn} = \int_\alpha^\beta \lambda_m \lambda_n d\zeta$
y_{mrn}	integral of shape functions: $y_{mrn} = \int_\alpha^\beta \lambda_m \lambda_r \lambda_n d\zeta$
y^n_{mr}	integral of shape functions: $y^n_{mr} = \int_\alpha^\beta \lambda_m \lambda_r \lambda_n' d\zeta$.
α	bottom material surface of a fluid sheet
β	top material surface of a fluid sheet
ϕ_0	thickness of the fluid sheet, $\phi_0 = \beta - \alpha$
ϕ_n	$\phi_n = \frac{1}{n+1}(\beta^{n+1} - \alpha^{n+1})$, n = 0, 1, 2, ...

η	non-dimensionalized thickness of fluid sheet, $\eta = \eta(\tilde{x}) = \frac{\phi_0}{H_1}$
φ	thickness of the fluid sheet, $\varphi = \beta - \alpha$
$\lambda_n(\zeta)$	shape or weighting function
ρ	density
ξ	mid-surface of the fluid sheet, $\xi = (\alpha + \beta)/2$
ζ	vertical coordinate used to replace x_3

Acknowledgements

It is an uneven, long and hard journey to complete this dissertation. There are many people to whom I feel in debt for their guidance, support and assistance that make this completion possible.

I would like to express my deepest gratitude to my advisor Professor William C. Webster. I am obliged to Professor Webster for his enlightening guidance, support and encouragement. Studying under his instruction during the past four years has been a precious experience for me and has been changing my whole life. I feel privileged to have known and worked with him. I would like to thank Professor Ronald W. Yeung for being my dissertation committee member and for his kindly help and valuable suggestions to my dissertation. Also special thanks to Professor Rodney J. Sobey for being my dissertation committee member.

I would like to thank Professor Alaa E. Mansour for chairing my qualifying examination. His excellent teaching and kindly assistance are very helpful to me to pursue my academic my academic goal. I am also grateful to Professor Alexandre J. Chorin and Professor David B. Bogy for being my qualifying committee members. I am thankful to Professor Robert G. Bea for excellent teaching. I am also grateful to Professor Mostafa A. Foda for providing the financial support in the last year of my studying. Special thanks to Lydia Briedis, who made my life on the Berkeley campus much easier by helping me through the administration.

This research was supported in part by National Sea Grant College, National Oceanic and Atmospheric Administration, US Department of Commerce and the California State Resource Agency. Without their support, this work could have not been accomplished.

I would like to extend my appreciation to Professor Hong-ru Yu (Chinese Academy of Sciences), whose personal influence helped me to determine my career goal. His support and encouragement made it possible for me to pursue opportunity on Berkeley campus.

Finally, I wish to express my sincere gratitude to my wife Lu Xu for her love, patience and encouragement during this work. I am also grateful to my parents and parents-in-law, my family in China for their selfless sacrifice and support.

Chapter 1

Introduction

1. Motivation

Wave breaking is a common phenomenon in nature. Along any coastline one can be impressed by the dramatic transformation of water waves as they advance onto a beach. The waves with a relatively smooth water surface offshore transform to those with rough white fronts of spray and bubbles when they arrive at the shoreline. Although there is no exact definition of wave breaking, the term 'wave breaking' is generally used to describe the transformation process from a smooth wave to the quasi-steady state with a white-water front rather than to any particular instant within the transition.

An approximate classification of breaker types was first made by Mason (1952). He divided breakers into two types: spilling and plunging. The generally employed classification, described by Galvin (1968, 1972) according to empirical knowledge of the breaking process, has four types of breakers according to their initial motion: spilling, plunging, collapsing and surging. Of course, this division is approximate, and there often seems to be a smooth gradation between them. On the other hand, because of the existence of various environments, it is not difficult to find occasions when waves do not fit well into one of these descriptions.

There are a variety of reasons to study breaking waves. They play a significant role in numerous aspects of air-water interactions, such as energy transfer from wind to sea surface, momentum transfer from waves to currents, etc. It is believed that wave breaking serves to limit the height of surface waves, mix the surface waters, generate ocean currents, and enhance air-sea fluxes of heat, mass, and momentum through the generation of turbulence and the entrainment of air. Melville (1996) made a survey and review on the role of wave breaking in air-sea interaction. In addition, breaking waves are hydrodynamic sources of noise near a beach or a harbor. They also are responsible for large hydrodynamic loads on coastal marine structures, such as levee, harbor and platforms.

Breaking waves are of particular importance to naval architecture for several reasons. The motion of ships is almost always accompanied by spilling breakers in the surrounding water, both at the bow and elsewhere. The white water thus produced, which surrounds the ship and trails aft, is one of the most easily observed features of the ship disturbance. The breaking waves before and near the bow of the ship hull can contribute appreciably to the ship's wave resistance (Baba, 1969; Dagan & Tulin, 1970, 1972; Tulin 1979; Inui, 1981). On the other hand, modern ships are not immune to severe damage, or even total loss due to breaking waves. Smaller ships such as yachts and trawlboats may capsize, while larger ships may suffer structure damage that may cause loss of lives. In a harbor, breaking waves can make loading and unloading of docked ships difficult, and can cause collisions between ships and a dock if sufficient protection is not provided.

In view of this, there is obviously a need to understand and study wave breaking, including its process, its mechanism, and its kinematic and dynamics properties. Actually, the study of wave breaking has continued for more than one hundred years. Unfortunately, because of its complexity, advancement towards understanding wave breaking has been relatively slow. Wave breaking remains one of the most challenging problems in hydrodynamics. As pointed out by Bonmarin (1989), there are several reasons for the difficulties arising in the study of wave breaking. From a theoretical point of view, the equations of motion and the boundary conditions are fully nonlinear; in addition, these equations and conditions must be applied at the free surface whose location is not known beforehand and varies with time. From an experimental point of view, observations and measurements are not easy. First, wave breaking is an unsteady phenomenon occurring intermittently, starting suddenly and evolving rapidly. Second, it presents three-dimensional and multiphase aspects. Third, the experimental conditions are extremely adverse in the field, while in the laboratory, measurements can not always be strictly extended to sea conditions because they may not easily be scaled-up due to the relatively great importance of surface tension and viscosity at small scale. From a numerical point of view, direct calculation of wave breaking is completely impossible at this time, and will probably be so far into the future for all of the reasons enumerated above. However, with the development of computing technology, especially during the last three decades, it is possible to numerically calculate more and more complicated "simplified" problems. Thus numerical simulation plays an increasingly important role in the study of wave breaking. Experimental, theoretical, and numerical methods are the

primary tools in the study of wave breaking. However, because of the complexity of wave breaking, any method will involve some kind of simplification.

The study of breaking waves on a beach up to the early eighties of twentieth century was reviewed by Peregrine (1983). Among these numerous works, the systematic experiments of Duncan (1981, 1983), who uses a towed hydrofoil to produce a steady breaker, for the first time provided not only careful qualitative observation but also a set of measurements relating breaker and wave dimensions. The ground-breaking work by Longuet-Higgins & Cokelet (1976) provided the numerical simulation of the wave overturning for the first time. Since then, many papers have been published to calculate the overturning of a wave crest with different forms of the free surface boundary conditions: Longuet-Higgins & Cokelet (1978), Cokelet (1978), Peregrine et al. (1980), McIver & Peregrine (1981). A review of the methodology in this period may be found in Yeung (1982).

In the last two decades, great progress has been made in both experimental and theoretical studies of breaking waves. By means of a visualization technique, Bonmarin (1989) observed the time space evolution of a steep water wave reaching the breaking stage, especially the asymmetry of the wave profile in the near-breaking region. He also observed the shape evolution of a plunging crest after breaking and the related splash-up phenomenon. His measurements at breaking onset on a sample of breaking waves show a relation between the rate of asymmetry growth and the breaker type. Grosenbaugh & Yeung (1989), in an experimental and numerical study, correlated the unsteady breaking

of waves in front of a blunt bow with different bow shapes. Even the effects of viscosity and surface tensions were considered in the generation of breaking bow waves (Yeung 1991) and in the wave generation by a translating body (Yeung & Ananthakrishnan 1997). At the same time, since instability of wave crest plays a very important role in the analysis of wave breaking, many efforts have been made on the study of instabilities of wave crests, and many papers have been published: Tanaka (1983, 1986, 1995), Longuet-Higgins & Cleaver (1994), Longuet-Higgins, Cleaver & Fox (1994), Longuet-Higgins & Dommermuth (1997).

As reviewed by Peregrine (1983), there are two major theoretical approaches to the problem of finding where waves break on a beach: shallow-water steepening & refraction and waves of limiting steepness. In his review, the origination and development of the theories are described in detail. In summary, shallow-water steepening is based on the work of Airy (1845) in response to Russell's (1834) observation of the existence of the solitary wave, and lends to the well-known Boussinesq equations. The Refraction method is based on the existence of a limiting wave steepness for traveling waves, which has been well known since Stokes (1880) studied the flow near the crest of such a wave, that is, the well-known and oft-quoted Stokes 120° corner flow.

Shallow-water steepening and limiting-steepness waves have provided a starting point for theoretical studies of wave breaking. However, both of the approaches are appropriate only under certain assumptions. For instance, shallow-water steepening theory is obtained by assuming that the water-surface slopes are sufficiently gentle that

water-particle accelerations are negligible compared with gravity. With wave steepening, the water accelerations will increase, and to certain degree they will have a significant effect on the pressure so that this must be taken into consideration. Then a "near-linear" approximation is made in order to handle the problem analytically, that is, only the "first" nonlinear terms are included. With this approximation, the resulting equations are the Boussinesq equations. Studies show that either refraction methods or integration of the Boussinesq equations will fail or become unreliable as waves approach the steepness that limits periodic waves, or the maximum solitary-wave height.

A completely different method has been proposed by Green and Naghdi in 1974, which is originated from techniques often used in analysis of solid shell-like structures. Since the appearance of this method, so-called Green-Naghdi theory or the theory of directed fluid sheets, many problems have been solved through this unique method. In particular, the Green-Naghdi method of fluid sheets has been used successfully for a variety of two-dimensional problems where nonlinear effects play a critical role. The success of the Green-Naghdi method in these large-amplitude wave problems provided the motivation to attempt to use it to study the wave-breaking problem. Before going further, it is useful to discuss the differences between the classical perturbation method, and Green-Naghdi method.

2. Perturbation method & Green-Naghdi method

As mentioned in above section, the limiting-steeping wave theory and the shallow-water steepening theory are the major analytical methods to study wave breaking. The former method relies on the expansion series of Stokes' corner-flow; and the latter applies the "near-linear" approximation and results in the Boussinesq equations. In essence, both of them are perturbation methods, e.g., Boussinesq equation is a perturbation or asymptotic method based on two non-dimensional parameters: the ratio of wave height to water depth, and the ratio of depth to wavelength.

In general, perturbation methods, both ordinary and singular, introduce some mathematical approximation to reduce the complexity of the model to the point where it can be solved. One advantage of these methods is that one obtains governing equations for the flow, and from those both specific solutions can be obtained and generalizations of the behavior of the flow can be made.

In perturbation analyses, reference scales appropriate for the particular problem at hand are introduced. These scales are used to non-dimensionalize the variables and to identify a non-dimensional perturbation parameter (or parameters) that can be considered small (or large). For time invariant problems, the flow is decomposed into a sequence of flows of presumably decreasing importance, each of which is a correction to the sum of the previously computed flows. The assumed sequence is inserted into the field equations

and boundary conditions and the perturbation parameters are used to segregate these into a corresponding sequence of perturbation problems. Typically, each of these problems is linear in the unknowns at its level, although it may involve higher-order terms of quantities determined already in previous (lower-order) solutions. At the same time, although it is implicitly assumed that this sequence is convergent this is almost never proven. In some flow problems, such as two-dimensional water waves in both shallow and deep water, there is ample evidence of the convergence, while in problems such as the flow about thin airfoils, the lack of convergence is well known. Theoretically, one can obtain solutions to whatever level of accuracy one wants, if the perturbation sequence converges. A particular advantage of the perturbation approach is that, since perturbation parameters are used to size quantities, the ingredients of this parameter give an insight into the types of problems for which the approximation is appropriate. However, it does not yield quantitative measures of the accuracy to be expected for a particular problem. This information can only be obtained from an analysis of higher order problems or from comparison with experiments.

In addition, Green and Naghdi (1974, 1976a, 1976b) pointed out that the perturbation methods results in a model that is not consistent in a physical sense. Frequently, neither mass nor momentum is conserved, nor are the surface boundary conditions exactly satisfied, since parts of the exact problem are thrown away (i.e., the higher-order terms). Moreover, some of these even violate the principle of invariance, that is, any order of the perturbation theory is not Galilean invariant. As a result, different results can be obtained for the same problem depending on the frame or reference from which it is analyzed.

As an alternative to the perturbation methods, Green and Naghdi have proposed a completely different scheme for obtaining approximate governing equations for three-dimensional problems. Green-Naghdi theory originated from techniques often used in analysis of solid shell-like structures and was initially called the "Theory of Cosserat surfaces" or the "Theory of Directed Fluid Sheets." According to Green & Naghdi, thin deformable media can be modelled by a surface embedded in a Euclidean 3-space, together with K ($K \geq 1$) directors (i.e. deformable vectors) assigned to every point of the surface. This surface, called Cosserat surface or directed surface, is three-dimensional in character, but depends only on two space variables and time.

Green, Laws & Naghdi (1974) proposed a direct formulation of a theory of water waves when the fixed bottom of the stream is level and used a Lagrangian frame. In 1986, Green & Naghdi recast this theory in an Eulerian frame so that it is much easier to apply to fluid flow problems and suitable for deep waters.

A new derivation of the direct sheet theory was given by Shields & Webster (1988), which employed a variational procedure due to Kantorovich called "the method for reduction to ordinary differential equations". This derivation does not use the concept of directors, which is included in the physically motivated derivations given by Green and Naghdi. It is presented as a straightforward approximation of the three-dimensional equations of motion. In this derivation, the dependence of the kinematic structure of the solutions along one coordinate direction is prescribed. This direction is usually the

vertical direction for shallow water flows. This makes it feasible to study higher-order approximations of the theory, beyond the most basic "restricted theory" by Green and Naghdi. As a result, this theory produces approximate field equations, but satisfies boundary conditions exactly.

Other than involving any simplifications, one can directly solve the original problem by purely numerical techniques. Finite difference, finite element and panel methods are such schemes. These methods are comparable to physical experiments in that each computation yields another result corresponding to a single realization of the flow. Generalization about the behavior of the flow requires induction from many of these specific solutions.

Green-Naghdi fluid sheet theory lies in the middle of the spectrum. It achieves simplification by reducing the dimensionality from three dimensions to two. This theory yields governing equations for the flow and these are more efficient to solve numerically than those from three-dimensional finite element or finite difference models.

Shields and Webster (1988) used this method ---Green-Naghdi method, to study waves in shallow water. Their results are compared well with experimental data. Later on, Demirbilek and Webster (1992) studied shoaling of a random wave train passing over submerged bar. Green-Naghdi Level II theory was used to yield the wave elevation at three locations: before the bar, at the bar and beyond the bar. Their results show that the wave patterns after passing over the bar are much different as a result of the nonlinear

interaction. Webster & Wehausen (1995) studied the reflection of a train of regular waves from a sinuous bottom. This reflection is due entirely to nonlinear interaction within the wave system. That is, linear theories do not predict reflection from either this type of bottom or as a result of shoaling. Application of Green-Naghdi theory to this problem yields predictions that match very closely those from careful laboratory experiments. As a result, these studies demonstrated Green-Naghdi theory's capability to reproduce several kinds of nonlinear behavior in complex wave systems. Thus the Green-Naghdi theory of fluid sheets appears to be attractive for the prediction of wave breaking, whereby nonlinear interactions play a critical role. However, when Demirbilek and Webster(1992) studied wave shoaling, their numerical calculation broke down at the moment when the velocity of a particle at the wave crest is nearly equal to the wave velocity. That is the computation broke down when according to the generally employed criterion, wave breaking should start. The same thing happens to the limiting steepening wave theory and the shallow water steepening theory. In order to calculate the overturning of a breaking wave, a new method or some modification is clearly necessary.

3. Application of Green-Naghdi Methods to Breaking Waves

Before we proceed further, imagine the picture of a typical plunging wave. An element of the water surface becomes vertical; a portion of the surface then overturns, projects forward, and forms a jet of water. We find that at this jet of water, the water surface is a multi-valued function of a horizontal coordinate. However, for the Green-Naghdi model, just as in shallow-water theory, variables must be single-valued functions

of the underlying coordinate system. Recall that in the Green-Naghdi model, the continuum representing the fluid flow has been reduced to the horizontal variables only. For the two-dimensional wave system under consideration, this means that the variables describing the flow kinematics are functions of one horizontal coordinate (say, x) and time, t. As a result, the water surface must be single valued. Therefore, the place where wave breaking occurs is where Green-Naghdi model breaks down. This was confirmed by Demirbilek & Webster (1992) when they studied the wave shoaling. However, this does not mean that it is not possible to calculate the overturning of a breaking wave by means of the Green-Naghdi model. Recall the picture of a steady plunging breaker, it consists of a relative smooth water surface before the crest and a jet of water. After the projection point of the jet, the water surface returns to be smooth. In view of this, we can divide the whole flow region of water into two regions by the point whose tangent is vertical, as shown in Figure 1.1. The advantage of this division is obvious. After the division, in each region the fluid is bounded by a top and a bottom surface, and both surfaces are single functions of space. Then, we can apply Green-Naghdi method to the two regions separately. Note that the interface used to divide the flow region has the kinematic properties, that is, there are transfers of mass, momentum and energy across this interface, and the interface varied with time during the unsteady development of the wave breaking.

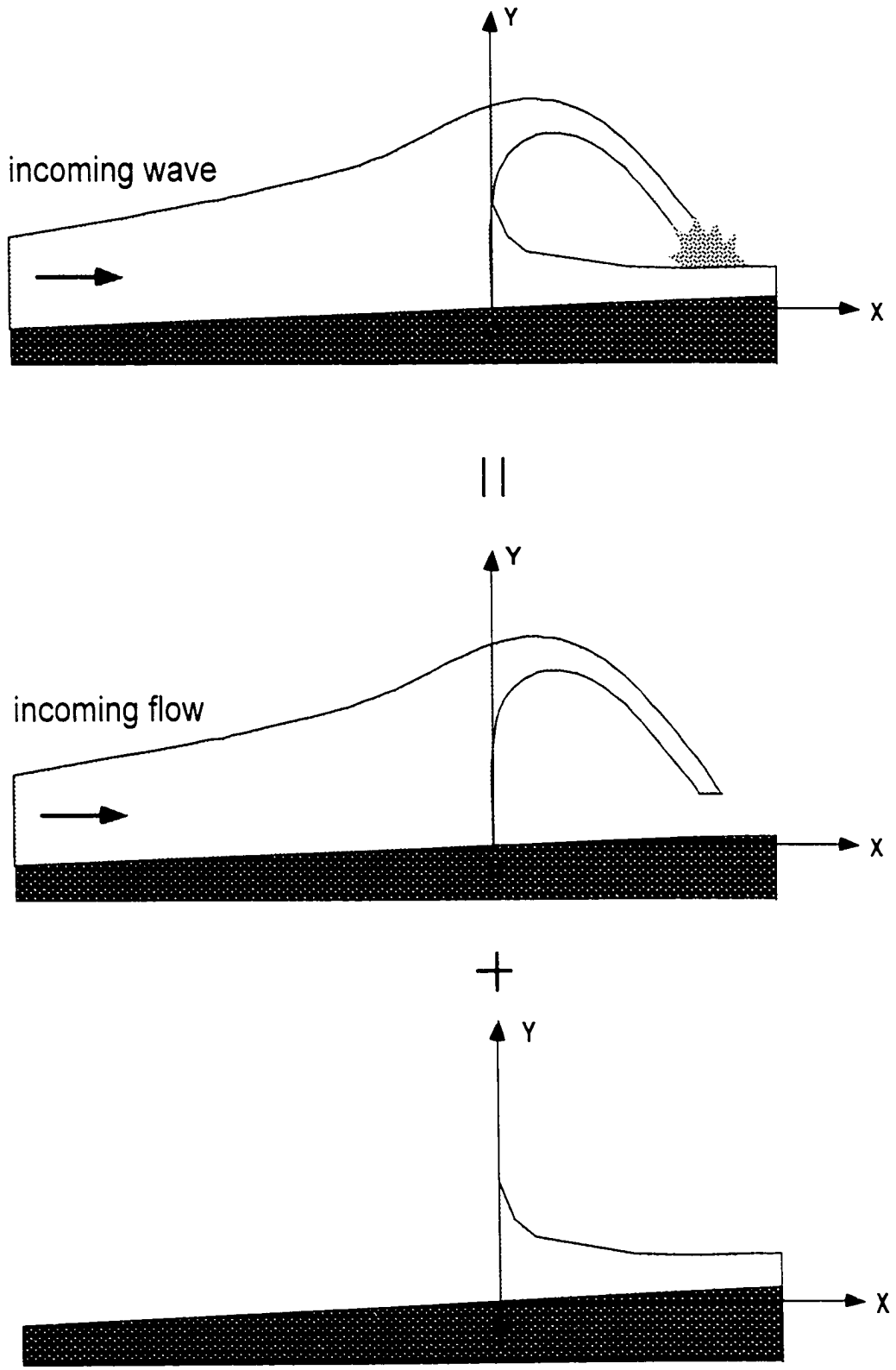

Figure 1.1 Schematic of Division of Plunging Breaker into two parts

Application of this division requires a criterion for detection of breaking. Shields (1986) had shown that the exact criterion for breaking (crest particle velocity equal to the phase velocity) is also the criterion for existence of a solution of the shallow water Green-Naghdi model at any level. Since both crest particle velocity and phase velocity are known everywhere at any instant of time in Green-Naghdi models, it is possible to use this criterion to apply the division. However, there exists an easily observed visual criterion for the onset of plunging waves: the breaking begins with the occurrence of a vertical crest front. Usually, the elevation of the water surface is what we want to know and this also known at any instant of time in Green-Naghdi models. Thus, it is much better to use this criterion as a trigger for invoking the division.

There, however, arises another problem, i.e., how to join the solutions for each region together again after calculation of each region, since what we pursue is a uniform solution for the whole region. These solutions do not make sense unless these solutions can match with each other at the joint. In the development of the Green-Naghdi theory, it was recognized early on that situations would arise similar to the bifurcation of the breaking wave described above. A procedure for dealing with these, called jump conditions was introduced by Naghdi and Rubin (1981) to deal with the bow wave of a planning boat. It appears attractive therefore to try to expand this approach to deal with the breaking wave phenomenon. Therefore, the study of jump conditions associated with Green-Naghdi theory becomes our main concern in this dissertation. Besides the breaking

waves, there are many problems that need the jump conditions to obtain a uniform solution throughout the flow region, as we will discuss later.

The jump conditions are associated with the integral balance laws of Green-Naghdi theory. The idea of jump conditions in fluid mechanics is not new but very common in dealing with many other problems in hydrodynamics and aerodynamics. A well-known case in aerodynamics is shock waves, across which there exist discontinuities of velocity, pressure, density, special entropy and temperature. The hydraulic jump is an oft-quoted example in hydraulics of jump conditions. It is instructive to examine some of these common applications to get a sense of the approach that is required.

Application of jump conditions is usually associated with discontinuities of one or more physical characters. We can learn this very clearly from the history of the study of shock waves. At the beginning of nineteenth century, Poison (1808) determined what was, in effect, a simple wave solution of the differential equation of flow in an isothermal gas. However, after forty years Challis (1848) observed that such an equation can not always be solved uniquely for the velocity u. To solve this uniqueness problem, Stokes (1848) proposed to assume that a discontinuity in the velocity begins at the time when the slope of velocity becomes infinite. Then he deduced two discontinuity conditions for an isothermal gas by means of the laws of conservation of mass and momentum. Stokes argued physically that discontinuities would never occur since viscous forces would smooth out any tendency toward a discontinuity. Furthermore he indicated that flows involving a discontinuity must also involve some phenomena of reflection.

Earnshaw (1858) and Riemann (1860) developed the theory of shocks independently. Unfortunately, Riemann made the incorrect assumption that the transition across a shock is adiabatic and reversible. Rankine (1869) showed that no steady adiabatic process in which the only forces are pressure forces can represent a continuous change over a small finite region from one constant state to another. He proposed instead that across this region a non-adiabatic process occurs subject to the condition that heat may be communicated from one particle to another but no heat is received from outside. Rankine's condition agrees with the principle of conservation of energy. But Rayleigh (1910) and Hugoniot (1887) were the first to point out clearly that an adiabatic reversible transition in a shock would violate the principle of conservation of energy. From the conservation of energy Hugoniot deduced the third shock condition in its customary form, which is preferable to Rankine's form, although in the case of a perfect gas, Rankine's three shock conditions are equivalent to those of Hugoniot. Rayleigh (1910) pointed out that the entropy must increase in crossing a shock front and that for this reason a rarefaction shock cannot occur in a perfect gas. Thus proper jump conditions across shock waves have been set up, and as a part of solution of shock waves, this has been proved a great advance in mathematics and fluid mechanics, especially for supersonic flows in aerodynamics.

Jump conditions for shock waves are derived from the "caloric equation of state," and the basic laws of physics: 1) conservation of mass, 2) conservation of momentum, 3) conservation of energy, and 4) increase or conservation of entropy. Taking into account

the assumptions that the fluid in hydrodynamics is incompressible, inviscid and homogenous, then the latest law, that is, increase or conservation of entropy, can be dropped. The others form the foundation to derive jump conditions in hydrodynamics.

Jump conditions involving overall concepts such as energy and momentum are much easier to apply in Green-Naghdi models than in other classical methods, because integral momentum and energy are basic variables in Green-Naghdi models while detailed flow kinematics are basic ingredients in other classical methods. Once the Green-Naghdi method was introduced in 1974, Green and Naghdi (1976) tried to solve the classic hydraulic jump problem with this method, where the simplest jump conditions have been applied. Since then, the jump conditions with various generality have been obtained and applied to various problems: Caulk (1976) to solve the problem of fluid under a sluice gate, Naghdi & Rubin (1981) to solve the planing of a boat, and Naghdi & Rubin (1981) to solve the free waterfall from a flat bottom. We need to point out that these jump conditions are derived for a theory with only one "director" from the Lagrangian form of the integral balance equations. After having realized the limitation of Green-Naghdi method in Lagrangian form, Green & Naghdi recast the governing equations in Eulerian form and established a one-to-one correspondence between the Lagrangian and Eulerian formulations. At the same time, the associated general jump conditions with K "directors" have been obtained with the limitation to steady flow and with the use of the rectangular Cartesian coordinates.

Recall that our primary need is to develop the jump conditions for Green-Naghdi theory in order to continue the numerical calculation of a plunging wave after it starts to break. In latest decade, there are many publications regarding the numerical calculation of a plunging wave as we have discussed in above sections. However, these calculation based on classical methods can only be valid just before the tip of the projection jet touches the front trough. Having realized the advantage of Green-Naghdi method over other classical methods on integral properties, we expect that the numerical calculation based on Green-Naghdi method may continue even after the projection of the jet. We shall not attempt to go so far here, but rather focus our attention to the derivation of the general jump conditions for Green-Naghdi theory. Then we will apply the jump conditions on various problems and further understand the advantages and disadvantages of the jump conditions in Green-Naghdi models, which we believe will form a solid foundation to solve more complicated problems such as breaking waves.

Recall that the plunging breaker can be divided into two parts to avoid the multi-valued problem, as shown in Figure 1.1. Even at the first glance, we can find that part 1 is very similar to the flow over a vertical weir, while part 2 is somehow like the flow under a sluice gate. Figure 1.2 shows the likeness between the plunging breaker and the weir flow and the flow through a sluice gate. This likeness is the motivation to study the weir flow and sluice gate to validate the jump conditions.

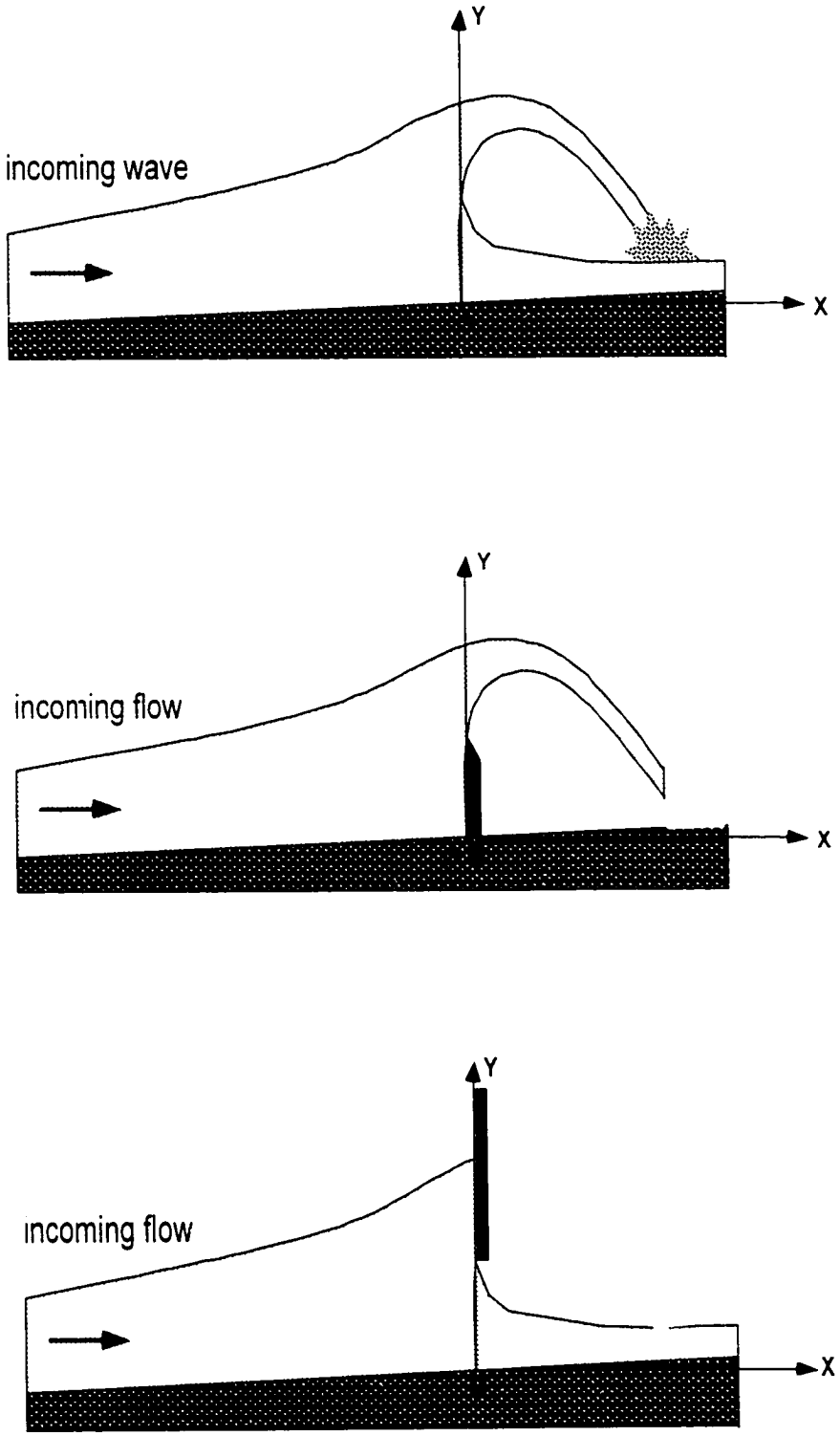

Figure 1.2 Schematic of Plunging Breaker
and Weir Flow and Sluice Flow

In the research that follows, we first attempt to derive the general jump conditions for Green-Naghdi method. Based on their formula of directed sheet theory, Green and Naghdi (1986) derived the general jump conditions for steady, two-dimensional problems. Here we will use the formula introduced by Shields & Webster, rather than adopt the formula of Green & Naghdi. Although the derivation given by Green & Naghdi may be elegant from a physical viewpoint, we find that the equivalent derivation by Shields & Webster (1986, 1988) is more straightforward and easier to understand, as well as obtained through a strictly mathematical approach. After having obtained the Green-Naghdi theory, Webster & Shields applied it to many problems, such as wave shoaling. However, jump conditions are not considered in their problems, and thus their derivation and applications do not include this development. Therefore, the jump conditions based on Shields & Webster's approach needs to be derived first.

After the governing equations and jump conditions based on different level of Green-Naghdi methods have been obtained, we will apply them to various problems. The main concern in this dissertation is the flow under a sluice gate and the flow over a weir. Before discussing these problems, we first consider some simple problems, such as the free waterfall problem, which form theoretical foundation to solve more complicated problems. The comparison between current results with those of Naghdi or others will be made when these results are available.

Chapter 2

Green-Naghdi Model

The Green-Naghdi model is a continuum model in which the kinematic character of the flow is prescribed in one direction beforehand, say, in the vertical direction in this thesis. This approach always yields a three-dimensional, unsteady model for particular flows. With the restriction of velocity profile, the equations for modeling a flow can satisfy the boundary conditions exactly, satisfy conservation of mass exactly. Moreover, the governing equations obtained through Green-Naghdi model are Gallilean invariant.

The governing equations derived by Green-Naghdi method are composed of: an exact statement of the conservation law of mass, an approximate statement of the conservation law of momentum, and exact statements for various boundary conditions. As a result of the formulation, the vertical coordinate no longer appears in the governing equations and all quantities are functions of horizontal coordinates and time. Therefore the obtained governing equations are two-dimensional in form and still three-dimensional in character, which is a great advantage of Green-Naghdi theory.

For later convenience, we derive briefly the governing equations for Green-Naghdi model, following the approach introduced by Shields & Webster (1988). For detail derivation, please refer to the paper of Shields & Webster (1988), or the Ph.D. dissertation of Shields (1986). In §2.1, we state clearly the idea of Green-Naghdi method and give out the general Green-Naghdi equations without detail derivations and

explanations. In §2.2, based on the assumed profile of the velocity (2.15), we obtain the particular Green-Naghdi equations for shallow water problems, which are the main concern in this thesis. Then in §2.3 and §2.4 we will obtain the Green-Naghdi Level I and II governing equations respectively.

§2.1 Derivation of the general Green-Naghdi equations

Before the derivation, we need to explain the notation adopted here. Let $\mathbf{x} = x_i$ (i = 1, 2, 3) be a system of fixed Cartesian coordinates in Euclidian space with base vectors $\mathbf{e}_i$, where $\mathbf{e}_3$ is oriented vertically upward. For convenience, we shall denote x_3 by ζ in the subsequent development because this dimension plays a much different role than the other two dimensions. In the following we shall use standard Cartesian tensor notation, with the summation convention implied for repeated indices. Latin indices are used for quantities having three spatial components and take on values of 1, 2, 3; Greek indices take on the values of 1, and 2 only. A comma in the subscript denotes differentiation by the following variable or that corresponding to the subsequent index. The fluid velocity vector at a point $\mathbf{x}$ and time t is given by $\mathbf{v} = \mathbf{v}(\mathbf{x}, t) = v_i e_i$.

Here we adopt the common assumption in hydrodynamics that the fluid is inviscid, incompressible and homogenous. Note that when Shields (1986) derived the directed theory, he did not restrict the property of the fluid. But in this dissertation we only consider the inviscid and incompressible fluid. The fluid is assumed to be bounded by two smooth and non-intersecting material surfaces. The material surfaces are given by

$\zeta=\alpha(x_1,x_2,t)$ and $\zeta=\beta(x_1,x_2,t)$, $\beta>\alpha$, respectively (see Fig. 2.1). Then the three-dimensional (Euler) equations resulting from the conservation laws of mass and momentum are

$$v_{i,i}=0, \tag{2.1}$$

$$\rho v_{i,t}+(\rho v_i v_j)_{,j}=-p_{,i}-\rho g e_3. \tag{2.2}$$

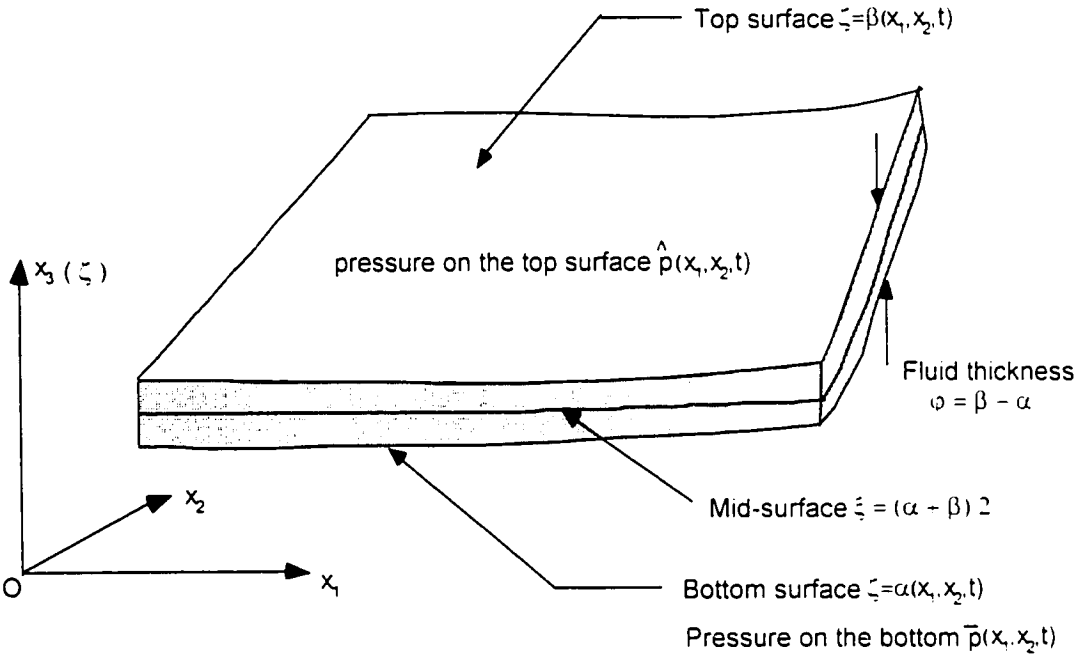

Fig. 2.1 Sketch of a fluid body bounded by two material surfaces

Since α and β are material surfaces, then the kinematic ("no leak") boundary conditions on these surfaces are:

$$\frac{D\beta}{Dt}=\left[v_3-\beta_{,t}-v_\gamma\beta_{,\gamma}\right]\Big|_{\zeta=\beta}=0,$$

$$\frac{D\alpha}{Dt} = \left[v_3 - \alpha_{,t} - v_\gamma \alpha_{,\gamma} \right]\Big|_{\zeta=\alpha} = 0. \qquad (2.3a, b)$$

where $\frac{D}{Dt}$ denotes the material derivative.

We now introduce a kinematic assumption that the velocity field of fluid can be approximately described as

$$v_i(x_1, x_2, \zeta, t) = \sum_{n=0}^{K} W_n^i(x_1, x_2, t)\lambda_n(\zeta). \qquad (i = 1, 2, 3) \qquad (2.4)$$

$\lambda_n(\zeta)$ is a "shape" function which depends upon ζ only, and is specified a priori. For instance, for particular problems such as shallow water problems, the polynomial weighing function $\lambda_n(\zeta) = \zeta^n$ is chosen. The coefficients W_n^i are unknown, time dependent vectors to be determined as part of the solution. The W_n^i correspond with the "directors" in the work of Green and Naghdi. For each choice of K, a complete, closed set of equations is developed which is independent from those for a different value of K. Thus, the kinematic models form a hierarchy depending on K and increasing in complexity with K. Since this hierarchy is different from a perturbation expansion, we adopt the terminology suggested by Shields & Webster (1988) to describe the complexity of the theory. We refer to a particular member of this hierarchy as the "K^{th} level approximation", or "Level K theory".

With the adoption of (2.4), the form of the solution is prescribed a priori in the vertical direction while is unknown in the other two directions. In addition, it is assumed that the vertical variation of the velocity field may be represented to a tolerable degree of

accuracy by the sum of different shape functions $\lambda_n(\zeta)$. Consequently, the otherwise three-dimensional governing equations are reduced to two-dimensional equations.

Then under this assumption, the kinematic boundary conditions, (2.3a, b), may be rewritten as

$$\sum_{n=0}^{K} W_n^3 \lambda_n(\alpha) = \alpha_{,t} + \sum_{n=0}^{K} W_n^\gamma \lambda_n(\alpha) \alpha_{,\gamma} . \tag{2.5}$$

$$\sum_{n=0}^{K} W_n^3 \lambda_n(\beta) = \beta_{,t} + \sum_{n=0}^{K} W_n^\gamma \lambda_n(\beta) \beta_{,\gamma} . \qquad (\gamma = 1, 2) \tag{2.6}$$

The continuity equation (2.1) likewise becomes

$$\sum_{m=0}^{K} W_{m,\gamma}^\gamma \lambda_m + \sum_{m=0}^{K} W_m^3 \lambda_{m,\zeta} = 0 . \tag{2.7}$$

It is convenient at this point to restrict the weighting function to those which possess the following property

$$\lambda_{m,\zeta} = \sum_{r=0}^{n} a_r^m \lambda_r \ , \quad (n \le m) \tag{2.8}$$

where the a_r are arbitrary constants. (2.8) means that the derivative of the shape function can be represented with the lower order of the polynomial function of the shape functions themselves. Here (2.8) is introduced in order to simplify the continuity equation (2.7). Because the shape function $\lambda_n(\zeta)$ is specified a priori, we can intently choose a function with the property of (2.8). There are many function sets that satisfy (2.8), such as exponential functions and polynomial functions. On the other hand, this property is not

essential in Green-Naghdi theory. If the chosen $\lambda_n(\zeta)$ does not satisfy (2.8), then the Krylov-Kantorovich method can be employed, as done by Shields (1986).

The function set $\{\lambda_m\}$ is therefore a finite closed set under differentiation. Inserting (2.8) into (2.7) we can express continuity equation as

$$\sum_{r=0}^{K}\left\{W^{\gamma}_{r,\gamma}+\sum_{m=0}^{K}W^{3}_{m}\,a^{m}_{r}\right\}\lambda_r(\zeta)=0\,. \tag{2.9}$$

or, since the terms in braces are not a function of ζ

$$W^{\gamma}_{r,\gamma}+\sum_{m=0}^{K}W^{3}_{m}\,a^{m}_{r}=0\,,\qquad \text{for } r=0,\ldots,K. \tag{2.10}$$

This is therefore the statement of conservation of mass for the flow given by the kinematic approximation (2.4).

Now let us turn to the conservation law of momentum. If we were to substitute (2.4) into the momentum equation (2.2), and require that the resulting coefficients of $\lambda_n(\zeta)$ be equal to zero (as we did for the continuity equation), we would obtain $3(K+1)$ equations. Remember that we have already obtained $(K+1)$ equations from (2.10), then we would have $4(K+1)$ equations. However, we have only $3(K+1)$ unknown velocity components, i.e., W^{i}_{n}, and the unknown pressure p. Therefore, we would have many more equations than unknowns. Consequently, the Krylov-Kantorovich method is employed. That is, the shape functions $\lambda_n(\zeta)$ are used as weighting functions to develop $3(K+1)$ approximate equations that express the conservation of momentum in some integral sense. At the same time, $K+1$ new unknowns, i.e., the integral pressure P_n, are introduced in this procedure.

As pointed out by Shields (1986), this procedure is equivalent to the *weak formulation* of a variational problem discussed by Yeung (1982), and it is equivalent to setting the depth-integrated weighted residuals of the field equations to zero. We multiply (2.2) by $\lambda_n(\zeta)$ and integrate through the vertical direction obtaining

$$\int_{\alpha}^{\beta}\left[(\rho v_i)_{,t}+(\rho v_i v_j)_{,j}\right]\lambda_n(\zeta)\,d\zeta=\int_{\alpha}^{\beta}\left[-p_{,i}-\rho g e_3\right]\lambda_n(\zeta)\,d\zeta. \qquad (2.11)$$

for n = 0, …., K.

We insert the kinematic assumption (2.4) into the above expression, and after a straightforward but tedious derivation, finally we can obtain

$$\sum_{m=0}^{K}\left\{\rho W^{1}_{m,t}\,y_{mn}+\sum_{r=0}^{K}\rho\,W^{1}_{m,\gamma}\,W^{\gamma}_{r}\,y_{mrn}+\sum_{r=0}^{K}\rho\,W^{1}_{m}\,W^{3}_{r}\,y^{m}_{rn}\right\}\;= \qquad (2.12)$$

$$\left(-P_n+\hat{p}\,\lambda_n(\beta)\beta_{,\gamma}-\bar{p}\,\lambda_n(\alpha)\alpha_{,\gamma}\right)e_{\gamma}+\left(P'_n-\rho g y_{n0}-\hat{p}\,\lambda_n(\beta)+\bar{p}\,\lambda_n(\alpha)\right)e_3,$$

for n = 0, …., K, and i = 1, 2, 3

where

$\hat{p}$ and $\bar{p}$ are the pressures on the top and bottom surfaces respectively, and

P_n and P'_n are the n^{th} integrated pressures:

$$P_n=\int_{\alpha}^{\beta}p\,\lambda_n\,d\zeta, \qquad P'_n=\int_{\alpha}^{\beta}p\,\lambda_n{}'\,d\zeta. \qquad (2.13)$$

and

$$y_{mn}=\int_{\alpha}^{\beta}\lambda_m\,\lambda_n\,d\zeta, \quad y_{mrn}=\int_{\alpha}^{\beta}\lambda_m\,\lambda_r\,\lambda_n d\zeta, \quad y^{n}_{mr}=\int_{\alpha}^{\beta}\lambda_m\,\lambda_r\,\lambda_n{}'\,d\zeta. \qquad (2.14)$$

Here the prime denotes the derivative with regard to ζ. For detail derivation, please refer to Shields & Webster(1988).

We have now completed the derivation of the general Green-Naghdi equations for an inviscid, incompressible fluid bound by two smooth, non-intersecting material surfaces. The governing equations for an inviscid flow are then: the two kinematic boundary conditions (2.5) and (2.6); the K+1 conservation of mass equations (2.10); and the 3(K+1) approximate conservation of momentum equations (2.12). The variables include 3(K+1) unknown components of W_n^i, K+1 integrated pressures, P_n, and two conditions on the bounding surfaces. On the top surface either β or $\hat{p}$ is unknown, depending on the problem. Similarly on the bottom surface either α or $\bar{p}$ is unknown. Thus, we have 4(K+1)+2 unknowns and the same number of equations, and the system is closed.

We can make several observations about the results so far. The equations depend only on x_1, x_2 and t and do not have any explicit dependence on the variable ζ. Thus the result of the derivation has been to reduce the dimensionality of the three-dimensional equations to a set of two-dimensional equations in x_1, x_2 and t. As such, these equations are reminiscent of equations for a membrane although, unlike a membrane, this "fluid sheet" has a much greater kinematic complexity. For instance, a membrane has only one kinematic variable, that is, the location of the membrane for a given x_1, x_2. The fluid sheet has variables W_n^i, one of which may be identified as the "location" of the sheet, but the others of which are clearly kinematic ingredients which have no counterparts as a membrane.

Recall that after the initial assumption of the form of the velocity distribution in the ζ direction was introduced, no terms were thrown out. Therefore, the governing equations, like the conservation laws from which they were derived, are Galilean invariant. Because no scale was introduced there is no explicit flow situation for which this theory is most applicable. Due to that assumption, the governing equations derived this way are, to be sure, an approximation. However, the limits of this approximation are implicit and must be determined by numerical or physical experiments. Even for the lowest level theory, the governing equations are nonlinear because both the conservation of momentum laws and the boundary conditions are.

As pointed out by Webster (1991), because the governing equations are approximate, they do not exactly satisfy Kelvin's theorem and the flow computed from these equations does not remain irrotational. Shields and Webster (1989) showed that the K^{th} level shallow water fluid sheet theory does satisfy conservation of circulation in an average sense across the fluid domain and the flow does remain approximately irrotational in an initial value problem when the initial state was quiescent. However, the treatment of steady flow (time invariant) problems does require some additional specifications of the average circulation (or of the vorticity distribution).

§2.2 Governing equations for shallow water

In the above section we have obtained the general Green-Naghdi equations for an inviscid, incompressible fluid. However, the general Green-Naghdi governing equations require that the shape function, or say, weighting function, $\lambda_n(\zeta)$ should be given a priori. Different shape functions will yield different realizations of the theory that will yield different answers to a given problem. That is, the solutions are not unique due to different chosen $\lambda_n(\zeta)$. It is assumed, however, that the answers from two such realizations will not be fundamentally different for a given problem if the shape functions are appropriate to the problem. For shallow water problems, the study of Shields and Webster (1988) shows that the adoption of the polynomial weighting function is relatively simply and yields satisfactory results.

With the choice of the polynomial weighting function, that is $\lambda_n(\zeta)=\zeta^n$, which satisfies the property (2.8), it is possible to reduce the general equations further. Then according to (2.4) and (2.5), the velocity field is given by

$$v_\gamma = \sum_{n=0}^{K} W_n^\gamma \zeta^n , \qquad v_3 = \sum_{n=0}^{K} W_n^3 \zeta^n . \tag{2.15}$$

Note that γ ranges from 1 to 2.

Then the kinematic boundary conditions (2.6a, b) become

$$\sum_{n=0}^{K} W_n^3 \alpha^n = \alpha_{,t} + \sum_{n=0}^{K} W_n^\gamma \alpha^n \alpha_{,\gamma} .$$

$$\sum_{n=0}^{K} W_n^3 \beta^n = \beta_{,t} + \sum_{n=0}^{K} W_n^\gamma \beta^n \beta_{,\gamma} . \qquad (2.16a, b)$$

The continuity equation becomes

$$\sum_{n=0}^{K} W_{n,\gamma}^\gamma \zeta^n + \sum_{n=0}^{K} W_n^3 \, n \zeta^{n-1} = 0 . \qquad (2.17)$$

After separating the K^{th} term in the first summation and changing the index n to n+1, we obtain

$$W_{K,\gamma}^\gamma \zeta^K + \sum_{n=0}^{K-1} \left\{ W_{n,\gamma}^\gamma + (n+1) W_{n+1}^3 \right\} \zeta^n = 0 . \qquad (2.18)$$

If (2.18) is to hold everywhere, we may set each coefficient of ζ^n to zero, that is,

$$W_{K,\gamma}^\gamma = 0 . \qquad (2.19)$$

$$W_{n,\gamma}^\gamma + (n+1) W_{n+1}^3 = 0 . \quad \text{for } n=0, 1, \ldots, K-1. \qquad (2.20)$$

We need to point out that (2.19) is related to the so-called "restricted theory". When Green & Naghdi introduced their theory, they restricted the last component of the director so that it remains vertical at all times. With this "restricted theory", Green & Naghdi make their theory self-consistent in its internal structure. Shields (1986) set $W_K^\gamma = 0$ (corresponding to a restricted director) in order to satisfy the continuity equations. However, Webster (1993) found that the restricted theory is needed in order to model shallow water problems whose fluid field is considered as irrotational. In the later

chapters, we introduce the "restricted theory" for particular problems, which we will discuss in detail later.

Finally the conservation law of momentum states

$$\sum_{m=0}^{K}\left\{\rho W_{m,t} H_{(m+n)}+\sum_{r=0}^{K}\rho W_{m,\gamma} W_r^{\gamma} H_{(m+r+n)}+\sum_{r=0}^{K}\rho m W_{,m} W_r^{3} H_{(r+n+m-1)}\right\} =$$

$$\left(-P_n+\hat{p}\beta^n\beta_{,\gamma}-\bar{p}\alpha^n\alpha_{,\gamma}\right)e_{\gamma}+\left(P'_n-\rho g H_n-\hat{p}\beta^n+\bar{p}\alpha^n\right)e_3 \qquad (2.21)$$

for n = 0, …., K

where

$$H_n=\int_{\alpha}^{\beta}\zeta^n\,d\zeta=\frac{1}{n+1}\left(\beta^{n+1}-\alpha^{n+1}\right) \qquad (2.22)$$

Therefore a closed system has been obtained, which consists of governing equations (2.16a, b), (2.19), (2.20) and (2.21). Note that in this governing system we did not include the restricted theory, as Shields (1986) did. However, the restricted theory will be applied in this thesis for simplification. As we will discuss later, under certain circumstance, (2.19) are equivalent to the restricted theory.

From the above derivation of Green-Naghdi governing equations, the total number of variables and equations depends on the assumed profile of the fluid velocity. For the governing system of shallow water flow, it depends on the highest order of the polynomial function, that is, the index K. Thus we can identify the level of Green-Naghdi model by means of the index K. When K=1, this responds Green-Naghdi Level-I theory, which is the simplest model. The higher the level is, the higher number of equations and

variables appears, as a result the more complicated the governing system becomes and more accurate results we can obtain. Notice that the appearance of the momentum equations in (2.21) is deceptively simple but note that there are two levels of summation. Actual evaluation of the equations is sufficiently tedious that it is impractical to carry out any but the first one or two levels without the use of computer programs to perform the calculus and the algebra. In the following two sections, we summarize the governing equations for Level-I and II for later convenience. We will focus our attention on two-dimensional problems. The governing equations for three-dimensional problems are similar, but more tedious.

§2.3 Green-Naghdi Level-I theory

According to Green-Naghdi method (Level-I), that is, the index K is set to 1, according to (2.15) the velocity profile (u, v) is assumed to be of the form:

$$\begin{aligned} u(x,\zeta,t) &= u_0(x,t) + u_1(x,t)\zeta; \\ v(x,\zeta,t) &= v_0(x,t) + v_1(x,t)\zeta. \end{aligned} \qquad (2.3.1a, b)$$

where, ζ denotes the vertical coordinate and x the horizontal coordinate. The corresponding restricted theory is

$$u_1 = 0. \qquad (2.3.2)$$

Hence we will get rid of u_1 from the governing system. Consequently, in this level, the horizontal velocity is uniform in the vertical direction, while the vertical velocity is assumed to be linear in the vertical direction (see Fig. 2.2).

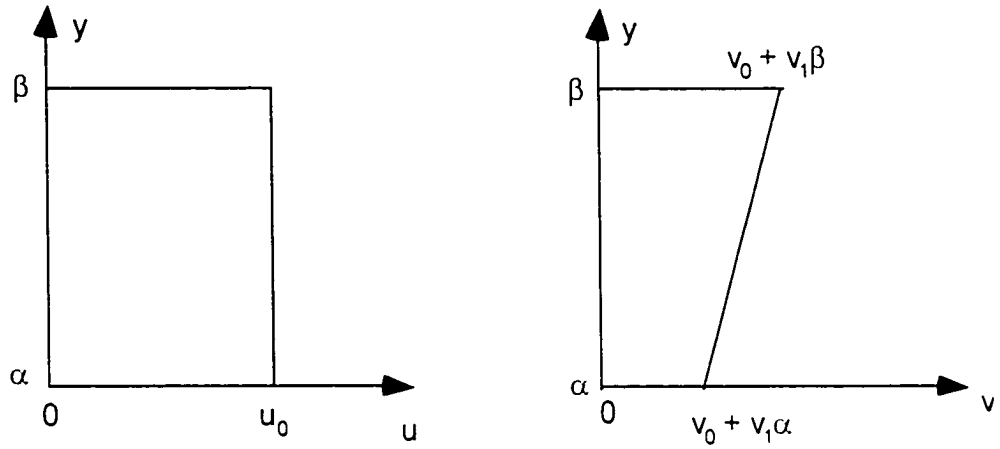

Fig. 2.2 Sketch of the velocity profile for Green-Naghdi Level-I theory

The fluid is assumed to be bounded by two smooth and non-intersecting material surfaces. The material surfaces, so called top and bottom surfaces, are denoted by $\zeta=\alpha(x,t)$ and $\zeta=\beta(x,t)$, $\beta>\alpha$, respectively. No matter whether they are given or unknown free surfaces, in principle, since they are material surfaces, then they will satisfy the kinematic ("no leak") boundary condition, that is,

$$\frac{D\beta}{Dt}=\left[v_3-\beta_t-v_\gamma\beta_\gamma\right]_{\zeta=\beta}=0, \qquad (2.3.3)$$

$$\frac{D\alpha}{Dt}=\left[v_3-\alpha_t-v_\gamma\alpha_\gamma\right]_{\zeta=\alpha}=0. \qquad (2.3.4)$$

Here f_t and f_γ denote $\frac{\partial f}{\partial t}$ and $\frac{\partial f}{\partial x_\gamma}$, respectively. From now on, we will use this notation.

In two-dimensional system, say x horizontal and y (or ζ) vertical, with use of the assumed velocity profile, the kinematic boundary conditions can be reduced to:

$$v_0+v_1\alpha=\alpha_t+u_0\alpha_x; \qquad (2.3.5a, b)$$
$$v_0+v_1\beta=\beta_t+u_0\beta_x.$$

where $\beta = \beta(x,t)$ and $\alpha = \alpha(x,t)$ represent the top and bottom surfaces respectively.

After applying the conservation law of mass and taking into account the velocity profile, we can obtain the continuity equation:

$$u_{0x} + v_1 = 0. \tag{2.3.6}$$

As for the conservation law of momentum, recall that there are two levels of summation in (2.21). The derivation is straightforward, but a little tedious. Without re-deriving them in detail, we just list the results as follows:

$$u_{0t}\phi_0 + \phi_0 u_0 u_{0x} = \frac{1}{\rho}(-P_{0x} + \hat{p}\beta_x - \bar{p}\alpha_x)$$

$$u_{0t}\phi_1 + \phi_1 u_0 u_{0x} = \frac{1}{\rho}(-P_{1x} + \hat{p}\beta\beta_x - \bar{p}\alpha\alpha_x)$$

$$v_{0t}\phi_0 + \phi_0 u_0 v_{0x} + \phi_0 v_0 v_1 + v_{1t}\phi_1 + \phi_1 u_0 v_{1x} + \phi_1 v_1 v_1 = \frac{1}{\rho}(-\rho g\phi_0 - \hat{p} + \bar{p}) \tag{2.3.7a-d}$$

$$v_{0t}\phi_1 + \phi_1 u_0 v_{0x} + \phi_1 v_0 v_1 + v_{1t}\phi_2 + \phi_2 u_0 v_{1x} + \phi_2 v_1 v_1 = \frac{1}{\rho}(P_0 - \rho g\phi_1 - \hat{p}\beta + \bar{p}\alpha)$$

where,

$\hat{p}$ and $\bar{p}$ are the pressures on the top and bottom surfaces respectively, and

$$\phi_0 = \beta - \alpha;$$
$$\phi_1 = \frac{1}{2}(\beta^2 - \alpha^2); \tag{2.3.8}$$
$$\phi_2 = \frac{1}{3}(\beta^3 - \alpha^3);$$

$$P_n = \int_{\alpha}^{\beta} p\zeta^n d\zeta . \quad (n = 0, 1, 2, \ldots)$$

Equations (2.3.5a, b), (2.3.6), and (2.3.7a-d) form the governing system with seven equations and nine variables, that is, α, β, u_0, v_0, v_1, P_0, P_1, $\hat{p}$ and $\bar{p}$. Two additional equations (or boundary conditions) are needed in order to form a closed governing system. We suppose that the remaining two equations will appear when particular problem is introduced. Thus, a well-posed governing system can be obtained.

Here we have to point out that, since P_1 only exists in equation (2.3.7b), it is then a dependent variable and need not be solved simultaneously with the other variables. Therefore, in practice, we will omit the governing equation (2.3.7b) together with the variable P_1 from the governing system

§2.4 Green-Naghdi Level II theory

According to Green-Naghdi Level-II method, that is, when the index K=2, in two dimensional system, say x horizontal and ζ vertical, the profiles of horizontal and vertical components of velocity (2.4) become:

$$u = u_0 + u_1 \zeta + u_2 \zeta^2 ,$$

$$v = v_0 + v_1 \zeta + v_2 \zeta^2 , \text{ respectively,} \qquad (2.4.1a, b)$$

where ζ denotes the vertical position. And the corresponding restricted theory is

$$u_2 = 0. \qquad (2.4.2)$$

From now on, we will get rid of u_2 from the governing system. As a result, the profile of the velocity is illustrated in Fig. 2.3.

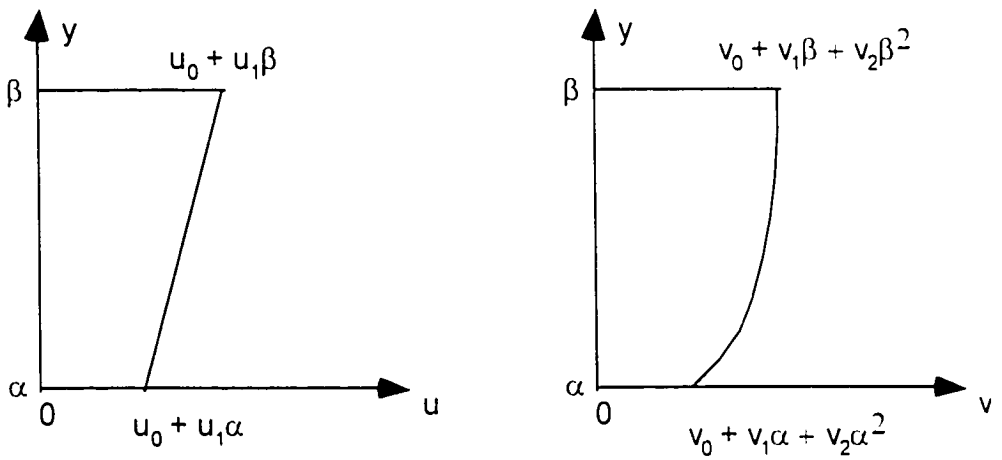

Fig. 2.3 Sketch of the velocity profile for Green-Naghdi Level-II theory

The kinematic boundary conditions on the top and bottom surfaces are:

$$\frac{D\beta}{Dt} = 0 \Rightarrow \beta_t + u_0\beta_x + u_1\beta\beta_x = v_0 + v_1\beta + v_2\beta^2;$$

$$\frac{D\alpha}{Dt} = 0 \Rightarrow \alpha_t + u_0\alpha_x + u_1\alpha\alpha_x = v_0 + v_1\alpha + v_2\alpha^2. \qquad (2.4.3a, b)$$

The continuity equation states:

$$u_{0x} + v_1 = 0,$$

$$u_{1x} + 2v_2 = 0. \qquad (2.4.4a, b)$$

The application of conservation law of momentum (2.21) leads to:

n=0, in horizontal direction.

$$(\beta-\alpha)(u_{0t}+u_0u_{0x}+u_1v_0)+\frac{1}{2}(\beta^2-\alpha^2)(u_{1t}+u_1u_{0x}+u_0u_{1x}+u_1v_1)$$
$$+\frac{1}{3}(\beta^3-\alpha^3)(u_1u_{1x}+u_1v_2)=-\frac{P_{0x}}{\rho}+\frac{\hat{p}}{\rho}\beta_x-\frac{\bar{p}}{\rho}\alpha_x$$

n=1, in horizontal direction.

$$\frac{1}{2}(\beta^2-\alpha^2)(u_{0t}+u_0u_{0x}+u_1v_0)+\frac{1}{3}(\beta^3-\alpha^3)(u_{1t}+u_1u_{0x}+u_0u_{1x}+u_1v_1)$$
$$+\frac{1}{4}(\beta^4-\alpha^4)(u_1u_{1x}+u_1v_2)=-\frac{P_{1x}}{\rho}+\frac{\hat{p}}{\rho}\beta\beta_x-\frac{\bar{p}}{\rho}\alpha\alpha_x$$

n=2, in horizontal direction.

$$\frac{1}{3}(\beta^3-\alpha^3)(u_{0t}+u_0u_{0x}+u_1v_0)+\frac{1}{4}(\beta^4-\alpha^4)(u_{1t}+u_1u_{0x}+u_0u_{1x}+u_1v_1)$$
$$+\frac{1}{5}(\beta^5-\alpha^5)(u_1u_{1x}+u_1v_2)=-\frac{P_{2x}}{\rho}+\frac{\hat{p}}{\rho}\beta^2\beta_x-\frac{\bar{p}}{\rho}\alpha^2\alpha_x$$

n=0, in vertical direction.

$$(\beta-\alpha)(v_{0t}+u_0v_{0x}+v_1v_0)+\frac{1}{2}(\beta^2-\alpha^2)(v_{1t}+u_1v_{0x}+u_0v_{1x}+v_1^2+2v_0v_2)$$
$$+\frac{1}{3}(\beta^3-\alpha^3)(v_{2t}+u_1v_{1x}+u_0v_{2x}+3v_1v_2)$$
$$+\frac{1}{4}(\beta^4-\alpha^4)(u_1v_{2x}+2v_2^2)=-g(\beta-\alpha)-\frac{\hat{p}}{\rho}+\frac{\bar{p}}{\rho}$$

n=1, in vertical direction.

$$\frac{1}{2}(\beta^2-\alpha^2)(v_{0t}+u_0v_{0x}+v_1v_0)+\frac{1}{3}(\beta^3-\alpha^3)(v_{1t}+u_1v_{0x}+u_0v_{1x}+v_1^2+2v_0v_2)$$
$$+\frac{1}{4}(\beta^4-\alpha^4)(v_{2t}+u_1v_{1x}+u_0v_{2x}+3v_1v_2)$$
$$+\frac{1}{5}(\beta^5-\alpha^5)(u_1v_{2x}+2v_2^2)=\frac{P_0}{\rho}-\frac{1}{2}g(\beta^2-\alpha^2)-\frac{\hat{p}}{\rho}\beta+\frac{\bar{p}}{\rho}\alpha$$

n=2, in vertical direction.

$$\frac{1}{3}(\beta^3-\alpha^3)(v_{0t}+u_0v_{0x}+v_1v_0)+\frac{1}{4}(\beta^4-\alpha^4)(v_{1t}+u_1v_{0x}+u_0v_{1x}+v_1^2+2v_0v_2)$$
$$+\frac{1}{5}(\beta^5-\alpha^5)(v_{2t}+u_1v_{1x}+u_0v_{2x}+3v_1v_2)$$
$$+\frac{1}{6}(\beta^6-\alpha^6)(u_1v_{2x}+2v_2^2)=2\frac{P_1}{\rho}-\frac{1}{3}g(\beta^3-\alpha^3)-\frac{\hat{p}}{\rho}\beta^2+\frac{\bar{p}}{\rho}\alpha^2$$

(2.4.5a-f)

There are twelve variables in the Green-Naghdi Level II governing equations, that is, α, β, u_0, u_1, v_0, v_1, v_2, P_0, P_1, P_2, $\hat{p}$ and $\bar{p}$. However, we have only ten equations, that is, (2.4.3a, b), (2.4.4a, b) and (2.4.5a-f). This means two extra conditions are needed to construct a well-posed system. These two extra conditions will depend on the particular problem in question and will be introduced in our discussion of each problem. For instance, for a free waterfall problem as we will discuss later, in the downstream the bottom surface and the pressure on the top surface is known, then only eleven variables are left. Thus a closed governing system can be set up.

Therefore, we have obtained both Green-Naghdi Level I governing equations and Level II equations for shallow water problems. In order to obtain the solutions, boundary conditions and initial conditions are need. These conditions must be specified for particular problems. Therefore, in the following chapters, application of these equations to particular problems will be demonstrated, and under particular problems, these governing equations can be further simplified.

Chapter 3

Jump Conditions for Green-Naghdi Theory

In chapter 2 we have obtained the general Green-Naghdi governing equations for an inviscid, incompressible fluid, simplified equations for shallow water problems, and the governing equations for Green-Naghdi Level I and II theory. For those problem where a set of governing equations are valid throughout the whole flow region and the variables are continuous everywhere, the governing equations, together with the particular boundary and initial conditions, are sufficient to obtain the solutions. However, under certain circumstances, different sets of governing equations are needed for different flow regions. For instance, the free waterfall over a cliff can be divided into two parts with distinct characteristics: part 1 is bounded by a given bottom and an unknown free surface; part 2 is bounded by two unknown free surfaces (see Fig. 4.1). Then it is convenient to derive different governing equations for them respectively, seek separate solutions for each region, and match these solutions where they join to obtain a uniform solution valid throughout both regions. Therefore, the jump conditions, or so-called matching conditions, become essential part of the solutions. Another possible application of jump conditions is when there are variables with discontinuity at certain discrete points, that is, there exist jumps on the values of some variables in the flow region. Both the flow over a weir and the flow through a sluice gate fall into this category. Obviously, because of the presence of the weir or the sluice gate, there exists a jump of the thickness of the fluid between upstream and downstream, as well as jumps of other variables as we will discuss later. When there are real physical jumps, the Green-Naghdi governing equations, which

require continuity of all variables involved, cannot be valid throughout the flow region. In this case, the Green-Naghdi theory must be applied separately to upstream and downstream flows respectively, even though the obtained governing equations are same in character, e.g. for sluice gate problems. Since the magnitudes of the jumps are unknown beforehand and the Green-Naghdi theory is a complex nonlinear theory at all levels, application of the jump conditions is a real challenge, as we will discuss in later chapters.

Green & Naghdi realized the importance of the jump conditions when they introduced the directed sheet theory. Jump conditions have been obtained with various degrees of generality by Green & Naghdi (1976, 1977), Caulk (1976) and Naghdi & Rubin (1981) for the theory with one director in the Lagrangian form. When they recast the directed fluid sheet theory in Eulerian frame in 1986, Green and Naghdi derived the general formula of jump conditions directly from the general governing equations.

In this thesis we have adopted the formula introduced by Shields and Webster (1988), as we presented in chapter 2. Their method appears much easier to understand from hydrodynamic point of view. However, they did not derive the jump conditions associated with their method, because the jump conditions are not needed for those problems they considered, such as wave shoaling. Therefore, we here need to derive the jump conditions based on their formula, which are different from, but equivalent to, those of Green and Naghdi. In the interest of simplicity, we restrict our attention only to jump conditions for steady two-dimensional flows, similar to what Green & Naghdi did. First

we derive the jump conditions associated with the general Green-Naghdi equations. Since this has never done before, we will present the derivation in detail. The results form the theoretical foundation of further application to a variety of problems.

§3.1 General formula of jump conditions for steady two-dimensional flows

We employ standard two-dimensional Cartesian coordinates with x horizontal and y (or ζ) vertical. We suppose that an inviscid, incompressible fluid is bounded by two non-intersecting material surfaces. According to the kinematic assumption, the velocity profile of the fluid is assumed to be

$$\mathbf{v}(x,\zeta)=\sum_{n=0}^{K} u_n(x)\zeta^n \mathbf{e}_x+\sum_{n=0}^{K} v_n(x)\zeta^n \mathbf{e}_y. \qquad (3.1)$$

where, ζ denotes the vertical coordinate instead of y; $u_n(x)$ and $v_n(x)$ are dependent on the horizontal coordinate x only since the flow is steady.

Then from the results obtained in chapter 2, for steady, two-dimensional flows, the kinematic boundary conditions for the bottom and top surfaces are given by

$$\sum_{n=0}^{K} v_n \alpha^n=\sum_{n=0}^{K} u_n \alpha^n \alpha_x,$$

$$\sum_{n=0}^{K} v_n \beta^n=\sum_{n=0}^{K} u_n \beta^n \beta_x, \text{ respectively.} \qquad (3.2a, b)$$

The continuity equations become

$u_{K,x} = 0$;

$$u_{n,x} + (n+1)\, v_{n+1} = 0, \qquad \text{for } n=0, \ldots, K-1. \tag{3.3a, b}$$

Note that here we do not use the restricted theory, that is, we do not assume that $u_K = 0$.

Then, from (3.3b) after changing the index n+1 to n, we have

$$v_n = -\frac{1}{n} u_{n-1,x}, \qquad \text{for } n = 1, \ldots, K. \tag{3.4}$$

Subtracting (3.2a) from (3.2b), we can obtain

$$\begin{aligned} \sum_{n=0}^{K} v_n (\beta^n - \alpha^n) &= \sum_{n=0}^{K} u_n (\beta^n \beta_x - \alpha^n \alpha_x) \\ &= \sum_{n=0}^{K} u_n \frac{1}{n+1} (\beta^{n+1} - \alpha^{n+1})_x \end{aligned} \tag{3.5}$$

Inserting (3.4) into the left-hand side of (3.5), we have

$$\begin{aligned} \text{LHS of (3.5)} &= v_0(\beta^0 - \alpha^0) + \sum_{n=1}^{K} -\frac{1}{n} u_{n-1,x} (\beta^n - \alpha^n) \\ &= -\sum_{n=1}^{K} \frac{1}{n} u_{n-1,x} (\beta^n - \alpha^n) \\ &= -\sum_{n=1}^{K} \frac{1}{n} u_{n-1,x} (\beta^n - \alpha^n) + \frac{1}{K+1} u_{K,x} (\beta^{n+1} - \alpha^{n+1}) \\ &= -\sum_{n=0}^{K} \frac{1}{n+1} u_{n,x} (\beta^{n+1} - \alpha^{n+1}) \end{aligned}$$

where, (3.3a) has been used. Then (3.5) becomes

$$\sum_{n=0}^{K} \frac{1}{n+1} u_n (\beta^{n+1} - \alpha^{n+1})_x + \sum_{n=0}^{K} \frac{1}{n+1} u_{n,x} (\beta^{n+1} - \alpha^{n+1}) = 0. \tag{3.6}$$

Finally we obtain a very simple formula

$$\sum_{n=0}^{K} \frac{1}{n+1}\left[u_n(\beta^{n+1}-\alpha^{n+1})\right]_x = 0. \qquad (3.7)$$

Obviously, (3.7) can be integrated. After integrating (3.7) with regard to x, we can obtain

$$\sum_{n=0}^{K} \frac{1}{n+1}\left[u_n(\beta^{n+1}-\alpha^{n+1})\right] = Q. \qquad (3.8)$$

where Q is a constant of integration. Q here has its own physical meaning, and actually is the flow flux across a vertical interface between the two material surfaces β and α. Recall that the horizontal velocity is assume to be

$$u(x,\zeta) = \sum_{n=0}^{K} u_n(x)\zeta^n. \qquad (3.9)$$

The flow flux across a vertical interface between the material surfaces β and α is

$$Q = \int_{\alpha}^{\beta} u(x,\zeta)\,d\zeta. \qquad (3.10)$$

Inserting (3.9) into (3.10) and integrating yields

$$Q = \int_{\alpha}^{\beta} \sum_{n=0}^{K} u_n(x)\zeta^n\,d\zeta = \sum_{n=0}^{K} \frac{1}{n+1}\left[u_n(\beta^{n+1}-\alpha^{n+1})\right]. \qquad (3.11)$$

Note that (3.11) is exactly same as (3.9). As a result, (3.9) implies that the flow flux across any vertical interface between β and α keeps constant. This result is consistent with the conservation law of mass.

Now we suppose that there is a discontinuity at $x = x_0$, for instance, there exists a jump on the value of the location of the bottom at $x = x_0$. Then the kinematic boundary condition for the bottom surface (3.2a) is not valid at $x = x_0$. However, the conservation law of mass is still valid across $x = x_0$. In other words, here the flow flux Q keeps constant across $x = x_0$. Consequently, we can obtain that

$$\| Q \|_{x=x_0} = 0, \tag{3.12}$$

where in the above formula the double bars, $\| \cdot \|$, indicates the magnitude of the jump defined by

$$\| f \|_{x=x_0} = f|_{x=x_0^+} - f|_{x=x_0^-} . \tag{3.13}$$

Making use of (3.11), we obtain finally

$$\left\| \sum_{n=0}^{K} \frac{1}{n+1} \left[u_n (\beta^{n+1} - \alpha^{n+1}) \right] \right\|_{x=x_0} = 0. \tag{3.14}$$

Before consideration of the conservation law of momentum, we derive some relations from the kinematic boundary conditions (3.2a, b), which will prove to be very useful to simplify the Green-Naghdi governing equations later, especially when Green-Naghdi Level I theory is applied.

Inserting (3.4) into (3.2a, b) respectively, we have

$$v_0 + \sum_{n=1}^{K}\left(-\frac{1}{n} u_{n-1,x}\, \alpha^n \right) = \sum_{n=0}^{K} u_n\, \alpha^n\, \alpha_x \,. \tag{3.15}$$

$$v_0 + \sum_{n=1}^{K}\left(-\frac{1}{n} u_{n-1,x}\, \beta^n \right) = \sum_{n=0}^{K} u_n\, \beta^n\, \beta_x \,. \tag{3.16}$$

Making use of (3.3a) and applying same process as we did in (3.6), from (3.15), we obtain

$$v_0 = \sum_{n=0}^{K} \frac{1}{n+1} \left(u_n\, \alpha^{n+1} \right)_x \,. \tag{3.17}$$

And similarly, (3.16) becomes

$$v_0 = \sum_{n=0}^{K} \frac{1}{n+1} \left(u_n\, \beta^{n+1} \right)_x \,. \tag{3.18}$$

Adding (3.17) and (3.18) together, we also obtain

$$v_0 = \frac{1}{2} \sum_{n=0}^{K} \frac{1}{n+1} \left(u_n\, \alpha^{n+1} + u_n\, \beta^{n+1} \right)_x \,. \tag{3.19}$$

This equation will prove to be very useful to eliminate the variable v_0 from the governing equations.

Now we return to the conservation law of momentum. For steady, two-dimensional flow, in the Green-Naghdi theory the conservation law of the horizontal and vertical momentum states that

$$\sum_{m=0}^{K}\left\{\sum_{r=0}^{K}\rho u_{m,x}u_r H_{(m+r+n)}+\sum_{r=0}^{K}\rho m u_m v_r H_{(r+n+m-1)}\right\} = \tag{3.20}$$

$$-P_{n,x}+\hat{p}\beta^n\beta_x-\bar{p}\alpha^n\alpha_x$$

$$\sum_{m=0}^{K}\left\{\sum_{r=0}^{K}\rho v_{m,x}u_r H_{(m+r+n)}+\sum_{r=0}^{K}\rho m v_m v_r H_{(r+n+m-1)}\right\} = . \tag{3.21}$$

$$P'_n-\rho g H_n-\hat{p}\beta^n+\bar{p}\alpha^n$$

for n = 0, …. K.

Integrating the above formulae between $x=x_0-\delta$ and $x=x_0+\delta$, and taking the limit as $\delta\to 0$, we obtain

$$\lim_{\delta\to 0}\int_{x=x_0-\delta}^{x=x_0+\delta}\sum_{m=0}^{K}\left\{\sum_{r=0}^{K}\rho u_{m,x}u_r H_{(m+r+n)}+\sum_{r=0}^{K}\rho m u_m v_r H_{(r+n+m-1)}\right\}dx+\left\| P_n \right\|_{x=x_0} =$$

$$\lim_{\delta\to 0}\int_{x=x_0-\delta}^{x=x_0+\delta}(\hat{p}\beta^n\beta_x-\bar{p}\alpha^n\alpha_x)dx \tag{3.22}$$

$$\lim_{\delta\to 0}\int_{x=x_0-\delta}^{x=x_0+\delta}\sum_{m=0}^{K}\left\{\sum_{r=0}^{K}\rho v_{m,x}u_r H_{(m+r+n)}+\sum_{r=0}^{K}\rho m v_m v_r H_{(r+n+m-1)}\right\}dx =$$

$$\lim_{\delta\to 0}\int_{x=x_0-\delta}^{x=x_0+\delta}(P'_n-\rho g H_n-\hat{p}\beta^n+\bar{p}\alpha^n)dx \tag{3.23}$$

n = 0, 1, …. K.

To this point, we have obtained jump conditions (3.14) derived from the conservation of mass, and (3.22) and (3.23), which are derived directly from the conservation law of momentum. These jump conditions (3.14), (3.22) and (3.23) are general formula that can be further simplified once the level of the Green-Naghdi theory is set.

Before further consideration of the jump conditions is applied in the context of a particular application in later chapters, we need to emphasize that the derivation of the jump conditions above is carried out in Eulerian frame, and the so-called "restricted theory" is not applied. These jump conditions seem different from what Green & Naghdi obtained, however, they are equivalent in principle, especially once the level of the Green-Naghdi theory is set, as we will find out later.

§3.2 Jump conditions for Green-Naghdi Level I theory

Now we proceed to obtain the jump conditions corresponding to Green-Naghdi Level I theory by specialization of the general results obtained in the above section. We apply the jump conditions to the location $x = x_0$, where discontinuities may exist such as the joint point between different regions. When the index level K=1, then (3.14) becomes

$$\left\| [u_0(\beta-\alpha)]+\frac{1}{2}[u_1(\beta^2-\alpha^2)] \right\|_{x=x_0} = 0. \qquad (3.24)$$

This is the jump condition associated with the conservation law of mass.

If the restricted theory is applied, that is, $u_1 = 0$ instead of $u_{1,x} = 0$, then we can obtain a very simple formula

$$\| u_0(\beta - \alpha) \|_{x=x_0} = 0. \tag{3.25}$$

For later convenience, we define

$$Q = u_0(\beta - \alpha). \tag{3.26}$$

Q corresponds the flow flux that, by continuity, is independent of x. Thus (3.25) can be rewritten

$$\| Q \|_{x=x_0} = 0, \tag{3.27}$$

which states that the flow flux keeps constant across the discontinuity interface.

Now we turn to the jump conditions derived from the law of conservation of momentum. The simplification of these jump conditions is more difficult and tedious and some manipulations are required. First we consider the conservation law of horizontal momentum. When K=1 and n=0, (3.22) becomes

$$\lim_{\delta \to 0} \int_{x_0 - \delta}^{x_0 + \delta} \rho u_{0x} u_0 (\beta - \alpha) dx + \| P_0 \|_{x=x_0} = \lim_{\delta \to 0} \int_{x=x_0 - \delta}^{x=x_0 + \delta} (\hat{p} \beta_x - \bar{p} \alpha_x) dx. \tag{3.28}$$

where the restricted theory and (3.18) have been used.

Note that since the flow rate is constant at the joint point, that is, $u_0(\beta - \alpha) \equiv Q$ everywhere, then (3.28) can be further simplified. With the help of (3.27), we can integrate the left-hand side of (3.28) as follows:

$$\text{LHS of (3.28)} = \lim_{\delta \to 0} \int_{x_0 - \delta}^{x_0 + \delta} \rho u_{0x} u_0 (\beta - \alpha) dx + \| P_0 \|_{x = x_0}$$

$$= \lim_{\delta \to 0} \int_{x_0 - \delta}^{x_0 + \delta} \rho u_{0x} Q dx + \| P_0 \|_{x = x_0}$$

$$= \| \rho Q u_0 \|_{x = x_0} + \| P_0 \|_{x = x_0}$$

Then we can arrive at

$$\| \rho Q u_0 + P_0 \| = \lim_{\delta \to 0} \int_{x = x_0 - \delta}^{x = x_0 - \delta} (\hat{p} \beta_x - \bar{p} \alpha_x) dx . \qquad (3.29)$$

The right-hand side of (3.29) still contains the integral form and the limit, but they cannot be treated with right now because they are dependent on the jump conditions at $x = x_0$.

In the same way, when K=1, n=1, (3.22) becomes

$$\lim_{\delta \to 0} \int_{x_0 - \delta}^{x_0 + \delta} \frac{1}{2} \rho Q u_{0x} (\beta + \alpha) dx + \| P_1 \|_{x = x_0} = \lim_{\delta \to 0} \int_{x = x_0 - \delta}^{x = x_0 + \delta} (\hat{p} \beta \beta_x - \bar{p} \alpha \alpha_x) dx . \quad (3.30)$$

Unfortunately, the left-hand side of this equation cannot be integrated.

Now let us consider the vertical component of conservation law of momentum. Before further proceeding, we define two new variables as

$$\varphi = \beta - \alpha ,$$

$$\xi = \frac{1}{2}(\beta + \alpha), \qquad (3.31a, b)$$

where, φ denotes the thickness of the fluid sheet, and ξ the center line of the fluid. On occasion it will be convenient to replace the variables α and β with the alternate representation ξ and φ.

In Green-Naghdi Level-I model, the kinematic boundary conditions on the top and bottom material surfaces are assumed to be

$$v_0 + v_1\alpha = u_0\alpha_x;$$
$$v_0 + v_1\beta = u_0\beta_x. \qquad (3.32a, b)$$

Adding (3.32a) and (3.32b) together and applying the definition (3.31b), we obtain

$$v_0 + v_1\xi = u_0\xi_x. \qquad (3.33)$$

Recall that $v_1 = -u_{0x}$. Using this we obtain a useful relation

$$v_0 = (u_0\,\xi)_x. \qquad (3.34)$$

Actually, (3.34) can be obtained directly from (3.19) when K = 1, and the restricted theory is used.

Let us turn back to the vertical component of the conservation law of momentum. When K=1 and n=0, (3.23) becomes

$$\lim_{\delta\to 0}\int_{x_0-\delta}^{x_0+\delta}\left[\rho v_{0,x}u_0(\beta-\alpha)+\rho v_{1,x}u_0\frac{1}{2}(\beta^2-\alpha^2)+\rho v_1 v_0(\beta-\alpha)+\rho v_1 v_1\frac{1}{2}(\beta^2-\alpha^2)\right]dx =$$
$$\lim_{\delta\to 0}\int_{x_0-\delta}^{x_0+\delta}\left[-\hat{p}+\bar{p}-\rho g(\beta-\alpha)\right]dx \qquad (3.35)$$

This equation looks very complicated because there are two levels of summation in (3.23). However, with the results we have obtained to date, we can simplify the left-hand side of (3.35).

With the definition of (3.31a, b), we rewrite (3.35) in terms of new variables φ and ξ as follows:

$$\lim_{\delta\to 0}\int_{x_0-\delta}^{x_0+\delta}\left[\rho v_{0,x} u_0 \varphi+\rho v_{1,x} u_0 \varphi\xi+\rho v_1 v_0 \varphi+\rho v_1 v_1 \varphi\xi\right]dx = \lim_{\delta\to 0}\int_{x_0-\delta}^{x_0+\delta}\left[-\hat{p}+\bar{p}-\rho g \varphi\right]dx \qquad (3.35a)$$

Recall that $u_0(\beta-\alpha)\equiv Q$ everywhere, that is, $u_0\varphi\equiv Q$. Using this, we can further simplify the left-hand side of (3.35a),

$$\text{LHS of (3.35a)} = \lim_{\delta\to 0}\int_{x_0-\delta}^{x_0+\delta}\left[\rho v_{0,x} Q+\rho v_{1,x} Q\xi+\rho v_1\,\varphi(v_0+v_1\xi)\right]dx$$
$$= \lim_{\delta\to 0}\int_{x_0-\delta}^{x_0+\delta}\left[\rho Q v_{0,x}+\rho Q v_{1,x}\xi+\rho v_1\,\varphi u_0\xi_x\right]dx$$

where (3.33) has been used.

Actually, with the help of (3.27) and (3.33), we can integrate the above expression as follows:

$$\text{LHS of (3.35a)} = \lim_{\delta \to 0} \int_{x_0 - \delta}^{x_0 + \delta} \left[\rho Q v_{0,x} + \rho Q (v_{1,x} \xi + \rho v_1 \xi_x) \right] dx$$

$$= \lim_{\delta \to 0} \int_{x_0 - \delta}^{x_0 + \delta} \left[\rho Q v_{0,x} + \rho Q (v_1 \xi)_x \right] dx$$

$$= \lim_{\delta \to 0} \int_{x_0 - \delta}^{x_0 + \delta} \left\{ \rho Q \left[v_{0,x} + (v_1 \xi)_x \right] \right\} dx$$

$$= \lim_{\delta \to 0} \int_{x_0 - \delta}^{x_0 + \delta} \left\{ \rho Q \left[u_0 \xi_x \right]_x \right\} dx$$

$$= \left\| \rho Q u_0 \xi_x \right\|_{x = x_0}$$

where, (3.27) and (3.33) have been used again.

Finally, (3.35) becomes

$$\left\| \rho Q u_0 \xi_x \right\|_{x = x_0} = \lim_{\delta \to 0} \int_{x_0 - \delta}^{x_0 + \delta} \left[-\hat{p} + \bar{p} - \rho g \varphi \right] dx . \qquad (3.36)$$

There still exists a limit in the right hand side of (3.36). This limit and the integral cannot be handled here, because they depend on the nature of the jump of the variables at the joint interface.

When K=1 and n=1, we have already obtained the jump condition (3.30), which is derived from the horizontal momentum. With the definition (3.31a, b), we rewrite (3.30) as

$$\lim_{\delta \to 0} \int_{x_0 - \delta}^{x_0 + \delta} \left[\rho Q u_{0,x} \xi \right] dx + \left\| P_1 \right\|_{x = x_0} = \lim_{\delta \to 0} \int_{x_0 - \delta}^{x_0 + \delta} \left(\hat{p} \beta \beta_x - \bar{p} \alpha \alpha_x \right) dx : \qquad (3.37)$$

When K=1 and n=1, (3.23) becomes

$$\lim_{\delta\to 0}\int_{x_0-\delta}^{x_0+\delta}\left[\rho v_{0,x}u_0\frac{1}{2}(\beta^2-\alpha^2)+\rho v_{1,x}u_0\frac{1}{3}(\beta^3-\alpha^3)+\rho v_1 v_0\frac{1}{2}(\beta^2-\alpha^2)+\rho v_1 v_1\frac{1}{3}(\beta^3-\alpha^3)\right]dx$$

$$=\lim_{\delta\to 0}\int_{x_0-\delta}^{x_0+\delta}\left[P'_1-\rho g\frac{1}{2}(\beta^2-\alpha^2)-\hat{p}\beta+\bar{p}\alpha\right]dx \qquad (3.38)$$

This equation cannot be integrated. However, we can simplify it to certain extent.

With the help of (3.31a, b), (3.38) can be rewritten as

$$\lim_{\delta\to 0}\int_{x_0-\delta}^{x_0+\delta}\left[\rho v_{0,x}u_0\varphi\xi+\rho v_{1,x}u_0\left(\frac{\varphi^3}{12}+\varphi\xi^2\right)+\rho v_1 v_0\varphi\xi+\rho v_1 v_1\left(\frac{\varphi^3}{12}+\varphi\xi^2\right)\right]dx$$

$$=\lim_{\delta\to 0}\int_{x_0-\delta}^{x_0+\delta}\left[P'_1-\rho g\varphi\xi-\hat{p}\beta+\bar{p}\alpha\right]dx \qquad (3.39)$$

Using $u_0\varphi \equiv Q$, the left-hand side of (3.39) can be simplified:

$$\text{LHS of (3.39)}=\lim_{\delta\to 0}\int_{x_0-\delta}^{x_0+\delta}\rho\left[v_{0,x}u_0\varphi\xi+\frac{\varphi^3}{12}v_{1,x}u_0+v_{1,x}u_0\varphi\xi^2+v_1v_0\varphi\xi+\frac{\varphi^3}{12}v_1^2+v_1^2\varphi\xi^2\right]dx$$

$$=\lim_{\delta\to 0}\int_{x_0-\delta}^{x_0+\delta}\rho\left[Qv_{0,x}\xi+\frac{\varphi^2}{12}Qv_{1,x}+\frac{\varphi^3}{12}v_1^2+Qv_{1,x}\xi^2+v_1\varphi\xi(v_0+v_1\xi)\right]dx$$

With the help of (3.33), the above expression becomes

$$\text{LHS of (3.39)}=\lim_{\delta\to 0}\int_{x_0-\delta}^{x_0+\delta}\rho\left[\frac{\varphi^2}{12}Qv_{1,x}+\frac{\varphi^3}{12}v_1^2+Qv_{0,x}\xi+Qv_{1,x}\xi^2+v_1\varphi\xi u_0\xi_x\right]dx$$

$$=\lim_{\delta\to 0}\int_{x_0-\delta}^{x_0+\delta}\rho\left[\frac{\varphi^2}{12}Qv_{1,x}+\frac{\varphi^3}{12}v_1^2+Qv_{0,x}\xi+Q\xi(v_{1,x}\xi+v_1\xi_x)\right]dx$$

$$=\lim_{\delta\to 0}\int_{x_0-\delta}^{x_0+\delta}\rho\left[\frac{\varphi^2}{12}Qv_{1,x}+\frac{\varphi^3}{12}v_1^2+Qv_{0,x}\xi+Q\xi(v_1\xi)_x\right]dx$$

After re-arranging the above expression, we have

$$\begin{aligned} \text{LHS of (3.39)} &= \lim_{\delta \to 0} \int_{x_0-\delta}^{x_0+\delta} \rho \left[\frac{\varphi^2}{12} Q v_{1,x} + \frac{\varphi^3}{12} v_1^2 + Q\xi (v_0 + v_1 \xi)_x \right] dx \\ &= \lim_{\delta \to 0} \int_{x_0-\delta}^{x_0+\delta} \rho \left[\frac{\varphi^2}{12} Q v_{1,x} + \frac{\varphi^3}{12} v_1^2 + Q\xi (u_0 \xi_x)_x \right] dx \end{aligned} \quad . \qquad (3.40)$$

where (3.33) has been used again.

Since $v_1 = -u_{0,x}$, the left-hand side of (3.39)

$$\text{LHS of (3.39)} = \lim_{\delta \to 0} \int_{x_0-\delta}^{x_0+\delta} \rho \left[Q\xi (u_0 \xi_x)_x - \frac{\varphi^2}{12} Q u_{0xx} + \frac{\varphi^3}{12} u_{0x}^2 \right] dx . \qquad (3.41)$$

Before further simplifying (3.41), we need to derive a particular relation. We differentiate the equation $u_0 \varphi = Q$ with respect to x and obtain

$$u_{0x} \varphi + u_0 \varphi_x = 0 . \qquad (3.42)$$

Thus,

$$u_{0x} = -\frac{Q\varphi_x}{\varphi^2} . \qquad (3.43)$$

Differentiating (3.43) again, we obtain

$$u_{0xx} = -\frac{Q\varphi_{xx}}{\varphi^2} + 2Q\frac{\varphi_x^2}{\varphi^3} . \qquad (3.44)$$

With these results, we can further simplify equation (3.39). Inserting (3.43) and (3.44) into (3.41), we have

$$\begin{aligned}
\text{LHS of (3.39)} &= \lim_{\delta\to 0}\int_{x_0-\delta}^{x_0+\delta}\rho\left[Q\xi(u_0\xi_x)_x - \frac{\varphi^2 Q}{12}\left(-\frac{Q\varphi_{xx}}{\varphi^2}+2Q\frac{\varphi_x^2}{\varphi^3}\right)+\frac{\varphi^3}{12}\left(-\frac{Q\varphi_x}{\varphi^2}\right)^2\right]dx \\
&= \lim_{\delta\to 0}\int_{x_0-\delta}^{x_0+\delta}\rho\left[Q\xi(u_0\xi_x)_x + \frac{Q^2}{12}\varphi_{xx} - \frac{1}{6}Q^2\frac{\varphi_x^2}{\varphi}+\frac{1}{12}\frac{Q^2\varphi_x^2}{\varphi}\right]dx \\
&= \lim_{\delta\to 0}\int_{x_0-\delta}^{x_0+\delta}\rho\left[Q\xi(u_0\xi_x)_x + \frac{Q^2}{12}\varphi_{xx} - \frac{1}{12}\frac{Q^2\varphi_x^2}{\varphi}\right]dx \\
&= \lim_{\delta\to 0}\int_{x_0-\delta}^{x_0+\delta}\rho\left[Q\xi(u_0\xi_x)_x + \frac{1}{12}Q^2\varphi\left(\frac{\varphi_{xx}}{\varphi}-\frac{\varphi_x^2}{\varphi^2}\right)\right]dx \\
&= \lim_{\delta\to 0}\int_{x_0-\delta}^{x_0+\delta}\rho\left[Q\xi(u_0\xi_x)_x + \frac{1}{12}Q^2\varphi\left(\frac{\varphi_x}{\varphi}\right)_x\right]dx
\end{aligned}$$

Recall the definition of the integral pressure P_n, as well as the kinematic assumption of velocity, that is, $\lambda_n(\zeta)=\zeta^n$, then we have

$$P'_n = n P_{n-1}, \qquad \text{for } n=1, \ldots, K. \tag{3.45}$$

where, the prime denotes the derivation with respect to ζ.

Finally, we obtain

$$\lim_{\delta\to 0}\int_{x_0-\delta}^{x_0+\delta}\left[\rho Q\xi(u_0\xi_x)_x + \frac{1}{12}\rho Q^2\varphi\left(\frac{\varphi_x}{\varphi}\right)_x\right]dx = \lim_{\delta\to 0}\int_{x_0-\delta}^{x_0+\delta}\left[P_0 - \rho g\varphi\xi - \hat{p}\beta + \bar{p}\alpha\right]dx . \tag{3.46}$$

Now we have completed the derivation of jump conditions for Green-Naghdi Level-I theory, that is, (3.27), (3.29), (3.36), (3.37) and (3.46). In the similar way, we can obtain

jump conditions for any level of Green-Naghdi theory, although the formulae are very complicated for higher levels.

We need to point out that although the momentum equations and energy are equivalent under our assumption that the fluid is inviscid and incompressible, sometimes it is more convenient to use energy equation rather than momentum equations to obtain jump conditions. The reason is that due to certain discontinuity, the jump of momentum across the joint interface is unknown a priori, but the mechanical energy may keep constant across the discontinuous point. We will not derive the general form of energy equation for Green-Naghdi theory in this chapter, instead, we will derive them for particular level of Green-Naghdi model as we will seen in later chapters.

We record below the jump conditions for Green-Naghdi Level I theory since they will often be used in the following chapters.

$$\| u_0(\beta-\alpha) \|_{x=x_0} = 0 : \text{Or} \| Q \|_{x=x_0} = 0 :$$

$$\| \rho Q u_0 + P_0 \| = \lim_{\delta\to 0} \int_{x_0-\delta}^{x_0+\delta} (\hat{p}\,\beta_x - \bar{p}\,\alpha_x)dx :$$

$$\| \rho Q u_0 \xi_x \|_{x=x_0} = \lim_{\delta\to 0} \int_{x_0-\delta}^{x_0+\delta} [-\hat{p} + \bar{p} - \rho g \varphi]dx :$$

$$\lim_{\delta\to 0} \int_{x_0-\delta}^{x_0+\delta} [\rho Q u_{0,x}\,\xi]dx + \| P_1 \|_{x=x_0} = \lim_{\delta\to 0} \int_{x_0-\delta}^{x_0+\delta} (\hat{p}\beta\beta_x - \bar{p}\alpha\alpha_x)dx :$$

$$\lim_{\delta\to 0} \int_{x_0-\delta}^{x_0+\delta} \left[\rho Q \xi (u_0 \xi_x)_x + \frac{1}{12}\rho Q^2 \varphi \left(\frac{\varphi_x}{\varphi} \right)_x \right] dx = \lim_{\delta\to 0} \int_{x_0-\delta}^{x_0+\delta} [P_0 - \rho g \varphi \xi - \hat{p}\beta + \bar{p}\alpha]dx .$$

It is of interest to provide a direct comparison between the jump conditions we obtained here and those obtained by Green & Naghdi (1987). First let us list their results here. The jump conditions Green & Naghdi obtained for Level I theory are equations (4.15), (4.16), (4.17), (4.18), (4.19) in their paper:

$$\|k\| = 0, \tag{4.15}$$

$$\|\rho^* k u\| = -\|p\| + F_1, \tag{4.16}$$

$$\left\|\tfrac{1}{2}\rho^* k \phi \omega\right\| = F_3, \tag{4.17}$$

$$\left\|\tfrac{1}{3}\rho^* k \phi^2 \omega\right\| - \tfrac{1}{3}\lim_{\delta\to 0}\int_{x_0-\delta}^{x_0+\delta}\rho^* \phi^3 \omega^2 dx = L_3, \tag{4.18}$$

$$\left\|\tfrac{1}{2}\rho^* k\{u^2 + \tfrac{1}{3}\phi^2\omega^2 + g\phi\}\right\| = \|-pu\| - \Phi, \tag{4.19}$$

where,

$$F_1 = \lim_{\delta\to 0}\int_{x_0-\delta}^{x_0+\delta}\hat{p}\phi' dx,$$

$$F_3 = -\lim_{\delta\to 0}\int_{x_0-\delta}^{x_0+\delta}(\hat{p}-\bar{p})dx, \tag{4.20}$$

$$L_3 = -\lim_{\delta\to 0}\int_{x_0-\delta}^{x_0+\delta}\hat{p}\phi dx,$$

and Φ is the rate of energy dissipation.

We need to point out that (4.18) and (4.19) are derived from the law of conservation of moment of momentum and the law of conservation of energy, respectively. Since we

do not use them here, we will ignore these two jump conditions during comparison. Before proceeding further, we introduce the following definition:

$$F_1 = \lim_{\delta \to 0} \int_{x=x_0-\delta}^{x=x_0+\delta} (\hat{p}\,\beta_x - \bar{p}\,\alpha_x)dx\,. \tag{3.47}$$

$$F_3 = \lim_{\delta \to 0} \int_{x_0-\delta}^{x_0+\delta} [-\hat{p} + \bar{p} - \rho g \varphi]dx\,. \tag{3.48}$$

Then the jump conditions (3.29) and (3.36) become

$$\| \rho Q u_0 + P_0 \|_{x=x_0} = F_1\text{, and} \tag{3.49}$$

$$\| \rho Q u_0 \xi_x \|_{x=x_0} = F_3\text{, respectively.} \tag{3.50}$$

Now let us compare our results with those of Green & Naghdi. Taking into consideration the different set of notations adopted, we can easily find that (3.27) and (3.49) are exactly same as (4.15) and (4.16) of Green & Naghdi respectively. (3.50) looks different from (4.17) of Green & Naghdi, but recall the definition of ω in Green & Naghdi's paper:

$$\omega = k\phi'/\phi^2\,, \tag{4.14}$$

where the prime denotes the derivative with respect to x. Plugging (4.14) into (4.17) and keeping in mind that the central line of the fluid sheet is one half of the thickness of the fluid sheet when the bottom surface is flat, we can finally show the equivalence between (3.50) and (4.17) of Green & Naghdi.

After brief comparison between our results and those of Green & Naghdi, we find that the jump conditions obtained here are equivalent to what Green & Naghdi obtained, and both sets of jump conditions are based on Eulerian frame.

Now that we have obtained both the Green-Naghdi governing equations and the corresponding jump conditions, in the following chapters we will demonstrate the application of this method to a variety of problems.

Chapter 4

Steady Inviscid Free Waterfall

This chapter is concerned with two-dimensional motion of an incompressible, inviscid fluid in a waterfall under the action of gravity. The general Green-Naghdi governing equations and the associated jump conditions are specialized for this situation. The equations and jump conditions obtained will form the basis for the investigation of the flow through a sluice gate and the weir flow in the following two chapters. Before proceeding further, we summarize the problem in the following paragraph for later reference.

Consider the steady two-dimensional flow of an inviscid, incompressible fluid under the action of gravity over a cliff leading to a free waterfall (as shown in Fig. 4.1). The effect of surface tension is assumed negligible. As shown in Fig. 4.1, we identify two distinct regions of flow are associated with this problem: the upstream region (region I) characterized by a free top surface and a smooth bottom, and the downstream region (labeled as III) where both the top and bottom surfaces of the fluid are free. Far upstream the fluid is assumed to flow as a uniform stream, while downstream the fluid falls freely under the action of gravity. Of particular interest in analyzing the problem is the prediction of the fluid height along the whole flow region and the determination of the downstream solution, i.e., the location of the free surfaces and the distribution of the vertical thickness of the jet.

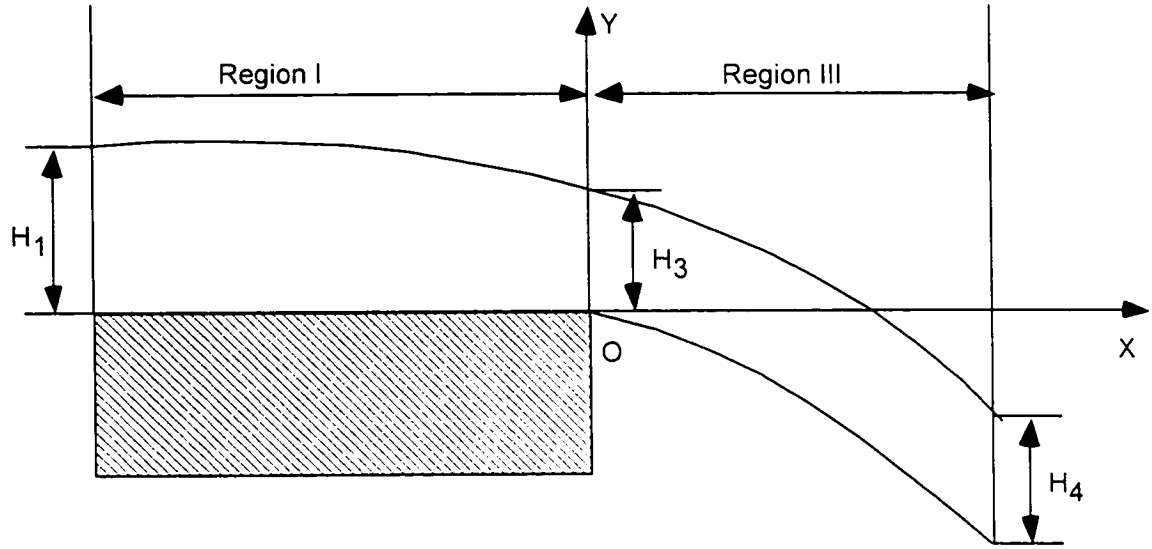

Fig. 4.1.1 Illustration of waterfall over a flat bottom

This problem seems very simple at the first glance. However, the unknown free surface and unknown velocity of particles on the free surface compose the rather complex nature of the flow. Moreover, in the downstream region, both top and bottom surfaces are free and unknown. As a result, although this problem is well-studied, the exact analytical solution of the problem has not been possible so far with the use of the three-dimensional equations of an incompressible, inviscid fluid. Instead, numerical procedures or asymptotic techniques are applied by previous researchers. Keller & Weitz (1957) have developed a series in powers of the jet thickness and obtained a solution for the region downstream of the fluid bed only. Clarke (1965) has solved the problem of waterfall for large Froude numbers with the use of matched asymptotic techniques and by utilizing an asymptotic expansion based on the reciprocal of Froude number in the upstream region and another expansion based on the thinness of the fall in the downstream region. A further discussion of the problem of overfall is included in a paper of Keller & Geer (1973), who consider asymptotic solutions of a class of problems based on the

slenderness ratio of the stream. An early numerical solution of the problem, employing relaxation, was given by Southwell & Vaisey (1946); and further results, again by relaxation method, were obtained by Markland (1965). Chow & Han (1979) obtained a numerical solution of the problem via the three-dimensional equations of an inviscid, incompressible fluid along with hodograph transformation. Later on, numerical solutions have been obtained by Smith and Abd-El-Malek (1983), Vanden-Broeck and Keller (1987), Dias et al. (1988) and Dias and Tuck (1991).

The first analytical solution of the waterfall problem was obtain by Naghdi & Rubin (1981), who employed a special case of the system of differential equation of a Cosserat (or a directed) fluid sheet, developed by Green & Naghdi (1976). The analytical solution, employing Green-Naghdi method, is quite simple, contrasted with the fairly intricate numerical work of Chow & Han (1979) or the asymptotic solution of Clarke (1965) which is valid only for large Froude numbers. Moreover, it proved that the upstream flow cannot be subcritical, which confirmed a speculative remark made by Chow & Han to the effect that 'the existence of subcritical case is doubtful in steady inviscid flow'.

In the paper of Naghdi & Rubin (1981), they gave the solution only for the waterfall problem with a flat bed. Actually, an analytical solution can be obtained only under this condition, as we will see later. Moreover, the Green-Naghdi governing equations they used are based on Lagrangian frame. In this chapter, we will use the governing equation and jump conditions, derived in previous chapters based on Eulerian frame, to solve the free waterfall problem with a smooth bottom, rather than the flat bottom. In addition, the

free waterfall problem with non-smooth a bottom is discussed and a simple case is illustrated.

§4.1 General solution through Green-Naghdi Level-I theory

From the statement of problem, we know that there are two distinct regions with different characters (see Fig. 4.1.1): the upstream region I associated with a unknown free surface and a smooth bottom; and the downstream region III bounded by two free surfaces, both of which are unknown. Recall that we have obtained a Green-Naghdi governing system in Chapter 2 for an unsteady, two-dimensional flow. Now we will specialize the system with the use of particular features associated with each region.

4.1.1 Governing equations for region I (flow over a smooth bottom)

First we consider the upstream region, that is, region I with a unknown free surface and a given smooth bottom. The pressure everywhere at the top free surface should be equal to the atmospheric pressure, which is assumed to be constant. Without loss of generality, we have the atmospheric pressure to be zero, that is, $\tilde{p} \equiv 0$ everywhere. For Green-Naghdi Level-I theory, the restricted theory states that

$$u_1 = 0. \tag{4.1.1}$$

From the continuity equation, we have

$$u_{0,x} + v_1 = 0. \tag{4.1.2}$$

Since the flow is steady, with the help of the restricted theory, the kinematic boundary conditions on the top and bottom surfaces become

$$v_0 + v_1\alpha = u_0\alpha_x; \tag{4.1.3}$$

$$v_0 + v_1\beta = u_0\beta_x. \tag{4.1.4}$$

For steady, two-dimensional flow, the governing equations (2.27a, c, d) derived from the conservation law of momentum become

$$\phi_0 u_0 u_{0x} = \frac{1}{\rho}(-P_{0x} - \bar{p}\alpha_x); \tag{4.1.5}$$

$$\phi_0 u_0 v_{0x} + \phi_0 v_0 v_1 + \phi_1 u_0 v_{1x} + \phi_1 v_1 v_1 = \frac{1}{\rho}(-\rho g\phi_0 + \bar{p}); \tag{4.1.6}$$

$$\phi_1 u_0 v_{0x} + \phi_1 v_0 v_1 + \phi_2 u_0 v_{1x} + \phi_2 v_1 v_1 = \frac{1}{\rho}(P_0 - \rho g\phi_1 + \bar{p}\alpha), \tag{4.1.7}$$

where the restricted theory and $\hat{p} \equiv 0$ have been used. And we do not use equation (2.27b) since the variable P_1 only appears in this equation. This implies that P_1 is dependent on other variables.

Since the bottom surface $\alpha(x)$ is given beforehand, then equations (4.1.2)-(4.1.7) form a closed governing system with six differential equations and six variables, that is, β, u_0, v_0, v_1, P_0 and $\bar{p}$. Once appropriate boundary conditions are applied, as discussed in section 4.1.4, these governing equations for region I can be solved.

After observing these governing equations obtained above, we find that they are coupled, quasi-linear first order differential equations, which can be solved numerically. However, in this particular case and with some manipulations, we can further simplify this governing system. Under certain condition, we can even obtain the analytical solutions for this governing system. Recall that for Green-Naghdi Level-I theory, the statement that the flow rate is constant everywhere is

$$u_0(\beta-\alpha)\equiv Q, \tag{4.1.8}$$

where Q denotes the constant rate of fluid flow.

Since the bottom is given, we can replace the top surface variable β with the variable ϕ_0, which stands for the thickness of the fluid according to its definition. Then (4.1.8) becomes

$$u_0\phi_0\equiv Q. \tag{4.1.9}$$

From (4.1.3), with the help of (4.1.2), we can obtain

$$v_0=(u_0\alpha)_x. \tag{4.1.10}$$

Inserting (4.1.2), (4.1.9) and (4.1.10) into (4.1.5) to eliminate u_0, v_0, v_1, and using (4.1.6) and (4.1.7) to replace P_0 and $\bar{p}$, finally we obtain after a tedious derivation a second-order differential equation in ϕ_0 only:

$$\frac{\phi_{0xx}}{\phi_0}-\frac{1}{2}\frac{\phi_{0x}^{2}}{\phi_0^{2}}+\frac{3}{2}(1+\alpha_x^{2})\frac{1}{\phi_0^{2}}+\frac{3g}{Q^2}(\phi_0+\alpha)+\frac{3}{2}\frac{\alpha_{xx}}{\phi_0}-3\frac{R_1}{Q^2}=0. \qquad (4.1.11)$$

where R_1 is integral constants and can be determined by appropriate upstream boundary conditions.

Once equation (4.1.11) is solved, from (4.1.7) and (4.1.6) we can obtain P_0 and $\bar{p}$ through the following equations:

(4.1.12)

$$\frac{P_0}{\rho}=\phi_0\left[R_1-\frac{1}{2}g\phi_0-g\alpha-\frac{1}{2}\frac{Q^2}{\phi_0^{2}}-\frac{1}{2}Q^2\frac{\alpha_x^{2}}{\phi_0^{2}}-\frac{1}{2}Q^2\frac{\alpha_x\phi_{0x}}{\phi_0^{2}}-\frac{1}{6}Q^2\frac{\phi_{0x}^{2}}{\phi_0^{2}}\right]$$

$$\frac{\bar{p}}{\rho}=g\phi_0-\frac{Q^2\phi_{0x}^{2}}{2\phi_0^{2}}-\frac{Q^2\alpha_x\phi_x}{\phi_0^{2}}+\frac{Q^2\phi_{0xx}}{2\phi_0}+\frac{Q^2\alpha_{xx}}{\phi_0}. \qquad (4.1.13)$$

respectively.

To this point, we have obtained the very simple governing system for region I of the waterfall problem, which includes (4.11), (4.12) and (4.13). If appropriate boundary conditions are specified, (4.1.11) can be solved so to determine ϕ_0, the distribution of the thickness of fluid in region I. By means of (4.1.9), (4.1.10), (4.1.12) and (4.1.13), u_0, v_0, P_0 and $\bar{p}$ can be obtained respectively.

When we derived the governing equations, we emphasized that the bottom should be smooth. In (4.1.11), the second-order derivative of the bottom surface appears. Hence, for Green-Naghdi Level I theory, we can define that the bottom is smooth enough if at least

the bottom surface is continuous through the second derivative. If under certain circumstance, this requirement may not be met, then jump conditions must be applied at the point where discontinuity appears. We will discuss this problem in some detail later.

Now let us discuss a particular case, that is, the bottom is flat. Without loss of generality, in this case we can set up the coordinate system so that the bottom surface function $\alpha(x)=0$ in region I. Then α can be eliminated from the solution equations (4.1.11), (4.1.12) and (4.1.13) and the corresponding simplified equations are as follows:

$$\frac{\phi_{0xx}}{\phi_0}-\frac{1}{2}\frac{\phi_{0x}^{2}}{\phi_0^{2}}+\frac{3}{2}\frac{1}{\phi_0^{2}}+\frac{3g}{Q^{2}}\phi_0-3\frac{R_1}{Q^{2}}=0; \tag{4.1.14}$$

$$\frac{P_0}{\rho}=\phi_0\left[R_1-\frac{1}{2}g\phi_0-\frac{1}{2}\frac{Q^{2}}{\phi_0^{2}}-\frac{1}{6}Q^{2}\frac{\phi_{0x}^{2}}{\phi_0^{2}}\right]; \tag{4.1.15}$$

$$\frac{\bar{p}}{\rho}=g\phi_0-\frac{Q^{2}\phi_{0x}^{2}}{2\phi_0^{2}}+\frac{Q^{2}\phi_{0xx}}{2\phi_0}\ . \tag{4.1.16}$$

These equations derived here are different from what Naghdi & Rubin (1981) used when they dealt with same problem. However, when same far upstream boundary conditions are employed, we can recover their results by means of these equations, as we will discuss later.

4.1.2 Discussion of the restricted theory

From the derivation of the governing equations, we know that the application of the restricted theory, that is, $u_1 = 0$, simplifies the Green-Naghdi level I governing equations

significantly. When Shields first used the restricted theory, he just pointed out that this theory corresponds to a restricted director employed by Green & Naghdi, but did not give out any further reasons. Here in this problem we can see the necessity of the restricted theory and we can even derive the restricted theory from the continuity equation and the far upstream boundary conditions. Recall that in Green-Naghdi Level I theory, the velocity profile is assumed to be

$$u(x,\zeta) = u_0(x) + u_1(x)\zeta;$$
$$v(x,\zeta) = v_0(x) + v_1(x)\zeta. \qquad (4.1.17a, b)$$

In the statement of problem, we have assumed that the flow at far upstream is uniform. Then, we can obtain that at far upstream,

$$u_0(-\infty) = u_{-\infty},$$
$$u_1(-\infty) = 0. \qquad (4.1.18a, b)$$

The continuity equations state that (see equations (4.1.1) and (4.1.2))

$$u_{1,x} = 0,$$
$$u_{0x} + v_1 = 0. \qquad (4.1.19a, b)$$

From equation (4.1.19a) we know that $u_{1,x} = 0$ everywhere, while from (4.1.18b) we know that the far upstream boundary condition for u_1 states that $u_1(-\infty) = 0$. Thus we can deduce that

$$u_1(x) = 0, \text{ everywhere,} \qquad (4.1.20)$$

which is exactly the assumption of the restricted theory.

4.1.3 Governing equations for region III (free waterfall)

Now let us consider the right region, that is, region III bounded by two unknown free surfaces. The pressure at both top and bottom surfaces are equal to the atmospheric pressure. As we did before, without loss of generality, we set the atmospheric pressure be equal to zero. Thus, in region III $\hat{p} \equiv 0$ and $\overline{p} \equiv 0$ everywhere. In Green-Naghdi Level-I theory, the kinematic boundary conditions on the top and bottom surfaces are

$$v_0 + v_1\beta = u_0\beta_x ; \tag{4.1.21}$$

$$v_0 + v_1\alpha = u_0\alpha_x . \tag{4.1.22}$$

where the restricted theory has been applied.

The continuity equation states that

$$u_{0x} + v_1 = 0 . \tag{4.1.23}$$

Taking into account that $\hat{p} \equiv 0$ and $\overline{p} \equiv 0$ everywhere, as well as the restricted theory $u_1(x)=0$, for steady, two-dimensional flow, we can obtain the momentum conservation laws for Green-Naghdi Level I theory:

$$\phi_0 u_0 u_{0x} = -\frac{1}{\rho} P_{0x} ; \tag{4.1.24}$$

$$\phi_0 u_0 v_{0x} + \phi_0 v_0 v_1 + \phi_1 u_0 v_{1x} + \phi_1 v_1 v_1 = -g\phi_0 ; \tag{4.1.25}$$

$$\phi_1 u_0 v_{0x} + \phi_1 v_0 v_1 + \phi_2 u_0 v_{1x} + \phi_2 v_1 v_1 = \frac{1}{\rho}(P_0 - \rho g \phi_1) . \tag{4.1.26}$$

Therefore, a closed governing system has been obtained, which is composed of six coupled, quasi-linear differential equations (4.1.21)-(4.1.26) and six variables α, β, u_0, v_0, v_1 and P_0. With appropriate boundary conditions, this governing system for region III is well posed.

Although the governing equations can be solved numerically, we prefer to obtain the analytical solution if possible. Before proceeding further, we replace α, β with ϕ_0 (which is, as before, the thickness of the fluid) and another variable ψ, which is height of center of the fluid sheet. These are defined as

$$\phi_0 = \beta - \alpha; \tag{4.1.27}$$

$$\psi = \frac{1}{2}(\beta + \alpha). \tag{4.1.28}$$

Subtracting (4.1.21) from (4.1.22) and using (4.1.23), we can derive that (4.1.9) still holds in region III, that is

$$u_0 \phi_0 \equiv Q. \tag{4.1.29}$$

Adding (4.1.21) and (4.1.22) and by means of (4.1.23), we can get

$$v_0 = (u_0 \psi)_x. \tag{4.1.30}$$

Substituting (4.1.23), (4.1.29) and (4.1.30) into (4.1.24), (4.1.25) and (4.1.26) respectively, to eliminate u_0, v_0 and v_1, and replacing α, β with ϕ_0 and ψ, after integrating and multiplying, finally we can obtain

$$\frac{1}{12}Q^2\phi_{0x}^2 = Q^2 - 2S_3\phi_0 + 2R_3\phi_0^2; \tag{4.1.31}$$

$$\frac{P_0}{\rho} = -\frac{Q^2}{\phi_0} + S_3; \tag{4.1.32}$$

$$Q^2\left(\frac{\psi_x}{\phi_0}\right)_x = -g\phi_0. \tag{4.1.33}$$

where R_3 and S_3 are integral constants that can be determined by appropriate boundary conditions. Thus the simplified Green-Naghdi Level I governing equations for region III of the waterfall problem has been obtained, and only three variables are involved, that is, ϕ_0, P_0 and ψ. Once the distribution of the thickness of the fluid is obtained through (4.1.31), P_0 and ψ can be obtained through (4.1.32) and (4.1.33) together with appropriate boundary conditions.

After comparing these results with what Naghdi & Rubin (1981) obtained, we find that (4.1.31), (4.1.32) and (4.1.33) are exactly same as (4.1.2), (4.1.1) and (3.4c) respectively in the paper of Naghdi & Rubin (1981), who used the directed theory with one restricted director.

4.1.4 Boundary conditions

Now that we have obtained the governing equations for regions I and III of the waterfall problem, we need to consider the boundary conditions necessary to solve the governing equations. Since the flow is assumed to be steady, initial conditions are not

needed. Let us first consider the left boundary conditions in region I. Recall that we have assumed that the flow is uniform at the far upstream. then the far left boundary conditions in region I can be described as follows:

$$\begin{aligned} &\text{as } x \to -\infty, \\ &\phi_0 \to H_1,\ \phi_{0x} \to 0,\ u_0 \to U_1,\ P_0 \to \tfrac{1}{2}\rho g H_1^2, \end{aligned} \tag{4.1.34}$$

where H_1 denotes the thickness of the fluid at far upstream. and U_1 denotes the uniform velocity of the flow at far upstream. Both H_1 and U_1 are given beforehand. In addition. we suppose that the bottom is flat at far upstream and is equal to zero. that is. $\alpha = 0$.

As for the right boundary conditions in region III. the only force acting on the fluid after departing from the cliff is the gravity and this force acts only in the vertical direction. As a result. we expect that the horizontal velocity of the fluid will approach a constant. and that the pressure inside the fluid will approach that on the free surfaces. i.e.. atmospheric pressure. Therefore the far right boundary conditions in region III can be described as

$$\begin{aligned} &\text{as } x \to +\infty, \\ &\phi_0 \to H_4,\ \phi_{0x} \to 0,\ u_0 \to U_4,\ P_0 \to 0. \end{aligned} \tag{4.1.35}$$

where H_4 denotes the thickness of the fluid at far downstream. and U_4 the horizontal velocity of the fluid at far downstream. Both of these variables are unknown and need to be determined as a part of the solution. This assumption about the far downstream conditions is same as that of Naghdi & Rubin (1981).

With these boundary conditions, we can determine several integral constants appearing in the governing equations for both regions I and III. First, let us consider region I. Obviously, Q can be determined immediately from (4.1.9), that is,

$$Q = U_1 H_1 . \tag{4.1.36}$$

Usually a non-dimensional number, so called Froude number, is introduced to replace the velocity. Here we define the Froude number as

$$Fr = \frac{U_1}{\sqrt{gH_1}} . \tag{4.1.37}$$

Then we can obtain Q in terms of the thickness of fluid and the given Froude number:

$$Q = Fr\sqrt{gH_1}\, H_1 . \tag{4.1.36a}$$

Then we can determine R_1 in terms of H_1 and Q from equation (4.1.11) since the bottom is flat at far left of region I:

$$R_1 = gH_1 + \frac{1}{2}\frac{Q^2}{H_1^2} . \tag{4.1.38}$$

In the same way, in region III, substituting the boundary conditions (4.1.35) into (4.1.32), we can get S_3 in terms of H_4 and Q:

$$S_3 = \frac{Q^2}{H_4} . \tag{4.1.39}$$

Inserting (4.1.35) and (4.1.39) into (4.1.31), we find R_3 in terms of H_4 and Q:

$$R_3 = \frac{Q^2}{2H_4^2}. \qquad (4.1.40)$$

However, contrary to the integral constants in region I, S_3 and R_3 are still unknown since H_4 is to be determined. Once H_4 is given, both of them can be found. Even so, we still lack sufficient conditions to solve the governing equations in region III. Recall that region I and region III have different characters and thus the governing equations are different. However, both of the solutions of the governing equations must be valid at the junction between region I and III. Therefore, the so-called jump conditions, or matching conditions, must be set up to match the solutions at the junction. In this problem, the constants of integration are also determined by the application of jump conditions, and the jump conditions will provide the conditions to solve the governing equations in Region III.

Before we advance to the jump conditions, we can simplify equation (4.1.31) by means of (4.1.39) and (4.1.40). Substituting (4.1.39) and (4.1.40) into (4.1.31), (4.1.31) yields the following differential equation for the vertical thickness of the fluid:

$$\frac{1}{12} H_4^2 \phi_{0,x}^2 = (\phi_0 - H_4)^2. \qquad (4.1.41)$$

Integrating (4.1.41) and making use of the assumption of far downstream boundary conditions (4.1.35), we arrive at

$$\phi_0 = H_4 + A e^{-Bx}, \qquad (4.1.42)$$

where the constant $B = \frac{2\sqrt{3}}{H_4}$, and A is a constant of integration to be determined as part of the solution. Thus the governing equations for Region III become (4.1.42), (4.1.32) and (4.1.33). Obviously, when the constants in (4.1.42) are determined, what we obtain is an analytical solution for Region III for the waterfall problem.

4.1.5 Jump conditions

As we have pointed out, in order to obtain the constants of integration, as well as a solution which holds throughout the whole flow, connection between two regions must be set up and the solutions in region I and III must be matched at the joint point, say x = 0. We have obtained the general Green-Naghdi jump conditions derived from the integral physical laws. Now we need to apply these general jump conditions to the waterfall problem to link two regions together.

Recall that we have obtained the physical jump conditions for Green-Naghdi Level-I theory in Chapter 3. Then in this waterfall problem, we can rewrite these jump conditions as follows:

$$\| Q \|_{x=0} = 0, \tag{4.1.43}$$

$$\| \rho Q u_0 + P_0 \|_{x=0} = \lim_{\delta \to 0} \int_{-\delta}^{+\delta} (\hat{p}\, \beta_x - \bar{p}\, \alpha_x) dx, \tag{4.1.44}$$

$$\| \rho Q u_0\, \psi_x \|_{x=0} = \lim_{\delta \to 0} \int_{-\delta}^{+\delta} [-\hat{p} + \bar{p} - \rho g \varphi] dx, \tag{4.1.45}$$

$$\lim_{\delta\to 0}\int_{-\delta}^{+\delta}\left[\rho Q u_{0,x}\psi\right]dx+\|P_1\|_{x=0}=\lim_{\delta\to 0}\int_{-\delta}^{+\delta}(\hat{p}\beta\beta_x-\bar{p}\alpha\alpha_x)dx. \tag{4.1.46}$$

$$\lim_{\delta\to 0}\int_{-\delta}^{+\delta}\left[\rho Q\psi(u_0\psi_x)_x+\frac{1}{12}\rho Q^2\varphi\left(\frac{\varphi_x}{\varphi}\right)_x\right]dx=\lim_{\delta\to 0}\int_{-\delta}^{+\delta}\left[P_0-\rho g\varphi\psi-\hat{p}\beta+\bar{p}\alpha\right]dx. \tag{4.1.47}$$

Before simplifying the jump conditions further, we turn to the geometric relations between region I and III at the junction x=0. For steady flow, since the bottom is smooth, we expect that the fluid departs from the cliff smoothly. Therefore, the top and bottom surfaces are continuous at the joint point x=0, that is,

$$\|\beta\|_{x=0}=0.$$

$$\|\alpha\|_{x=0}=0. \tag{4.1.48a, b}$$

Then from the definition of ϕ_0 and ψ, we have

$$\|\phi_0\|_{x=0}=0.$$

$$\|\psi\|_{x=0}=0. \tag{4.1.49a, b}$$

According to (4.1.43), from (4.1.49a) we can deduce that

$$\|u_0\|_{x=0}=0. \tag{4.1.50}$$

Since we have set the pressure at the top free surface $\hat{p}\equiv 0$ everywhere, then (4.1.44) becomes

$$\| \rho Q u_0 + P_0 \|_{x=0} = \lim_{\delta \to 0} \int_{-\delta}^{+\delta} (-\bar{p}\, \alpha_x) dx . \qquad (4.1.51)$$

For $0 \leq x \leq \delta$, the integrand, $-\bar{p}\, \alpha_x$, in (4.1.51) is identically zero. If the integrand remains bounded for $-\delta \leq x \leq 0$, the right-hand side of (4.1.51) is equal to zero, even if there exists a jump in $-\bar{p}\, \alpha_x$ at the joint point. Thus we have

$$\| \rho Q u_0 + P_0 \|_{x=0} = 0 . \qquad (4.1.52)$$

Substituting (4.1.43) and (4.1.50) into (4.1.52), (4.1.52) yields

$$\| P_0 \|_{x=0} = 0 . \qquad (4.1.53)$$

In the same way, the right-hand side of (4.1.45) is equal to zero and we arrive at

$$\| \rho Q u_0 \psi_x \|_{x=0} = 0 , \text{ or} \qquad (4.1.54)$$

$$\| \psi_x \|_{x=0} = 0 , \qquad (4.1.55)$$

where (4.1.50) and (4.1.43) have been applied.

Using (4.1.43), (4.1.49a, b), (4.1.50), (4.1.53) and (4.1.55), (4.1.47) yields

$$\| \phi_{0x} \|_{x=0} = 0 . \qquad (4.1.56)$$

At the same time, from (4.1.46) we can deduce that the first order integral pressure, P_1, remains unchanged across the joint point x=0. However, this jump condition is not necessary to solve the governing equations for region I and III, since we have eliminated this variable from the governing systems.

Therefore, we have finished the derivation of the necessary jump conditions at the joint point x=0 between the two regions of the overfall problem. For later convenience, we summarize the jump conditions as follows:

$$\begin{aligned} &\|u_0\phi_0\|_{x=0} = 0; \quad \|\beta\|_{x=0} = 0; \quad \|\beta_x\|_{x=0} = 0; \\ &\|\alpha\|_{x=0} = 0; \quad \|\alpha_x\|_{x=0} = 0; \quad \|P_0\|_{x=0} = 0. \end{aligned} \tag{4.1.57}$$

We need to point out that the above jump conditions (4.1.57) are based on the assumption that the flow departs from the cliff smoothly. Under certain circumstances, this assumption may not be valid. Then these jump conditions are not applicable to that problem and new jump conditions are needed.

With the help of these jump conditions, along with the boundary conditions, we can solve the waterfall problem throughout the whole region. In the following sections, we discuss several cases to illustrate the development of solutions.

§4.2 Free waterfall over a flat bottom

First we consider a very simple case, that is, the bottom surface in region I is flat. Naghdi & Rubin solved this problem with the directed fluid sheet theory with one director and obtained the analytical solutions for the first time. Their method is based on Lagrangian frame since the Eulerian form of Green-Naghdi theory had not been developed yet. Now we will solve this problem with the Green-Naghdi Level I theory developed above, which is in Eulerian form.

4.2.1 Solution of the problem

Because the general form of the governing equations for such problems has been obtained, it is relatively easy to obtain analytical solutions. In this case the bottom in region I is flat, then we can set up the coordinates such that the bottom surface function $\alpha \equiv 0$ everywhere in region I. Recall that we have obtained the governing equations for such cases. Using the assumption on the far upstream, (4.1.34), then in region I, these governing equations are:

$$\frac{\phi_{0xx}}{\phi_0} - \frac{1}{2}\frac{\phi_{0x}^2}{\phi_0^2} + \frac{3}{2}\frac{1}{\phi_0^2} + \frac{3g}{Q^2}\phi_0 - 3\frac{R_1}{Q^2} = 0; \tag{4.2.1}$$

$$\frac{P_0}{\rho} = \phi_0\left[R_1 - \frac{1}{2}g\phi_0 - \frac{1}{2}\frac{Q^2}{\phi_0^2} - \frac{1}{6}Q^2\frac{\phi_{0x}^2}{\phi_0^2}\right]; \tag{4.2.2}$$

$$\frac{\bar{p}}{\rho} = g\phi_0 - \frac{Q^2\phi_{0x}^2}{2\phi_0^2} + \frac{Q^2\phi_{0xx}}{2\phi_0}. \tag{4.2.3}$$

where, the constants of integration are

$$Q = Fr\sqrt{gH_1}\,H_1. \tag{4.2.4}$$

$$R_1 = gH_1 + \frac{1}{2}\frac{Q^2}{H_1^2}. \tag{4.2.5}$$

In this case, the second order differential equation (4.2.1) can be integrated. Substituting (4.2.5) into (4.2.1), multiplying by ϕ_{0x}/ϕ_0, integrating and multiplying the resulting expression by $2\phi_0^2$, we finally obtain

$$\frac{1}{3}Q^2\phi_{0x}{}^2+g\phi_0{}^3-2R_1\phi_0{}^2+2S_1\phi_0-Q^2=0. \tag{4.2.6}$$

where S_1 is another constant of integration, and can be determined by boundary conditions.

With the help of far upstream boundary conditions (4.1.34), from (4.2.6) we can obtain the constant of integration

$$S_1=\frac{1}{2}gH_1{}^2+\frac{Q^2}{H_1}. \tag{4.2.7}$$

After substituting (4.2.7) into (4.2.6), we can reduce the differential equation (4.2.6) to the following form:

$$\frac{1}{3}Q^2\phi_{0x}{}^2=\left(\frac{Q^2}{H_1{}^2}-g\phi_0\right)(\phi_0-H_1)^2. \tag{4.2.8}$$

This differential equation can be integrated again, and thus the analytical solution can be obtained. However, since (4.2.8) involves the boundary conditions at negative infinity, we need the jump conditions to determine a constant that will appear when integrating (4.2.8). Before proceeding further, we consider the governing equations in region III. From the above section, we know that they are

$$\phi_0=H_4+Ae^{-Bx}; \tag{4.2.9}$$

$$\frac{P_0}{\rho}=-\frac{Q^2}{\phi_0}+S_3; \tag{4.2.10}$$

$$Q^2\left(\frac{\psi_x}{\phi_0}\right)_x = -g\phi_0. \tag{4.2.11}$$

where,

$$A = H_3 - H_4. \tag{4.2.12}$$

$$B = \frac{2\sqrt{3}}{H_4}. \tag{4.2.13}$$

$$S_3 = \frac{Q^2}{H_4}. \tag{4.2.14}$$

H_3 here denotes the thickness of the fluid at the joint point x =0, and needs to be determined as a part of the solution.

In this case, the jump conditions (4.1.57) imply that at the joint point x = 0,

$\phi_0^+ = \phi_0^- = H_3$, $\phi_{0x}^+ = \phi_{0x}^- = K$, $\psi^+ = \psi^- = \frac{1}{2}H_3$, $\psi_x^+ = \psi_x^- = \frac{1}{2}K$, and

$$Q^+ = Q^- = Q,\ S^+ = S^-, \tag{4.2.15a-f}$$

where Q represents the constant rate of flow, K is the slope of the thickness of the fluid at the joint point x=0.

The constant H_4 in (4.2.9) can now be determined by using (4.2.7), (4.2.14) and jump condition (4.2.15f) and is given by

$$H_4 = Q^2\left[\tfrac{1}{2}gH_1^2 + \frac{Q^2}{H_1}\right]^{-1}. \tag{4.2.16}$$

So the constants B and S_3 are determined as well:

$$B=\frac{2\sqrt{3}}{Q^2}\left(\tfrac{1}{2}gH_1^{\,2}+\frac{Q^2}{H_1}\right). \tag{4.2.17}$$

$$S_3=\tfrac{1}{2}gH_1^{\,2}+\frac{Q^2}{H_1}. \tag{4.2.18}$$

After evaluating (4.2.6) and differentiating (4.2.9) at x=0, with the use of the jump conditions (4.2.15a, b) to eliminate the constant K, along with (4.2.16), (4.2.17) and (4.2.18), finally we obtain the cubic equation

$$gH_3^{\,3}+\left(\frac{4S_1^{\,2}}{Q^2}-2R_1\right)H_3^{\,2}-6S_1H_3+3Q^2=0 \tag{4.2.19}$$

for the determination of the vertical thickness H_3. Although three roots can be obtained from (4.2.19), only one has physical meaning. Once H_3 is determined, the constant A can be determined too. From (4.2.9) we can obtain the distribution of the thickness of the fluid in region III. Once the distribution of the fluid thickness in region III is determined, with the help of jump conditions (4.2.15c) and (4.2.15d), we can integrate (4.2.11) twice to obtain the function of central line of the fluid in region III, that is,

$$\psi=-\frac{gH_4^{\,2}}{2Q^2}x^2+CH_4x+\frac{gAH_4}{Q^2B}xe^{-Bx}-\frac{gA^2}{2Q^2B^2}e^{-2Bx}-\frac{AC}{B}e^{-Bx}+D. \tag{4.2.20}$$

where, C and D are constants of integration, and can be determined through the jump conditions (4.2.15c) and (4.2.15d).

Once the terms in (4.2.9) are determined, the integral pressure P_0 can be easily determined through (4.2.10) together with (4.2.14). Thus the solution for region III has been obtained.

Now let us turn back to Region I. With the help of the jump conditions (4.2.15), (4.2.8) can be integrated and the solution for region I thus can be obtained. The integral pressure P_0 and the bottom pressure $\bar{p}$ can be obtained through (4.1.15) and (4.1.16) respectively. Thus, the analytical solution for the whole region of the waterfall problem has been obtained.

4.2.2 Results and discussion

Here we do not give the results in detail because the solutions obtained are exactly same as those of Naghdi & Rubin, although their method was based on the Lagrangian frame while our method is based on Eulerian form. Comparing these results with the paper of Naghdi and Rubin (1981), we find that equations (4.2.8), (4.2.9), (4.2.10) and (4.2.11) are just same as (4.10), (4.5a), (4.1) and (3.4c) in their paper respectively. The only difference is that they did not obtain explicitly the formula to calculate the integral pressure P_0 and the bottom pressure $\bar{p}$ in region I, that is, equations (4.2.2) and (4.2.3) here.

By way of illustration, Fig. 4.2.1 shows the solution for three values of the Froude number Fr=1.25, 2.0 and 4.0 and for an upstream height H_1 = 1m. Fig. 4.2.2 shows the comparison between our solution, the experimental results of Rouse (1936), and the numerical solution of Southwell & Raisey (1946) using relaxation method for the Froude number Fr = 1 and H_1 = 1m. After comparison, we find that the results are in good

agreement with the experimental results of Rouse (1936). In particular, our calculation predicts that the brink depth $y_b = 0.717$, which is quite close to the experimental mean value 0.716 reported by Rouse (1936). At the same time, as pointed out by Naghdi & Rubin (1981), in the full range of Froude numbers, the predictions of the present solution for the height H_3 at the edge of the cliff are almost identical to those obtained numerically from the three-dimensional equations by Markland (1965).

On the other hand, through our calculation we find that there are no solutions when the Froude number, say Fr, is less than 1. In other words, there are only supercritical solutions for the free waterfall problem. This is consistent with the results obtained by Dias and Tuck (1991), who employed a completely different method, i.e., the conformal mapping. Their study showed that wave-free waterfall exists only for $Fr > 1$. Note that this result should not be confused with the physical results due to the adopted assumption that the fluid is inviscid. In reality there do exist physical solutions for the Froude number $Fr < 1$ due to the viscosity of the fluid and fraction of the bottom. In fact, for the steady flow, the gravity will be balanced with the friction, and thus the fluid far upstream cannot be uniform stream. This condition completely changes the nature of the waterfall problem because different boundary conditions are applied, and needs further effort to study. Thus it is beyond the discussion in this dissertation.

Fig. 4.2.3 depicts the distribution of the integral pressure P_0 throughout the flow region for three different values of Froude number, and Fig. 4.2.4 illustrates the corresponding distribution of the bottom pressure $\bar{p}$ in the upstream. From Fig. 4.2.3 we

find that the integral pressure P_0 is continuous everywhere in the flow region. However, Fig. 4.2.4 indicates that the bottom pressure $\overline{p}$ is discontinuous at the departure point x= 0, since the bottom pressure is zero in the downstream. This result is consistent with the claim of Naghdi and Rubin (1981), that is, although the jump conditions require the continuity of various quantities at the edge of the cliff x = 0, certain discontinuities remain with Green-Naghdi method. Both the present solution and that of Naghdi & Rubin (1981) indicate that the bottom pressure is discontinuous at the departure point x =0. The reason is unclear. Naghdi & Rubin (1981) did not make any comments when they pointed out this discontinuity.

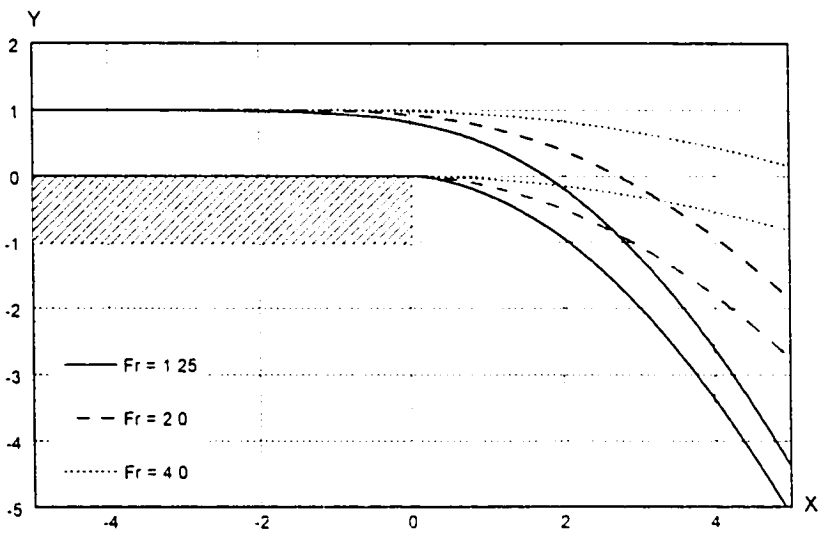

Fig. 4.2.1 A plot of the solution exhibiting profiles of the fluid sheet for an upstream height H_1 = 1 meter and for three values of the Froude number Fr, that is, Fr=1.25, 2.0, and 4.0.

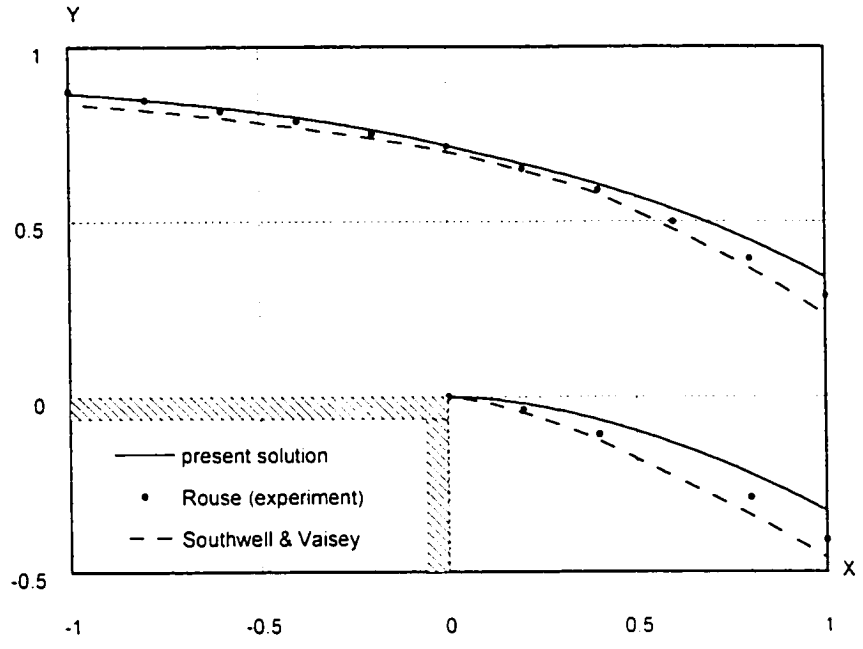

Fig. 4.2.2 Comparison between present solution, experimental results of Rouse (1936) and the solution of Southwell & Raisey (1946) for Fr = 1 and H_1 = 1 m.

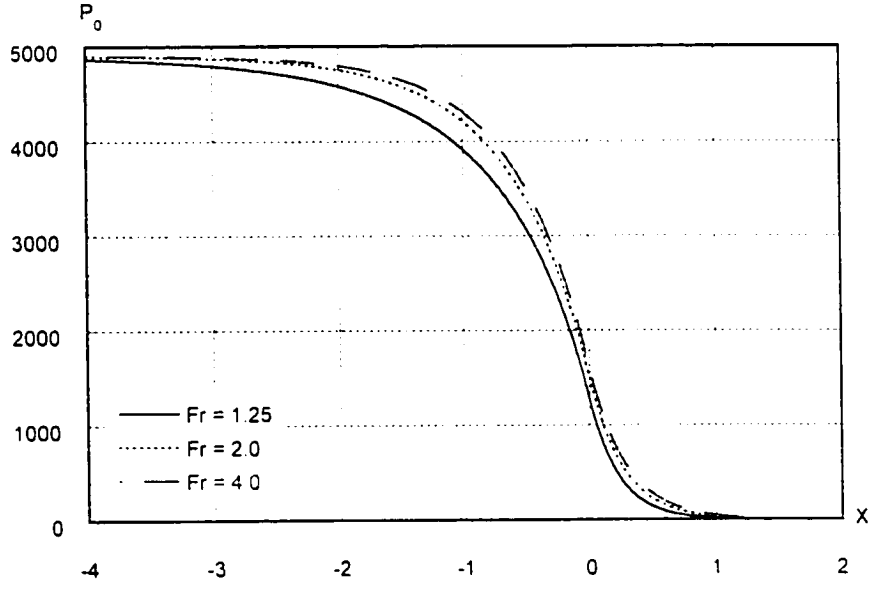

Fig. 4.2.3 The integral pressure throughout the flow region for different values of Fr

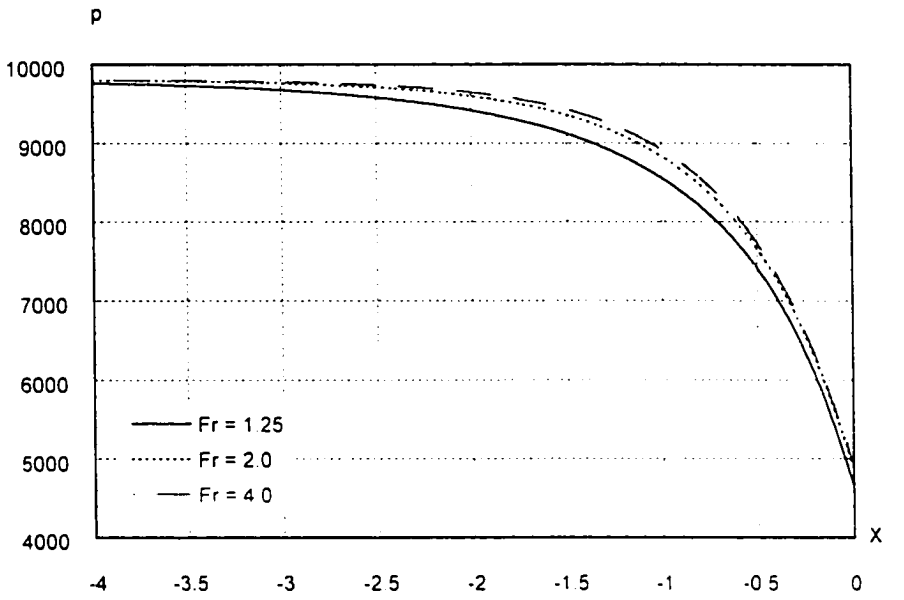

Fig. 4.2.4 The bottom pressure in the upstream for different values of Fr

§4.3 Free waterfall over an arbitrary, smooth bottom

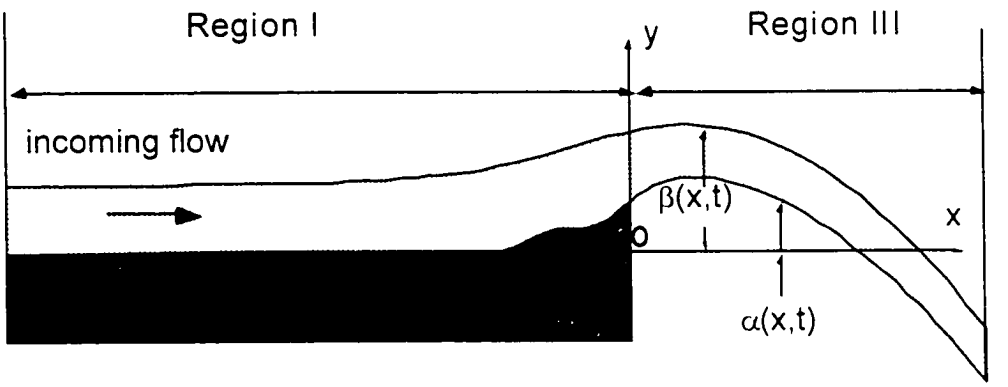

Fig 4.3.1 Schematic of waterfall over a smooth bottom

As we pointed out before, Naghdi and Rubin (1981) only obtained the solutions for the free waterfall problem with a flat bottom, as we did in §4.2. Now we consider the general case, that is, the bottom is smooth rather than flat (as shown in Fig 4.3), which will complicate the problem. Recall that for Green-Naghdi Level I theory we have defined that the bottom is smooth if its second derivative is continuous everywhere. For simplification, we still suppose that at far upstream the bottom is flat and assume that the upstream flow is uniform.

4.3.1 Solution of the problem

We still divide the whole flow region into two regions (shown in Fig. 4.3): region I where the fluid is bounded by a smooth bottom surface, which is given, and a unknown

free surface; and region III where the fluid is bounded by two unknown free surfaces. Then from above sections, we can obtain the governing equations for region I as follows:

$$\frac{\phi_{0xx}}{\phi_0}-\frac{1}{2}\frac{\phi_{0x}^{2}}{\phi_0^{2}}+\frac{3}{2}(1+\alpha_x^{2})\frac{1}{\phi_0^{2}}+\frac{3g}{Q^{2}}(\phi_0+\alpha)+\frac{3}{2}\frac{\alpha_{xx}}{\phi_0}-3\frac{R_1}{Q^{2}}=0. \tag{4.3.1}$$

$$\frac{P_0}{\rho}=\phi_0\left[R_1-\frac{1}{2}g\phi_0-g\alpha-\frac{1}{2}\frac{Q^{2}}{\phi_0^{2}}-\frac{1}{2}Q^{2}\frac{\alpha_x^{2}}{\phi_0^{2}}-\frac{1}{2}Q^{2}\frac{\alpha_x\phi_{0x}}{\phi_0^{2}}-\frac{1}{6}Q^{2}\frac{\phi_{0x}^{2}}{\phi_0^{2}}\right]. \tag{4.3.2}$$

$$\frac{\bar{p}}{\rho}=g\phi_0-\frac{Q^{2}\phi_{0x}^{2}}{2\phi_0^{2}}-\frac{Q^{2}\alpha_x\phi_x}{\phi_0^{2}}+\frac{Q^{2}\phi_{0xx}}{2\phi_0}+\frac{Q^{2}\alpha_{xx}}{\phi_0}. \tag{4.3.3}$$

where,

$$Q=Fr\sqrt{gH_1}\,H_1. \tag{4.3.4}$$

$$R_1=gH_1+\frac{1}{2}\frac{Q^{2}}{H_1^{2}}. \tag{4.3.5}$$

Compared with (4.2.1), (4.3.1) is more complicated since there are several items arising from the smooth bottom surface in region I. As a result, (4.3.1) can not be integrated as we did in §4.2. It does not seem possible to obtain the analytical solution to this problem. Instead, numerical calculation will be employed.

Now we consider the governing equations for region III. Here we still adopt the assumption that because the only acting force on the free waterfall is the gravity, at the far downstream the variables do not change along the vertical direction. Under this assumption and with the associated boundary conditions at far downstream, the governing equations are as follows:

$$\phi_0 = H_4 + A e^{-Bx}; \tag{4.3.6}$$

$$\frac{P_0}{\rho} = -\frac{Q^2}{\phi_0} + S_3; \tag{4.3.7}$$

$$Q^2\left(\frac{\psi_x}{\phi_0}\right)_x = -g\phi_0, \tag{4.3.8}$$

where,

$$A = H_3 - H_4, \tag{4.3.9}$$

$$B = \frac{2\sqrt{3}}{H_4}, \tag{4.3.10}$$

$$S_3 = \frac{Q^2}{H_4}. \tag{4.3.11}$$

Here the variables and notations have the same meaning as in §4.2.

Now that we have obtained the governing equations for region I and region III, we need to consider the jump conditions to obtain the uniform solution. Just as in §4.2, in order to obtain these constants of integration, jump conditions must be applied at the junction, which we will locate, as before, at x=0. As long as the bottom in region I is smooth, we still adopt the assumption that the fluid departs from the cliff smoothly. Then the jump conditions (4.1.57) are still valid in this problem, that is,

$$\begin{aligned} &\|Q\|_{x=0} = 0; \quad \|\beta\|_{x=0} = 0; \quad \|\beta_x\|_{x=0} = 0; \\ &\|\alpha\|_{x=0} = 0; \quad \|\alpha_x\|_{x=0} = 0; \quad \|P_0\|_{x=0} = 0. \end{aligned} \tag{4.3.12}$$

When we replace α and β with ϕ_0 and ψ, the jump conditions (4.3.12) become

$$\begin{aligned} &\|u_0\phi_0\|_{x=0} = 0; \quad \|\phi_0\|_{x=0} = 0; \quad \|\phi_{0x}\|_{x=0} = 0; \\ &\|\psi\|_{x=0} = 0; \quad \|\psi_x\|_{x=0} = 0; \quad \|P_0\|_{x=0} = 0. \end{aligned} \tag{4.3.13}$$

Considering the notation we adopted, we can deduce from the jump conditions (4.3.13a-e) that

$$\begin{aligned} &\phi_0^+ = \phi_0^- = H_3, \qquad \phi_{0,x}^+ = \phi_{0,x}^- = K, \\ &\psi^+ = \psi^- = \frac{1}{2}H_3 + H_b, \quad \psi_x^+ = \psi_x^- = \frac{1}{2}K + K_b \end{aligned} \tag{4.3.14}$$

and

$$Q^+ = Q^- = Q, \tag{4.3.15}$$

where K denotes the slope of thickness of the fluid at the junction, and H_3 the thickness of the fluid at the junction, while H_b denotes the height of the bottom at the joint point and K_b the slope of the bottom at the joint point. K and H_3 are to be determined while H_b and K_b are specified beforehand.

The jump condition (4.2.15f) is not valid here because of the effect of the non-flat bottom. However, by means of (4.3.13f), we can deduce the corresponding jump condition to (4.2.15f). Inserting (4.3.5) into (4.3.2) and plugging (4.3.11) into (4.3.7), and substituting the equations into the jump condition (4.3.13f) and with the help of other jump conditions (4.3.14) and (4.3.15), finally we can obtain the following nonlinear algebraic equation relating the critical heights (H_1, H_2, H_3), the slopes at the junction (K, K_b) and the flow rate Q.

$$\frac{1}{H_4}-\frac{gH_1H_3}{Q^2}-\frac{H_3}{2H_1^2}+\frac{gH_3^2}{2Q^2}+\frac{gH_3H_b}{Q^2}-\frac{1}{2H_3}+\frac{K_b^2}{2H_3}+\frac{K_bK}{2H_3}+\frac{K^2}{6H_3}=0\,. \quad (4.3.16)$$

Since the constant flux of fluid Q, the far upstream thickness H_1 and the slope of bottom at $x = 0^-$ are given, from above expression we know that the slope of fluid thickness K, the thickness of the fluid at x=0 H_3 and the thickness at far downstream H_4 are related. Once two of them are determined, the other is determined by (4.3.16).

Note that jump conditions (4.3.14c) and (4.3.14d) involve the value and the slope of the central line at x = 0. At $x = 0^-$, these values are related with the thickness since the bottom surface is specified in region I. However in region III both top and bottom surface are free and to be determined, so we need to get the equations with regard of the central line of fluid and its slope. Recall that only (4.3.8) involves the central line, and actually it is a second-order differential equation. However, with the help of (4.3.6), we can integrate (4.3.8). Substituting (4.3.6) into (4.3.8) and integrating, we can obtain

$$\psi_x=-\frac{gH_4^2}{Q^2}x+\frac{gAH_4}{Q^2B}e^{-Bx}+CH_4-\frac{gAH_4}{Q^2}xe^{-Bx}+\frac{gA^2}{Q^2B}e^{-2Bx}+ACe^{-Bx}\,. \quad (4.3.17)$$

where C is a constant of integration to be determined, and is given by

$$C=\frac{\psi_x}{\phi_0}+\frac{gH_4}{Q^2}x-\frac{gA}{BQ^2}e^{-Bx}\Big|_{x=0}\,. \quad (4.3.18)$$
$$=\frac{K_b+K/2}{H_3}-\frac{gA}{BQ^2}$$

(4.3.17) can be integrated again. After integrating (4.3.17), we arrive at

$$\psi = -\frac{gH_4^2}{2Q^2}x^2 + CH_4 x + \frac{gAH_4}{Q^2B}xe^{-Bx} - \frac{gA^2}{2Q^2B^2}e^{-2Bx} - \frac{AC}{B}e^{-Bx} + D. \quad (4.3.19)$$

where D is another constant of integration to be determined, and given by

$$\begin{aligned} D &= \psi|_{x=0} + \frac{gA^2}{2Q^2B^2} + \frac{AC}{B} \\ &= \frac{1}{2}H_3 + H_b + \frac{gA^2}{2Q^2B^2} + \frac{AC}{B} \end{aligned} \quad (4.3.20)$$

Obviously, the constants of integration C and D are to be determined through the application of jump conditions (4.3.14c) and (4.3.14d).

4.3.2 Results and discussion

To date, we have obtained enough equations and jump conditions, together with boundary conditions, to solve the free waterfall problem over an arbitrary smooth bottom. However, explicit results cannot be obtained, as we did for the flat bottom case. As a result, numerical calculation is employed for non-flat smooth bottom cases. By way of illustration, several solutions are computed for different Froude numbers and different bottom shapes in region I. For all of the computations the thickness of the fluid far upstream H_1 is set equal to unity. Unfortunately, we have not found any experimental data to make a comparison.

Fig. 4.3.2 shows the numerical results of the flows for three different far upstream Froude numbers over the same smooth bottom, that is, Fr = 1.25, 2.0 and 4.0. The bottom profile is: $\alpha = 0$ for $x < -3$, $\alpha(x) = 0.0037x^3 + 0.033x^2 + 0.1x + 0.1$ for $-3 \le x \le 0$. An

enlarged figure is showed in Fig. 4.3.3 for the region near the lip of the waterfall. We find from these figures that the thickness of the fluid at the junction increases with the upstream Froude number. Meanwhile, we find that the highest elevation of the free surface is located before the junction for small Froude numbers, i.e., Fr = 1.25, while for higher Froude numbers it moves forward and is behind x = 0 for Fr = 4.0.

Fig. 4.3.4 shows the flows of the same Froude number, Fr = 2.0, over different smooth bottoms. Three different smooth bottoms corresponding to $\alpha(x)$, $3\alpha(x)$ and $5\alpha(x)$ have been considered. It is obvious that the elevation of the free surface depends on the shape of the bottom surface in region I. The higher the bottom is, the higher the elevation of the free surface becomes, as shown in Fig. 4.3.4. On the other hand, the horizontal velocity and the local Froude number will change sharply due to the steep slope of the bottom. Fig. 4.3.5 shows the distribution of the horizontal velocity along the x-axis over different bottoms, and Fig. 4.3.6 depicts the local Froude number throughout the flow region. After observation of Fig. 4.3.5 and Fig. 4.3.6, we find that the steeper the bottom is, the more rapidly the horizontal velocity and local Froude number change along the x-axis, in particular in the neighborhood of the junction. At the same time, after observing Fig. 4.3.6, we find that the local Froude number decreases initially when the flow approaches the non-flat part of the bottom, and increases again in the neighborhood of the junction and approach a constant far downstream. Another result we need to point out is that the Froude number downstream decreases as the non-flat smooth bottom becomes steeper, as shown in Fig. 4.3.6. When the bottom in region II is $5\alpha(x)$, the Froude number downstream is less than that at far upstream, while for other two cases,

the Froude number downstream is greater than that at far upstream. It is easy from these results to conclude that the steeper non-flat smooth bottom has more effect on the free waterfall.

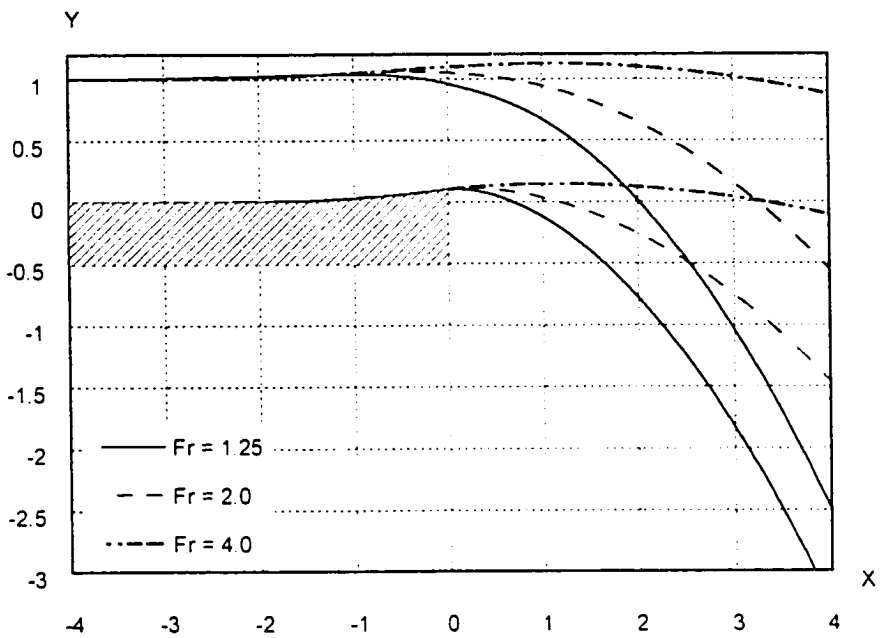

Fig. 4.3.2 A plot of the solution exhibiting profiles of the fluid sheet for an upstream height H_1 = 1 meter and the bottom surface $\alpha = 0$ when $x < -3$, and $\alpha = 0.0037x^3 + 0.033x^2 + 0.1x + 0.1$ when $-3.0 \le x \le 0$, for different Froude numbers, Fr = 1.25, 2.0, and 4.0 respectively.

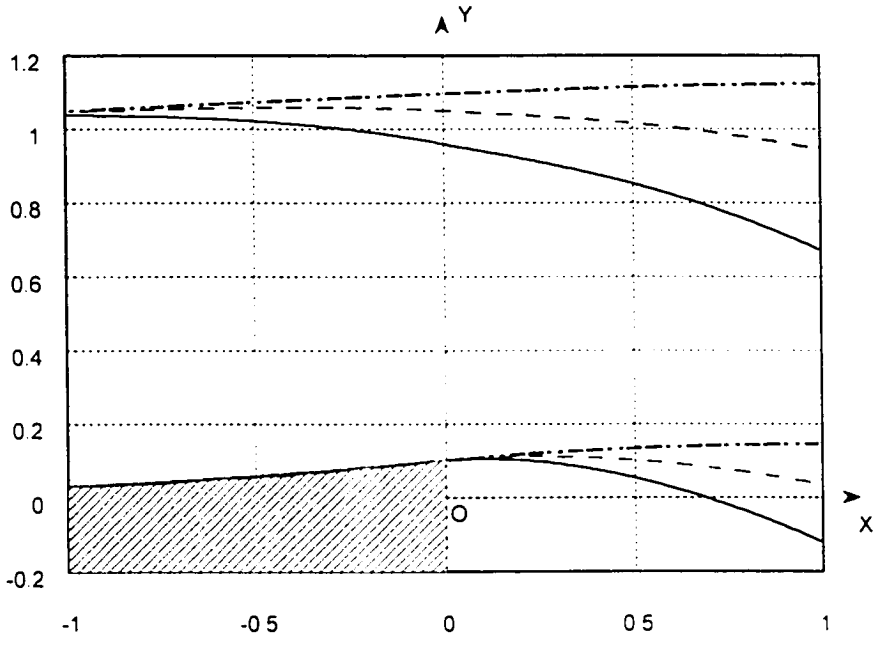

Fig. 4.3.3 Close look near the junction x = 0 for Fig. 4.3.2

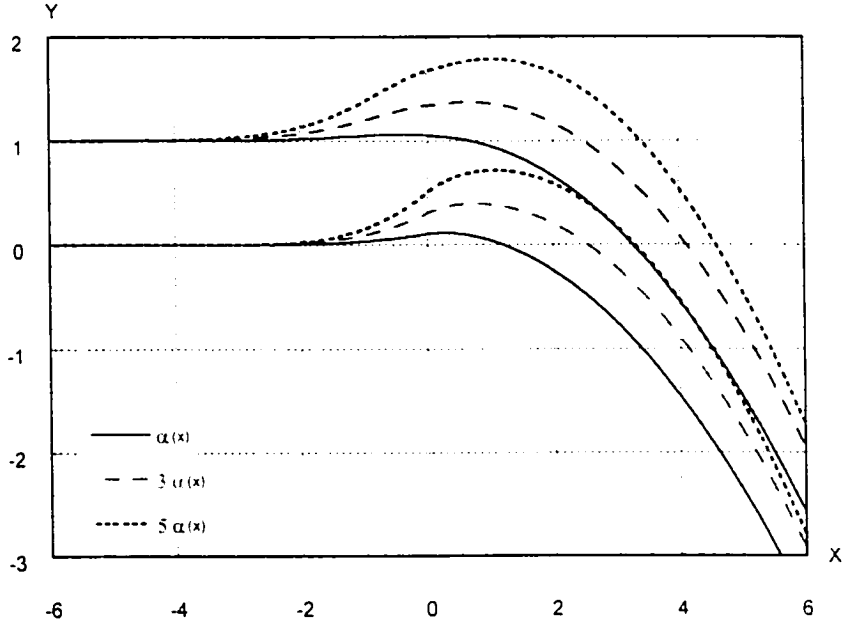

Fig. 4.3.4 Plot of waterfall over different smooth bottoms at Fr =2.0

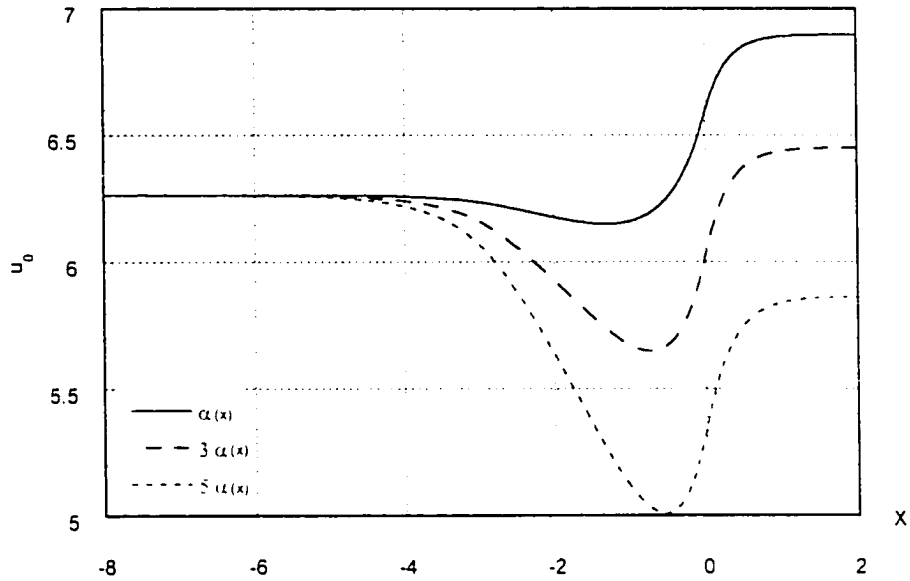

Fig. 4.3.5 Plot of the horizontal velocity u_0 for different bottoms

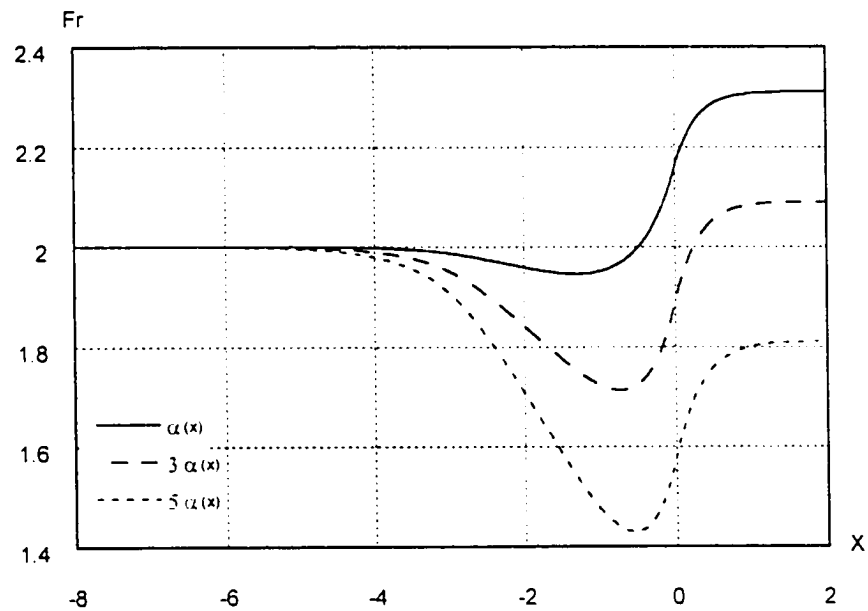

Fig. 4.3.6 Local Froude number for different non-flat smooth bottoms

From the numerical calculation, we also found that the existence of solutions depends on the Froude number at far upstream. Our numerical results show that there is no solution if the Froude number Fr < 1.0 at far upstream, which is consistent with the results of flat bottom case. Moreover, the actual minimum Froude number upstream depends on the shape of the bottom surface, and maybe is greater than 1. For instance, when we calculated the solution for the bottom $\alpha(x) = 0.0111\ x^3 - 0.1\,x^2 - 0.3\,x - 0.3$ for $-3 \le x \le 0$, and $\alpha = 0$ for $x < -3$. We found that when the Froude number Fr < 1.282, there were no solutions at all. Thus we concluded that the minimum Froude number for this case is $Fr_{min} = 1.282$.

With a try to explain this phenomenon, we plotted the local Froude number along the top and bottom surfaces (see Fig. 4.3.7) and the vertical component of the fluid velocity on the top and bottom surfaces (see Fig. 4.3.8), when the Froude number far upstream is minimum. Fig. 4.3.7 indicates that the local Froude number decreases first and reaches a minimum value, and increases again. The initial decrease of the local Froude number is due to the upward non-flat smooth bottom in region II, which slows down the velocity of the fluid and transfers part of horizontal momentum into the pressure on the bottom. While the increase is due to the action of the gravity, which accelerates the flow in the neighborhood of the junction. Fig. 4.3.8 shows that on the bottom surface the vertical velocity is positive and corresponds to the shape of the bottom, while on the top surface the vertical velocity increases due to the effect of the upward bottom and then decrease again due to the action of the gravity. It is surprising that the minimum local Froude number is less than 1. As shown in Fig. 4.3.7, the minimum local Froude number is near

0.8, and there is little difference between the local Froude number on the top and bottom surfaces. Actually it is still arguable whether the minimum Froude number for free waterfall problem is greater than 1, and various results have been achieved by different researchers. Chow & Han (1979) have computed a solution for a Froude number of 0.9 while admitting that the existence of subcritical waterfalls was doubtful in steady inviscid flow. Smith & Abd-el-Malek (1983) have computed a solution for a Froude number of 0.8 without comments about the validity of such a solution. Later on, Dias & Tuck (1991) claimed that wave-free waterfalls exist only for $Fr > 1$. We need to point out that all of the mentioned results are based on the waterfall over a flat bottom. Our results show that for the waterfalls over a flat bottom, the claim of Dias & Tuck is corroborated, that is, only supercritical solutions exist. However, for the waterfalls over a smooth, non-flat bottom, the local Froude number can be less than 1, although the Froude number far upstream still must be greater than 1. After observing the difference between the waterfalls over a flat bottom and over a smooth upward bottom, we noticed that for the waterfall over a flat bottom, due to the effect of the gravity, the fluid velocity in region I is accelerated and the free surface is "pulled down". Consequently, the local Froude number is always greater than that far upstream, and is always greater than 1 to obtain a solution. On the contrary, for the waterfall over a smooth bottom, the presence of a steep bottom will "slow down" the flow somewhat and "lift up" the free surface in region I before the action of the gravity becomes dominant, say near the lip of the waterfall. As a result, the local Froude number will decrease somewhat and increase again as the flow accelerates under the action of the gravity, as shown in Fig. 4.3.7. Therefore, the local Froude number is less than that at far upstream in the neighborhood of the non-flat

portion of the bottom. This makes it possible that the local Froude number may be less than 1.

Fig. 4.3.9 depicts the distribution of the bottom pressure $\bar{p}$ in the flow region, and Fig. 4.3.10 shows the distribution of the integral pressure P_0 throughout the region, for the bottom surface $\alpha(x) = 0.0111\,x^3 - 0.1\,x^2 - 0.3\,x - 0.3$ for $-3 \le x \le 0$, and $\alpha = 0$ for $x < -3$ when the Froude number Fr = 1.282. From Fig. 4.3.10 we find that P_0 is continuous throughout the region and decreases to zero rapidly in the downstream region. Fig. 4.3.9 indicates that $\bar{p}$ is continuous in the upstream region, but there exists a jump at $x = 0$, which is consistent with what we obtained for the waterfall problem over a flat bottom.

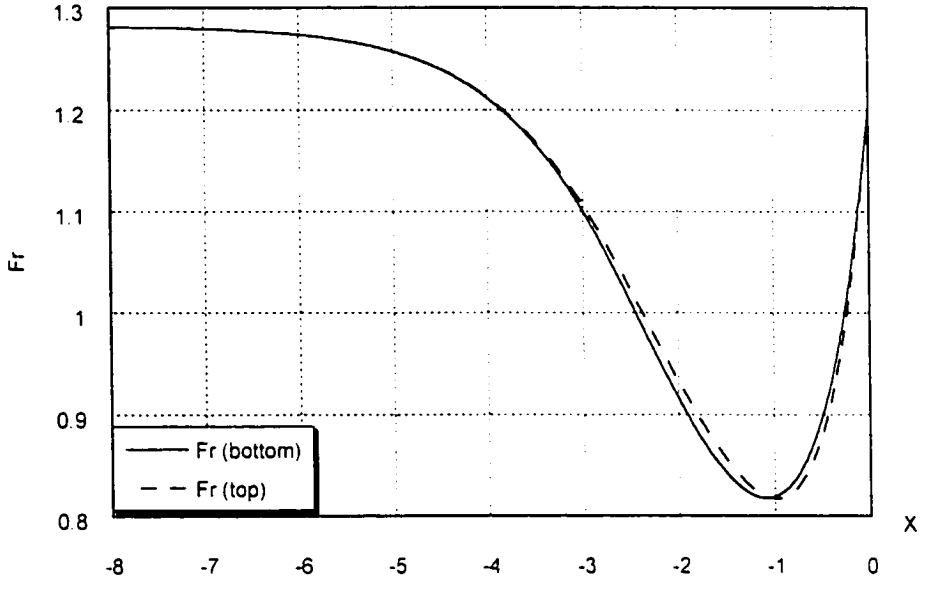

Fig. 4.3.7 Local Froude number when the Froude number upstream is minimum

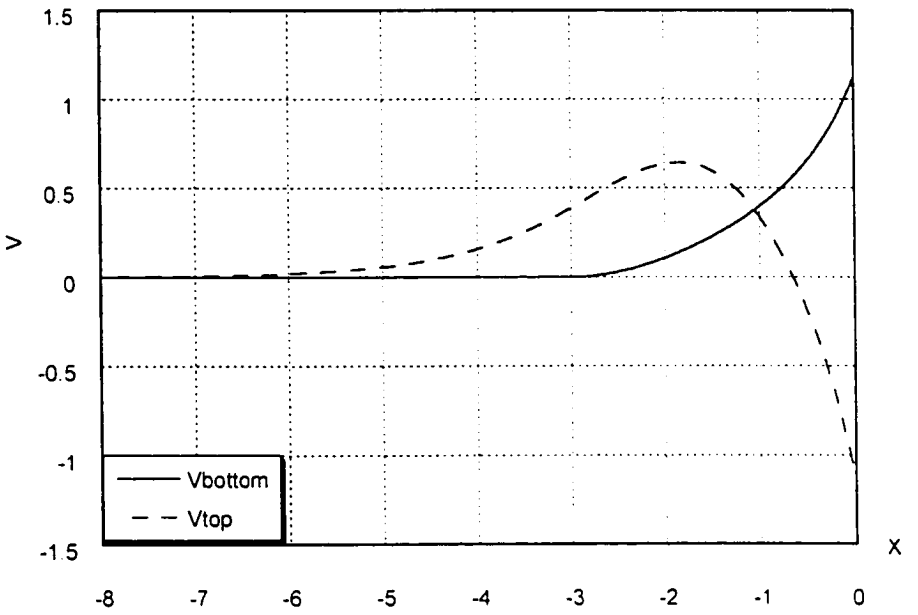

Fig. 4.3.8 Vertical velocity on the top and bottom in region I when the Froude number upstream is minimum

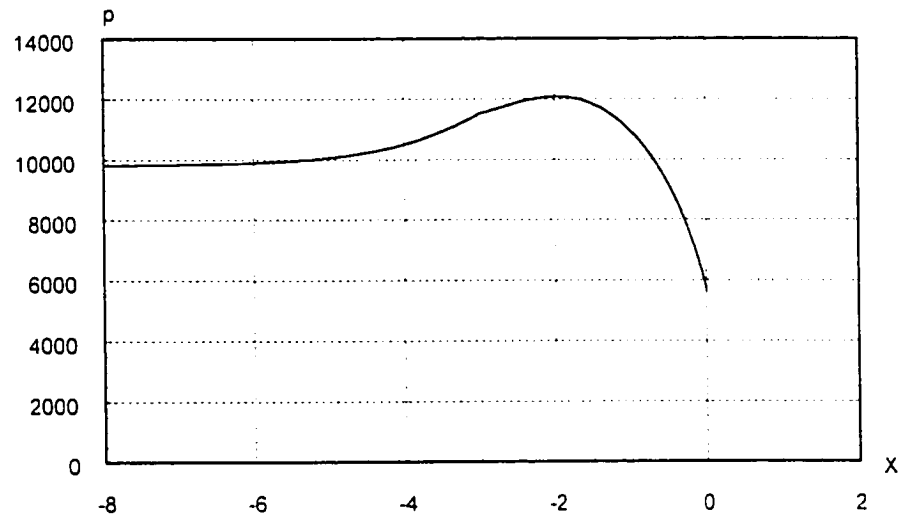

Fig. 4.3.9 The distribution of the bottom pressure when the Froude number Fr = 1.282, and the bottom $\alpha(x) = 0.0111\,x^3 + 0.1\,x^2 + 0.3\,x + 0.3$ for $-3 \le x \le 0$, and $\alpha = 0$ for $x < -3$

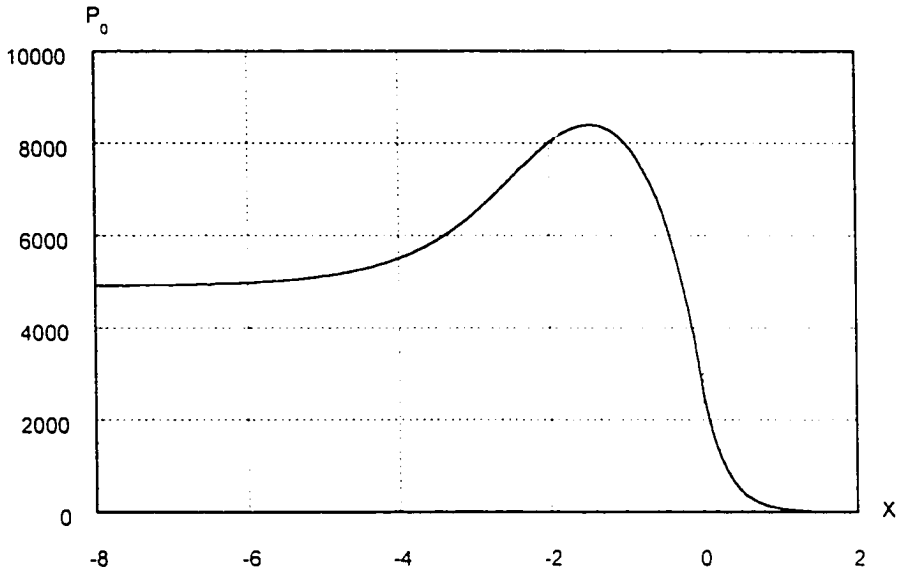

Fig. 4.3.10 The distribution of the integral pressure when the Froude number Fr = 1.282.

and the bottom $\alpha(x) = 0.0111\,x^3 + 0.1\,x^2 + 0.3\,x + 0.3$ for $-3 \le x \le 0$. and $\alpha = 0$ for $x < -3$

§4.4 Free waterfall over a non-planar bottom

In the statement of the waterfall problem, we have assumed that the bottom is smooth. The derived governing equations are all based on this assumption, and by means of these governing equations, together with appropriate jump conditions, we have solved these free waterfall problems either analytically or numerically in the two previous sections. However, the waterfall over a continuous, but non-planar cliff may exist in practice. In this section we will consider the free waterfall over a continuous, but non-planar bottom. As we will see later, because of the existence of the non-planar bottom, the waterfall problem becomes much more complicated, and special jump conditions are needed to consider the discontinuities in the process of the solution. On the other hand, just because there exist "real" discontinuities in this problem, it becomes a good example to test and apply the jump conditions derived in Chapter 3. As far as we know, no paper has dealt with such waterfall problems, especially with Green-Naghdi method. We will illustrate how to solve this problem with Green-Naghdi method and associated jump conditions by solving a simple case. Before further proceeding, we summarize the problem in the following paragraph for later convenience.

Consider the steady, two-dimensional flow of an inviscid, incompressible fluid under the action of gravity over a cliff leading to a free overfall. The bottom is flat at far left upstream and becomes steep with a constant slope at some distance from the departure point of the waterfall (as shown Fig 4.4.1). Here the effect of surface tension is assumed negligible. Far upstream the fluid is assumed to flow as a uniform stream, while in the

downstream the fluid falls freely only under the action of the gravity. Of particular interest in analyzing the problem is the prediction of the height of the whole flow region and the determination of the downstream solution, i.e., the location of the free surfaces and the distribution of the vertical thickness of the jet.

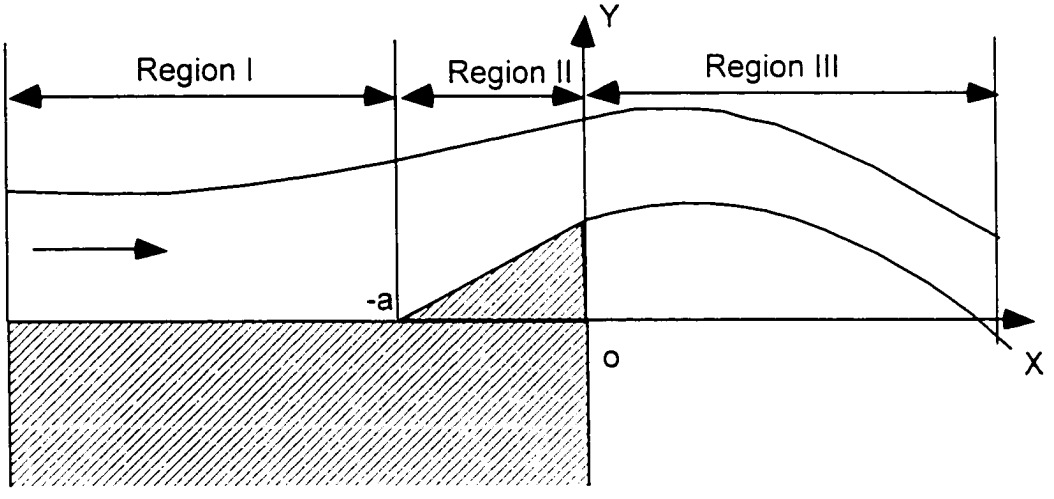

Fig. 4.4.1 Schematic of waterfall over a non-planar bottom

4.4.1 Formulation of the problem

Obviously, if we still divide the whole flow into two regions as we did before, that is, upstream region characterized by a free surface and a continuous but non-planar bottom, and downstream region bounded by two free surfaces, then the governing equations (4.1.42), (4.1.32) and (4.1.33) are still valid for the downstream region, while the governing equations (4.1.11), (4.1.12) and (4.1.13) are not valid any longer for the upstream region since they are derived on the basis of the assumption that the bottom is smooth. In order to apply these equations, we divide the upstream again into two separate

regions by the point where the discontinuity of the slope of the bottom is located, i.e., x = -a. Then we have three different regions: region I characterized with a free surface and a flat bottom; region II associated with a free surface and a steep bottom with constant slope; and region III with two free surfaces (see Fig. 4.4.1). Consequently, two sets of jump conditions need to be applied at two points, say x=-a and x=0, respectively, in order to link the solutions in three regions.

This problem is much more complex than the previous two cases. First three distinct regions exist, and we need to develop different governing equations for different regions. Secondly, in order to obtain the uniform solution, two sets of jump conditions are needed to apply to two junctions between three regions. Moreover, there exist discontinuities at x=-a, which implies that the jump conditions are not only used to link the solutions in different regions, but also to take into account the real jump of variables at x=-a. This is always difficult because the jumps of some variables are usually unknown beforehand. As we will see later, another jump condition, which can be obtained through the law of conservation of energy, is needed to solve this problem.

First we derive the governing equations for three different regions. Based on the results obtained in previous sections, we can easily state the governing equations without detail derivation. Obviously, region I and region III here are exactly same as the regions in §4.2. According to the statement of problem, the far upstream is uniform, then we have the same far upstream boundary conditions in region I as in §4.2. In addition, as for the free waterfall region, we still adopt the same assumption about the far downstream as

in §4.3. Therefore, we can use the simplified governing equations obtained in §4.2 and §4.3 for region I and region III here. Recall that the Green-Naghdi governing equations for region I are as follows

$$\frac{1}{3}Q^2\phi_{0x}{}^2=\left(\frac{Q^2}{H_1{}^2}-g\phi_0\right)(\phi_0-H_1)^2. \tag{4.4.1}$$

$$\frac{P_0}{\rho}=\phi_0\left[R_1-\frac{1}{2}g\phi_0-\frac{1}{2}\frac{Q^2}{\phi_0{}^2}-\frac{1}{6}Q^2\frac{\phi_{0x}{}^2}{\phi_0{}^2}\right]; \tag{4.4.2}$$

$$\frac{\bar{p}}{\rho}=g\phi_0-\frac{Q^2\phi_{0x}{}^2}{2\phi_0^2}+\frac{Q^2\phi_{0xx}}{2\phi_0}. \tag{4.4.3}$$

where,

$$Q=Fr\sqrt{gH_1}\,H_1. \tag{4.4.4}$$

$$R_1=gH_1+\frac{1}{2}\frac{Q^2}{H_1{}^2}. \tag{4.4.5}$$

And in region III, the governing equations are

$$\phi_0=H_4+Ae^{-Bx}; \tag{4.4.6}$$

$$\frac{P_0}{\rho}=-\frac{Q^2}{\phi_0}+S_3; \tag{4.4.7}$$

$$\psi=-\frac{gH_4{}^2}{2Q^2}x^2+CH_4x+\frac{gAH_4}{Q^2B}xe^{-Bx}-\frac{gA^2}{2Q^2B^2}e^{-2Bx}-\frac{AC}{B}e^{-Bx}+D. \tag{4.4.8}$$

where

$$B=\frac{2\sqrt{3}}{H_4}, \tag{4.4.9}$$

$$S_3 = \frac{Q^2}{H_4}. \tag{4.4.10}$$

$$\begin{aligned} C &= \frac{\psi_x}{\phi_0} + \frac{gH_4}{Q^2}x - \frac{gA}{BQ^2}e^{-Bx} \\ &= \frac{K_3 + K/2}{H_3} - \frac{gA}{BQ^2} \end{aligned}, \tag{4.4.11}$$

$$\begin{aligned} D &= \psi|_{x=0} + \frac{gA^2}{2Q^2B^2} + \frac{AC}{B} \\ &= \frac{1}{2}H_3 + H_b + \frac{gA^2}{2Q^2B^2} + \frac{AC}{B} \end{aligned}. \tag{4.4.12}$$

Now we need to derive the particular form of governing equations for Region II, which is bounded by a free surface and an inclined bottom. Note that in this region, the bottom is still smooth and thus the general Green-Naghdi governing equations are still valid in region II. For simplification we have specified that the slope of the bottom in region II is constant, although clearly we could have assumed a more general form. Taking this background into account, from the general Green-Naghdi Level I governing equations obtained in §4.1, that is, (4.1.11), (4.1.12) and (4.1.13), we can obtain the governing equations for region II:

$$\frac{\phi_{0xx}}{\phi_0} - \frac{1}{2}\frac{\phi_{0x}^2}{\phi_0^2} + \frac{3}{2}(1+K^2)\frac{1}{\phi_0^2} + \frac{3g}{Q^2}(\phi_0 + \alpha) - 3\frac{R_2}{Q^2} = 0, \tag{4.4.13}$$

$$\frac{P_0}{\rho} = \phi_0\left[R_2 - \frac{1}{2}g\phi_0 - g\alpha - \frac{1}{2}\frac{Q^2}{\phi_0^2} - \frac{1}{2}Q^2\frac{K^2}{\phi_0^2} - \frac{1}{6}Q^2\frac{\phi_{0x}^2}{\phi_0^2}\right]. \tag{4.4.14}$$

$$\frac{\bar{p}}{\rho} = g\phi_0 - \frac{Q^2\phi_{0x}{}^2}{2\phi_0^2} - \frac{Q^2K\phi_{0x}}{\phi_0^2} + \frac{Q^2\phi_{0xx}}{2\phi_0}, \tag{4.4.15}$$

where K denotes the constant slope of the bottom in region II, and R_2 is a constant of integration needed to be determined as part of solution.

4.4.2 Application of jump conditions

Now that we have obtained the governing equations for three regions that have taken into consideration the boundary conditions at far upstream and downstream, we now consider the jump conditions to determine the constants of integration in the governing equations, and to obtain the conditions to determine the solutions. First we consider the jump conditions at the junction between region II and region III, i.e. at x=0. We still assume that the fluid departs smoothly from the cliff. Then the jump conditions are just same as those in §4.3:

$$\begin{aligned} &\|Q\|_{x=0} = 0; \quad \|\beta\|_{x=0} = 0; \quad \|\beta_x\|_{x=0} = 0; \\ &\|\alpha\|_{x=0} = 0; \quad \|\alpha_x\|_{x=0} = 0; \quad \|P_0\|_{x=0} = 0. \end{aligned} \tag{4.4.16}$$

or

$$\begin{aligned} &\|u_0\phi_0\|_{x=0} = 0; \quad \|\phi_0\|_{x=0} = 0; \quad \|\phi_{0x}\|_{x=0} = 0; \\ &\|\psi\|_{x=0} = 0; \quad \|\psi_x\|_{x=0} = 0; \quad \|P_0\|_{x=0} = 0. \end{aligned} \tag{4.4.17}$$

With particular notation at x = 0, we have

$$\begin{aligned} &\phi_0^+ = \phi_0^- = H_3, \qquad \phi_{0,x}{}^+ = \phi_{0,x}{}^- = K_0, \\ &\psi^+ = \psi^- = \frac{1}{2}H_3 + H_b, \quad \psi_x{}^+ = \psi_x{}^- = \frac{1}{2}K_0 + K \end{aligned} \tag{4.4.18}$$

and

$$Q^{+} = Q^{-} = Q, \tag{4.4.19}$$

where K_0 denotes the slope of thickness of the fluid at the junction at x = 0, and H_3 the thickness of the fluid and H_b denotes the height of the bottom at this junction. K_0 and H_3 are to be determined.

Another jump condition derived from (4.4.17f) is

$$\frac{1}{H_4} - \frac{gH_1H_3}{Q^2} - \frac{H_3}{2H_1^2} + \frac{gH_3^2}{2Q^2} + \frac{gH_3H_b}{Q^2} - \frac{1}{2H_3} + \frac{K^2}{2H_3} + \frac{KK_0}{2H_3} + \frac{K_0^2}{6H_3} = 0. \tag{4.4.20}$$

where, H_4 denotes the thickness of the fluid at far downstream, and is to be determined as part of the solution.

Up to this point we have completed the derivation of the jump conditions at x = 0. It is relatively easy since we already have had the results from §4.2 and §4.3. Now we have to consider the jump conditions at the junction between region I and region II at x = -a. These require a development further than that above and this development is the major emphasis of this section.

First we apply the general jump conditions for Green-Naghdi Level-I theory to the joint point x = -a. After having set the atmospheric pressure equal zero, we can obtain the following jump conditions:

$$\| Q \|_{x=-a} = 0, \tag{4.4.21}$$

$$\| \rho Q u_0 + P_0 \|_{x=-a} = \lim_{\delta \to 0} \int_{-a-\delta}^{-a+\delta} (-\bar{p}\, \alpha_x) dx . \tag{4.4.22}$$

$$\| \rho Q u_0 \psi_x \|_{x=-a} = \lim_{\delta \to 0} \int_{-a-\delta}^{-a+\delta} [\bar{p} - \rho g \varphi] dx , \tag{4.4.23}$$

$$\lim_{\delta \to 0} \int_{-a-\delta}^{-a+\delta} [\rho Q u_{0,x} \psi] dx + \| P_1 \|_{x=-a} = \lim_{\delta \to 0} \int_{-a-\delta}^{-a+\delta} (-\bar{p} \alpha \alpha_x) dx . \tag{4.4.24}$$

$$\lim_{\delta \to 0} \int_{-a-\delta}^{-a+\delta} \left[\rho Q \psi (u_0 \psi_x)_x + \frac{1}{12} \rho Q^2 \varphi \left(\frac{\varphi_x}{\varphi} \right)_x \right] dx = \lim_{\delta \to 0} \int_{-a-\delta}^{-a+\delta} [P_0 - \rho g \varphi \psi + \bar{p} \alpha] dx \tag{4.4.25}$$

However, all of these conditions except (4.4.21) involve the limits. Unlike before, these limits are not identically zero and this makes it difficult to apply these jump conditions directly. Before proceeding further, we first consider the geometric relations near the junction at x = -a. There exists an obvious discontinuity of the slope of the bottom at x=-a, that is,

$$\| \alpha_x \|_{x=-a} = K . \tag{4.4.26}$$

Because of the discontinuity of the slope of the bottom, a hydraulic jump may occur. However, what we pursue here is a steady solution with a smooth free surface, so we expect that the top and bottom surfaces to remain continuous at this junction. Then we have the following geometric relations at x = -a:

$$\| \beta \|_{x=-a} = 0 ,$$

$$\| \alpha \|_{x=-a} = 0 ; \qquad (4.4.27a, b)$$

or

$$\| \phi_0 \|_{x=-a} = 0 ,$$

$$\| \psi \|_{x=-a} = 0 . \qquad (4.4.28a, b)$$

In addition, we expect that the top surface is smooth at this junction, that is,

$$\| \beta_x \|_{x=-a} = 0 . \qquad (4.4.29)$$

Since the slope of the bottom is discontinuous at the joint point x=-a, then the second-order derivative of the bottom with respect to x may be unbounded there. Consequently, in view of equations (4.4.2), (4.4.3) for region I and (4.4.14), (4.4.15) for region II, the bottom pressure $\bar{p}$ may be unbounded at x=-a as well, while the integral pressure P_{II} will remain bounded. Keeping this background in mind, we introduce the following definitions in conjunction with the jump conditions (4.4.22)-(4.4.24):

$$F_1 = \lim_{\delta \to 0} \int_{-a-\delta}^{-a+\delta} (-\bar{p}\, \alpha_x) dx,$$

$$F_3 = \lim_{\delta \to 0} \int_{-a-\delta}^{-a+\delta} [\bar{p}\,] dx ,$$

$$L = \lim_{\delta \to 0} \int_{-a-\delta}^{-a+\delta} [\bar{p}\, \alpha] dx . \qquad (4.4.30a, b, c)$$

Thus the jump conditions at x=-a become

$$\| u_0 \phi_0 \|_{x=-a} = 0 , \qquad (4.4.31)$$

$$\left\| \rho Q u_0 + P_0 \right\|_{x=-a} = F_1, \tag{4.4.32}$$

$$\left\| \rho Q u_0 \psi_x \right\|_{x=-a} = F_3, \tag{4.4.33}$$

$$\lim_{\delta \to 0} \int_{-a-\delta}^{-a+\delta} \left[\rho Q \psi (u_0 \psi_x)_x + \frac{1}{12} \rho Q^2 \varphi \left(\frac{\varphi_x}{\varphi} \right)_x \right] dx = L . \tag{4.4.34}$$

In addition, from (4.4.26) and (4.4.29) we have

$$\left\| \phi_{0x} \right\|_{x=-a} = -K . \tag{4.4.35}$$

$$\left\| \psi_x \right\|_{x=-a} = \tfrac{1}{2} K . \tag{4.4.36}$$

However, since F_1, F_3 and L are all unknown, the jump conditions (4.4.32)-(4.4.34) are of little help before the solution is obtained. On the other hand, in addition to the jump conditions derived from the geometric relations at x =-a, that is, (4.4.28a, b), (4.4.35) and (4.4.36), another jump condition is needed. Recall that when we assumed that the fluid is incompressible, inviscid and homogeneous, we noted that the conservation laws of energy and momentum are identical and thus we omitted the energy equation in the derivation of jump conditions for Green-Naghdi method. However, in present problem there are changes of momentum across x = -a due to the effect of discontinuity of the slope of the bottom, that is, some part of momentum will be transformed to the forces. These forces, say F_1 and F_3, are part of the solution and unknown beforehand. On the other hand, because the fluid is assumed to be inviscid and incompressible and no hydraulic jumps occur, it is expected that there is no changes of mechanical energy across x = -a. Consequently, the jump conditions based on the law of

conservation of momentum are of little help to solve this problem. Therefore, we now derive jump conditions based on the energy equation for Green-Naghdi Level-I theory. Because we did not give any results regarding of the energy equation, we have to start from the very beginning. The detail derivation is presented in Appendix A.

In Appendix A, we have obtained the general form of jump condition associated with the energy equation, that is,

$$\left\| \frac{1}{2}\rho u_0 \phi_0 \left(u_0^2 + u_0^2 \psi_x^2 + \frac{1}{12} u_0^2 \phi_{0x}^2 + 2g\psi \right) + u_0 P_0 \right\|_{x=-d} = 0. \qquad \text{(A.15a)}$$

or

$$\left\| \frac{1}{2}\rho Q \left(u_0^2 + u_0^2 \psi_x^2 + \frac{1}{12} u_0^2 \phi_{0x}^2 + 2g\psi \right) + u_0 P_0 \right\|_{x=-d} = 0. \qquad \text{(A.15b)}$$

Now we return to our original problem. Before we consider the jump condition (A.15), we consider the jump condition with respect to u_0. Actually, from the jump conditions (4.4.28a) and (4.4.31), we can immediately obtain

$$\| u_0 \|_{x=-d} = 0. \qquad \text{(4.4.37)}$$

Then taking into account the jump conditions (4.4.28b), (4.4.31) and (4.4.37), from (A.15) we obtain

$$\left\| \frac{1}{2}\rho Q \left(u_0^2 \psi_x^2 + \frac{1}{12} u_0^2 \phi_{0x}^2 \right) + u_0 P_0 \right\|_{x=-d} = 0. \qquad \text{(4.4.38)}$$

This is the desired remaining jump condition.

With the help of (4.4.38), we can obtain a relation between the constants of integration R_1 and R_2 in the governing equations (4.4.2) and (4.4.14). First let us consider the formula of (4.4.38) at the left side of x=-a, that is, $x = -a^-$. Substituting (4.4.2) into (4.4.38), we have

$$\left[\frac{1}{2}\rho Q\left(u_0^2\psi_x^2+\frac{1}{12}u_0^2\phi_{0x}^2\right)+u_0P_0\right]\Bigg|_{x=-a} = \rho Q\left(R_1-\frac{1}{2}g\phi_0-\frac{Q^2}{2\phi_0^2}+\frac{Q^2}{2\phi_0^2}\psi_x^2-\frac{Q^2}{8\phi_0^2}\phi_{0x}^2\right)_{x=-a} \quad (4.4.39)$$

In the same way, substituting (4.4.14) into (4.4.38) yields

$$\left[\frac{1}{2}\rho Q\left(u_0^2\psi_x^2+\frac{1}{12}u_0^2\phi_{0x}^2\right)+u_0P_0\right]\Bigg|_{x=-a^+} = \rho Q\left(R_2-\frac{1}{2}g\phi_0-g\alpha-\frac{Q^2}{2\phi_0^2}-\frac{Q^2}{2\phi_0^2}K^2+\frac{Q^2}{2\phi_0^2}\psi_x^2-\frac{Q^2}{8\phi_0^2}\phi_{0x}^2\right)_{x=-a^+} \quad (4.4.40)$$

With the use of jump conditions (4.4.28a, b), (4.4.31), (4.4.35) and (4.4.36), from (4.4.39) and (4.4.40) finally we can obtain

$$R_2 = R_1+\frac{Q^2}{2H_2^2}K^2-\frac{Q^2}{2H_2^2}K\phi_{0x}^- \quad . \quad (4.4.41)$$

where H_2 denotes the thickness of the fluid at x=-a, and ϕ_{0x}^- the slope of the thickness at the left side of x=-a.

Now we have obtained sufficient jump conditions at the joint point x=-a. For later convenience, we summarize them in the following:

Geometric jump conditions:

$$\left\| \phi_0 \right\|_{x=-a} = 0; \qquad \left\| \psi \right\|_{x=-a} = 0;$$

$$\left\| \phi_{0x} \right\|_{x=-a} = -K; \quad \left\| \psi_x \right\|_{x=-a} = \tfrac{1}{2}K.$$

Physical jump conditions:

$$\left\| Q \right\|_{x=-a} = 0;$$

$$\left\| \frac{1}{2}\rho Q\left(u_0^{\,2}\psi_x^{\,2} + \frac{1}{12}u_0^{\,2}\phi_{0x}^{\,2} \right) + u_0 P_0 \right\|_{x=-a} = 0.$$

Then with the help of the jump conditions and the governing equations, we can completely solve this problem by numerical calculation.

4.4.3 Results and discussion

By way of illustration, we calculated a case where the thickness of the fluid far upstream is H_1 = 1m, and the inclined bottom starts from x = -3m with a constant slope K = 0.1. Fig. 4.4.2 depicts the numerical results for three values of the Froude number Fr = 1.365, 2.0 and 3.0. It is clear from the figure that the fluid is "lifted up" due to the existence of the inclined bottom, and the inclined bottom appears to have more effect on lower Froude number cases. At the same time, Fig. 4.4.3 shows the distribution of local Froude number throughout the flow region. After observing Fig. 4.4.3, we find that although the local Froude number is continuous at x = -3m, the first-order derivative is discontinuous, where the discontinuity of the slope of bottom occurs. As a result, there is

a "corner" at x = -3.0m, as shown in Fig. 4.4.3. The higher the Froude numbers at far upstream, the sharp the corner becomes and the bigger the discontinuity is at this junction. Fig. 4.4.4 and Fig. 4.4.5 depict the integral pressure P_0 and the bottom pressure $\bar{p}$ throughout the flow region respectively. Here the Froude number far upstream Fr = 1.365, and the inclined bottom starts from x =-3m with the slope K = 0.1. From both figures, we find clearly that there exist sharp jumps on the value of P_0 and $\bar{p}$ at x = -3m. These jumps are obviously due to the discontinuous slope of bottom. At the same time, Fig. 4.4.4 indicates that the integral pressure P_0 is continuous at x = 0, while Fig. 4.4.5 shows that the bottom pressure $\bar{p}$ at $x = 0^-$ is not equal to zero, that is, $\bar{p}$ is not continuous at x =0. This result is consistent with what Naghdi & Rubin (1981) obtained when they dealt with the waterfall over a flat bottom.

Furthermore, during the calculation, we found that the minimum upstream Froude number for which a numerical solution was possible is greater than 1, which is consistent with what we concluded in §4.3. For instance, in this particular case we found that the minimum upstream Froude number Fr_{min} is around 1.365. Again, this result is different from the free waterfall problem, where the minimum Froude number is 1. It seems that more energy is needed to "overcome" the inclined bottom than the flat bottom. Under this particular case the minimum local Froude number is slightly below 1 (see Fig. 4.4.3). The minimum upstream Froude number was also obtained for another case, where the slope of the inclined bottom was half of that above, i.e., K = 0.05. We found that the minimum Froude number at far upstream for this case is Fr_{min} = 1.175, as shown in Fig. 4.4.7. Fig 4.4.6 indicates that the minimum local Froude number in this case is near 0.9. This result

is consistent with what we obtained for smooth bottoms in §4.3. That is, for free waterfalls over a non-flat bottom, the local Froude number may be less than 1. In our knowledge, this conclusion has not been obtained before.

Fig. 4.4.8, 4.4.9 and 4.4.10 describe the numerical results for different slopes of the bottom under the same Froude number at far upstream, that is, K = 0.25, 0.50 and 0.95. The distance in region II is set to be 1m and the Froude number far upstream Fr = 2.0. Investigation of these figures indicates that the steeper the slope K, the higher and steeper the elevation of the free surface. Under the same circumstance, in Fig. 4.4.11, the local Froude numbers throughout the region for different K are illustrated. From Fig. 4.4.11, we find that the Froude number downstream is greater than that upstream when K=0.25. However, when K = 0.5 and 0.95, the Froude number downstream is less than that upstream. This result means that the loss of momentum is higher for larger K. More precisely, more momentum is transferred to the force acting on the bottom for the steeper bottom in region II, which results in the decrease of the Froude number.

Actually, here the inclined bottom can be regarded as the inclined weir, thus this problem becomes the flow over a inclined weir in a channel with a finite depth. To our knowledge, supercritical solutions with an inclined weir in water of finite depth have not been calculated in the past. Of particular interest for the inclined weir problem is the thickness of the water over the top of the inclined weir, say H_3 here. Fig. 4.4.12 depicts the elevation of the free surface relative to the elevation of the top of the weir as a function of the slope of the inclined weir. During this calculation the Froude number is

fixed at Fr = 2.0 and the distance of the weir in the horizontal coordinate is fixed at a = 1.0m. In the range of the inclined weirs we calculated, the thickness of water H_3 increases with the slope K. However, limited by the nature of Green-Naghdi Level I theory, we can only calculate small values of K. When the slope is too steep, the assumption of the profile of the velocity is not valid any longer, thus the numerical calculation is perhaps not valid. Actually, the calculation breaks down when K is larger than a certain value. For instance, in this case the maximum value of K is $K_{max} = 1.0$. Fig. 4.4.10 shows the top and bottom surfaces when K is close to the maximum slope, that is, K = 0.95. In Fig. 4.4.11 the local Froude number throughout the region is illustrated. From Fig. 4.4.11 we find that the minimum local Froude number is below 0.7, and occurs somewhere after x = -1.0m, while for K=0.25 and 0.5 the minimum local Froude number is greater than 1 and occurs at x = -1m. Moreover, the Froude number far downstream is less than 1, although the Froude number far upstream is greater than 1. This means that the downstream flow is subcritical while the far upstream flow is supercritical. Actually, from Fig. 4.4.11 we can find that even from some distance before x = -1m, the flow has already become subcritical. Although the Froude number increases in the neighborhood of the lip of the waterfall, i.e., x =0, the flow keeps subcritical.

When the inclined bottom becomes vertical, this problem becomes the classical weir problem. A special approach needs to be employed in this case because the jump conditions at x=0 are not valid any longer. This problem will be discussed in a subsequent chapter.

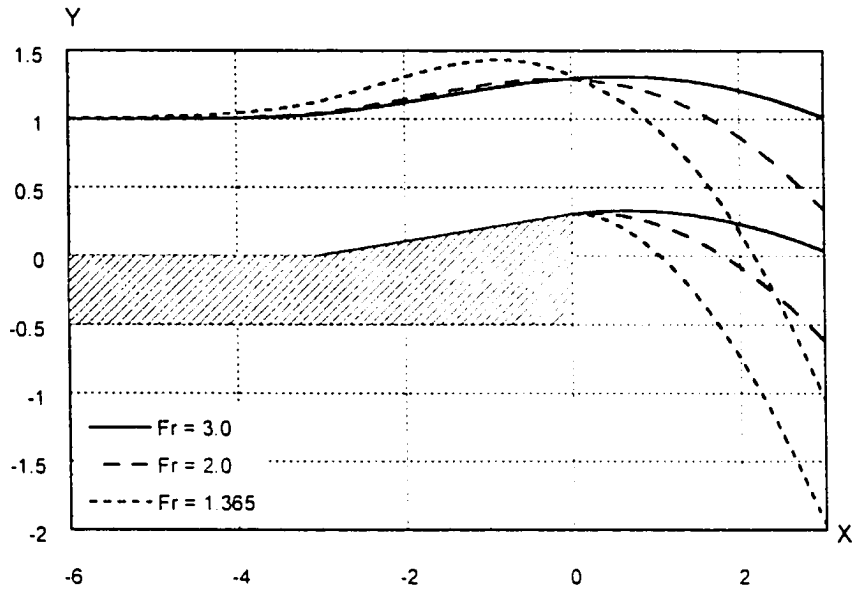

Fig. 4.4.2 Numerical results for flow over an inclined bottom for different Fr

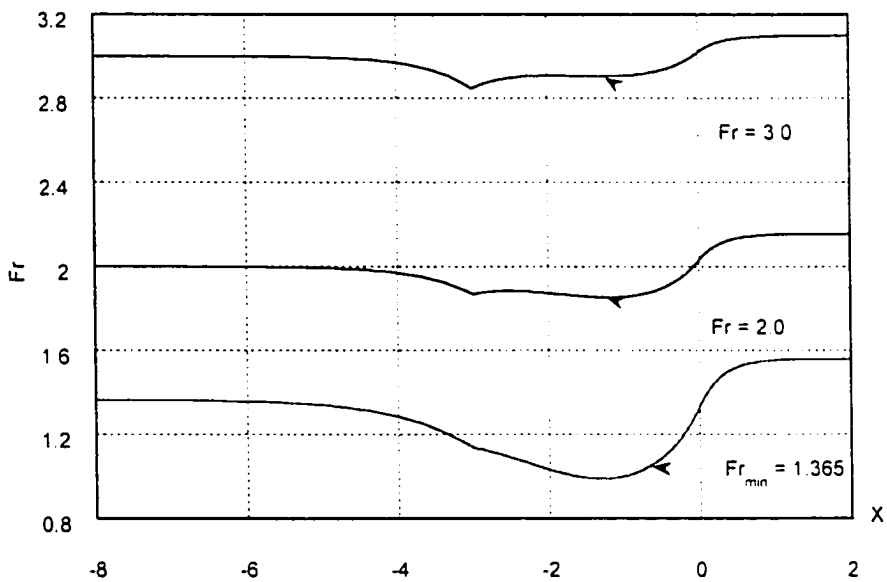

Fig. 4.4.3 Distribution of local Froude number under different Fr far upstream

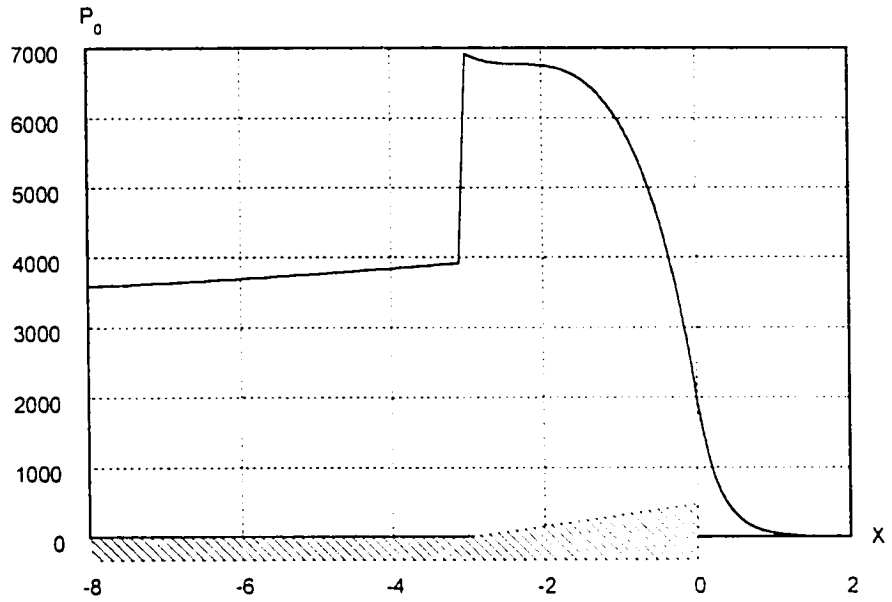

Fig 4.4.4 Plot of the integral pressure P_0 in the whole region (K=0.1, Fr = 1.365)

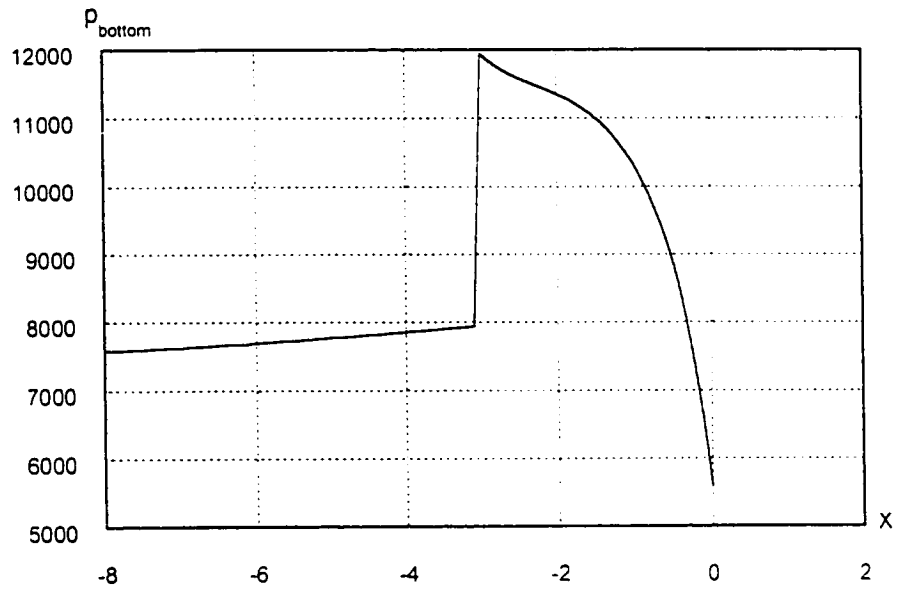

Fig. 4.4.5 Plot of the pressure on the bottom in region I (K=0.1, Fr=1.365)

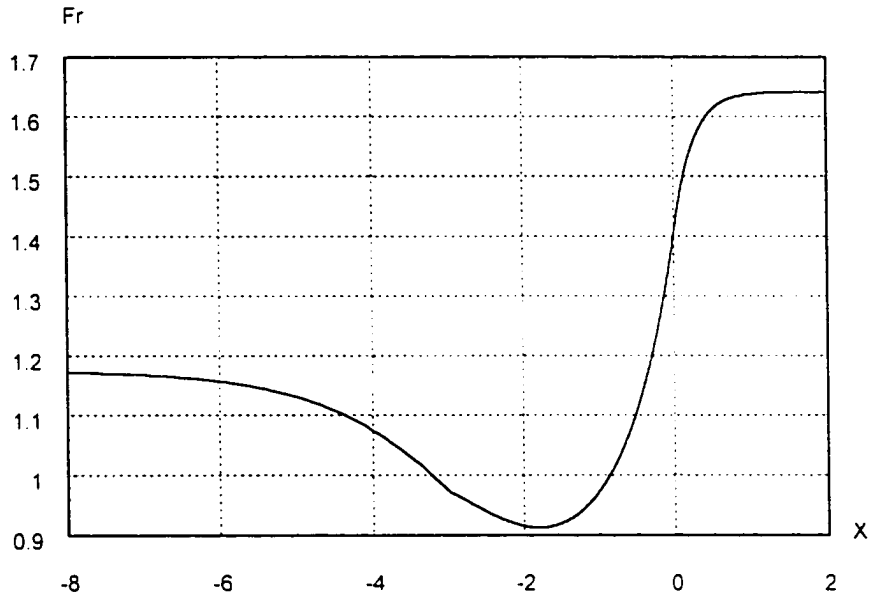

Fig. 4.4.6 Plot of local Froude number for the minimum Fr (K=0.05, a=3m)

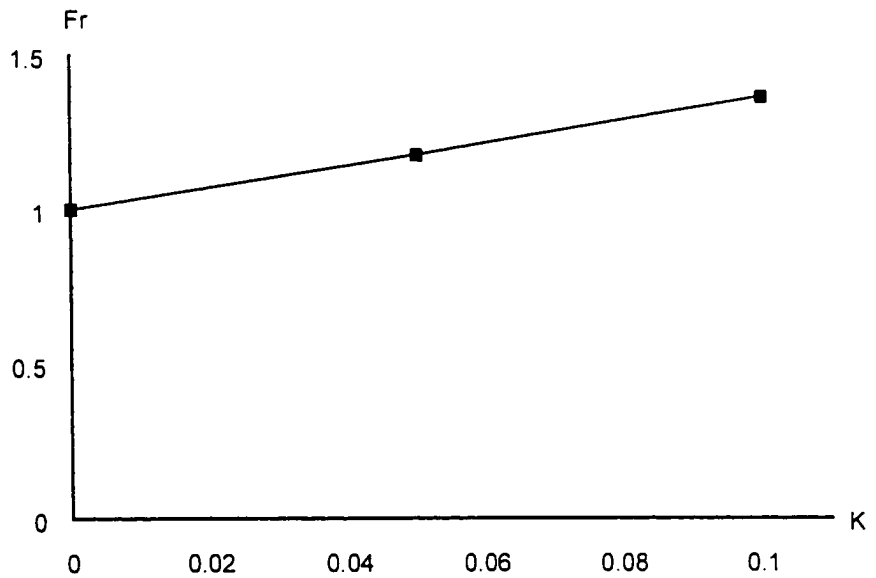

Fig. 4.4.7 Minimum upstream Froude number for different slopes of bottom K

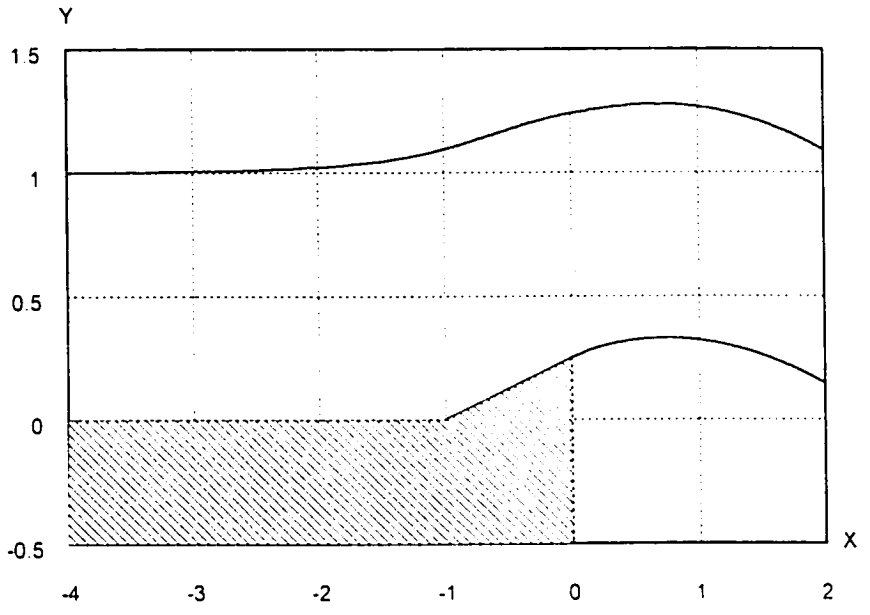

Fig. 4.4.8 Plot of the top and bottom surfaces for K = 0.25

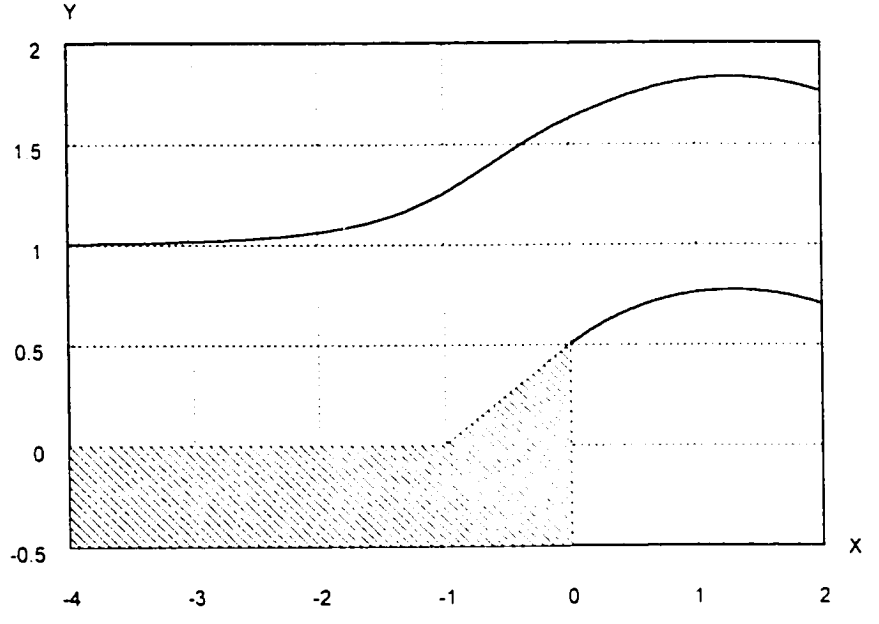

Fig. 4.4.9 Plot of top and bottom surfaces for K = 0.5

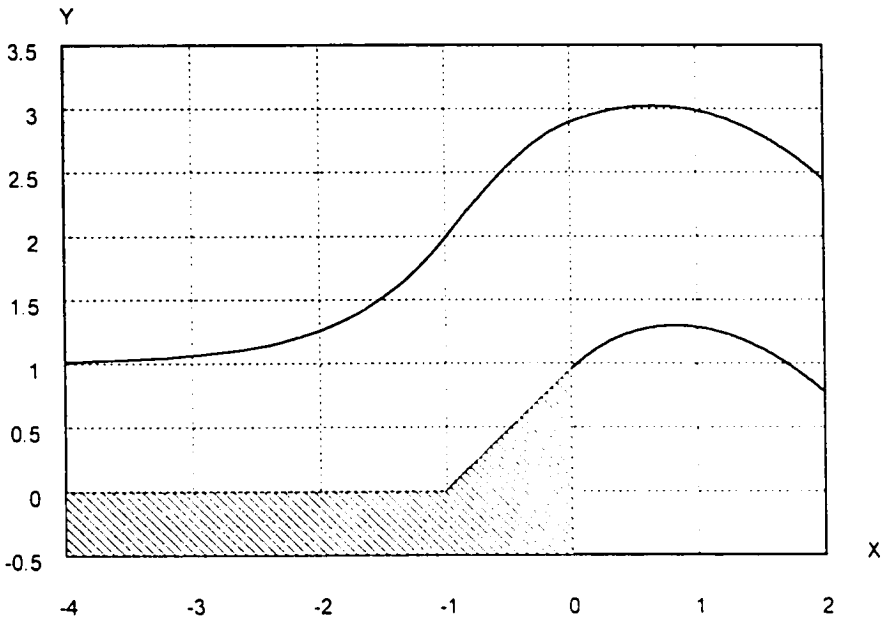

Fig. 4.4.10 Plot of the top and bottom surfaces for K = 0.95

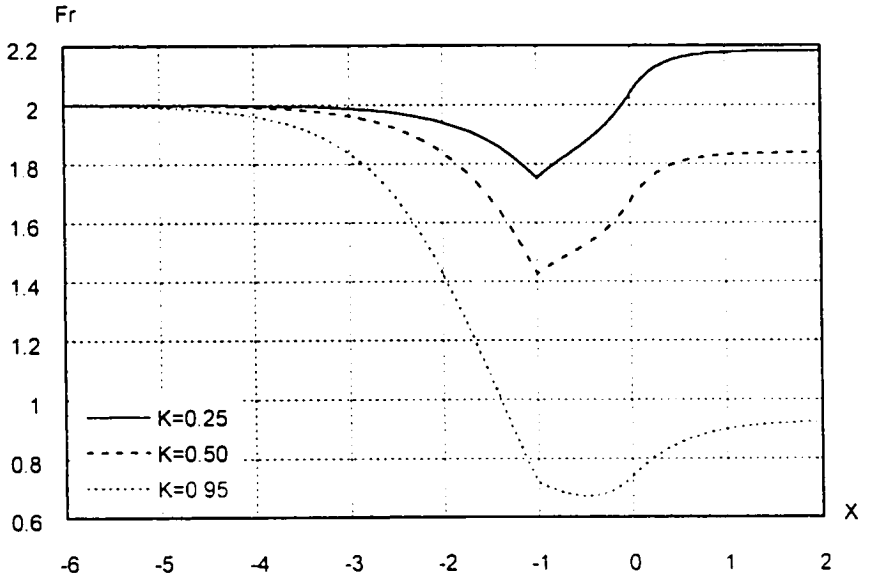

Fig. 4.4.11 Plot of the local Froude numbers for different K

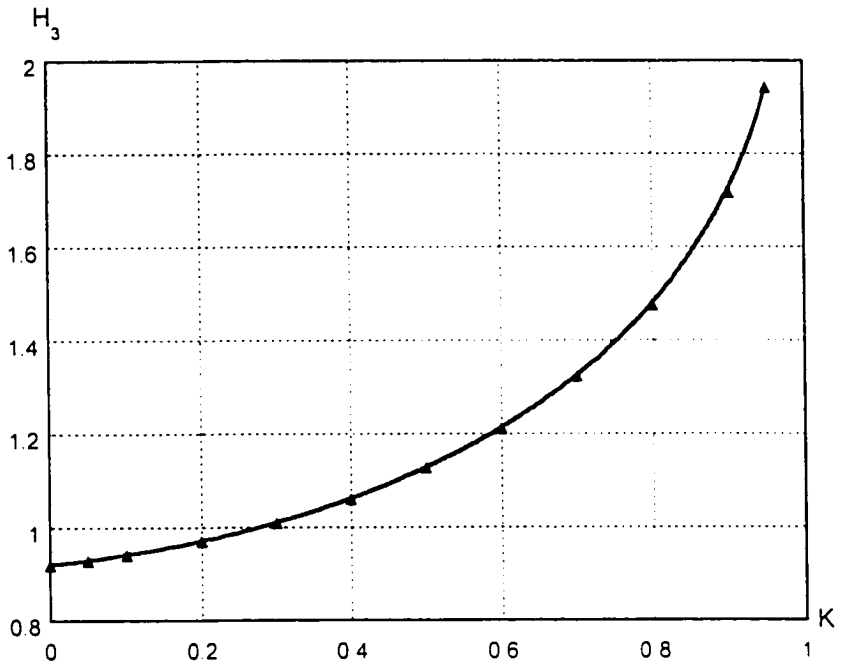

Fig. 4.4.12 The elevation of the free surface over the top of the inclined weir as a function of the slope of bottom K, and the triangle symbol indicates the data we calculated.

Chapter 5

Steady Inviscid Flow under a Sluice Gate

In Chapter 4 we have discussed the problems of free waterfall departing from different kinds of bottom surfaces by means of Green-Naghdi method and associated jump conditions. The results showed that the jump conditions are necessary and crucial to determine the solution of free waterfall problem. The application of jump conditions is required due to the characteristics of the bottom of the flow field, i.e., the sudden disappearance of the bottom or the discontinuities of the slope of the bottom at certain points. In this chapter, jump conditions will be applied due to different characteristics of top surfaces of the flow field. The flow under a sluice gate is a typical of this kind of flow and is the focus of this chapter. Another reason to consider the flow under a sluice gate is that the downstream part of the flow is similar in principle to the second region of the breaking wave (see Fig. 1.1). At the same time, other flows related to the flow under a sluice gate are also discussed.

The sluice gate problem, involving a free surface in the presence of gravity, is extremely difficult from the point of view of three-dimensional inviscid fluid theory. It is a typical hydraulic problem and is well studied. Mostly, conformal mapping is employed to solve this problem (Pajer1937, Marchi 1953, Birkhoff & Zarantonello 1957, Klassen 1967, Milne-Thomson 1968). Benjamin (1956) improved this method by considering separately a region in the vicinity of the sluice gate starting from a point somewhat downstream. After employing a different approximation of the three-dimensional

equations in each region, he joined the respective free surface lines at the selected point of division.

Caulk (1976) employed a completely different method, the two-dimensional theory of the directed fluid sheet, to solve this sluice problem without a priori restriction on the shape of the free surface. To date, this appears to be the only paper employing the directed theory to solve the sluice gate problem. However, due to the early stage of the development of the directed theory (Green-Naghdi theory), the method Caulk used is posed in Lagrangian frame. In this chapter we will use the Green-Naghdi governing equations and associated jump conditions to solve the same problem in an Eulerian frame. In addition, some particular problems related to the sluice gate problem are discussed and solved by means of Green-Naghdi method.

§5.1 Flow under a vertical sluice gate

A sluice gate is a frequently employed means of open channel control. As a result, it is well studied by means of classical theories, such as conformal mapping. Here we will study this problem with the Green-Naghdi theory and the jump conditions developed Chapter 2 and 3. At the same time, the results of previous chapters will be applied directly if appropriate. In this section, the sluice gate is restricted to be vertical. Before going further, it is expedient to explicitly state the problem for later reference.

Consider the steady two-dimensional flow of an inviscid, incompressible fluid through a fixed vertical sluice gate in the presence of gravity (see Figure 5.1.1). For the purpose of simplification, we suppose that on both sides of the sluice the fluid is flowing over flat bottom, and the top surface is free. The lower edge of the sluice is raised a distance d from the flat bottom. In addition, here we assume that the flow extends to a uniform stream at infinity in both directions.

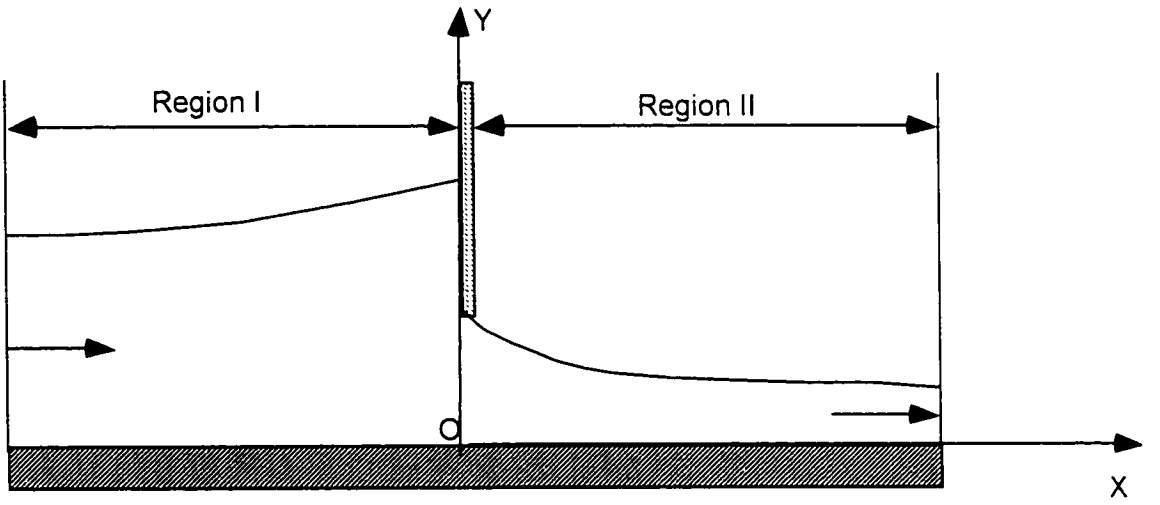

Fig. 5.1.1 Schematic of flow under a vertical sluice gate

From Fig. 5.1.1, we find that the flow region is divided into two parts by the vertical sluice gate. At the same time, due to the existence of the sluice gate, the free surfaces at sides of the gate are discontinuous. Before deriving the governing equations for each region, we choose a coordinate system such that the x-axis lies on the flat bottom surface and the origin of the x coordinate coincides with the position of the sluice gate, as shown in Fig 5.1.1. Then we distinguish the two regions as: (i) upstream region I, $x \leq 0$; and (ii) downstream region II, $x \geq 0$. We can find that both of the regions are characterized with a

free surface and a flat bottom. The difference relies only on the boundary conditions. Therefore, their governing equations are expected to be similar. For simplification, we may just derive the Green-Naghdi governing equations for region I. Then we apply the obtained governing equations to region II by replacing the boundary conditions in region I with those in region II.

5.1.1 Governing equations for region I and II

At the top free surface, the pressure is equal to the atmospheric pressure. Without loss of generality, we set the atmospheric pressure to be equal to zero. Then the pressure at the top surface for both regions is zero, that is, $\hat{p} \equiv 0$ everywhere. On the other hand, because we chose the x-axis to lie on the flat bottom, the bottom can be denoted by

$$\alpha = 0. \tag{5.1.1}$$

As for the boundary conditions, we have assumed that the flow far upstream is uniform. Then we can have the boundary conditions far upstream:

$$\begin{aligned} &\text{as } x \to -\infty, \\ &\phi_0 \to H_1,\ \ \phi_{0x} \to 0,\ \ u_0 \to U_1,\ \ P_0 \to \tfrac{1}{2}\rho g H_1^2. \end{aligned} \tag{5.1.2}$$

where, H_1 denotes the thickness of the fluid at far upstream, and U_1 denotes the uniform velocity of the flow at far upstream. The values of H_1 and U_1 are given beforehand.

Then, based on the results of previous chapter, the governing equations of region I can be derived as:

$$\frac{1}{3}Q^2\phi_{0x}{}^2=\left(\frac{Q^2}{H_1{}^2}-g\phi_0\right)(\phi_0-H_1)^2. \tag{5.1.3}$$

$$\frac{P_0}{\rho}=\phi_0\left[R_1-\frac{1}{2}g\phi_0-\frac{1}{2}\frac{Q^2}{\phi_0{}^2}-\frac{1}{6}Q^2\frac{\phi_{0x}{}^2}{\phi_0{}^2}\right]. \tag{5.1.4}$$

$$\frac{\bar{p}}{\rho}=g\phi_0-\frac{Q^2\phi_{0x}{}^2}{2\phi_0^2}+\frac{Q^2\phi_{0xx}}{2\phi_0}. \tag{5.1.5}$$

where the constants of integration are

$$Q=U_1H_1. \tag{5.1.6}$$

$$R_1=gH_1+\frac{1}{2}\frac{Q^2}{H_1{}^2}. \tag{5.1.7}$$

Now we consider the governing equations of region II. Recall that we have assumed that the flow far downstream approaches uniform. Then the boundary conditions far downstream can be described as:

$$\text{as } x\to+\infty,$$
$$\phi_0\to H_4,\ \phi_{0x}\to 0,\ u_0\to U_4,\ P_0\to\tfrac{1}{2}\rho gH_4{}^2. \tag{5.1.8}$$

where H_4 denotes the thickness of the fluid at far downstream, and U_4 the uniform velocity of the fluid at far downstream. Both of them are unknown and need to be determined as a part of the solution.

Since region II has similar characteristic to region I, then we can easily obtain the governing equations of region II:

$$\frac{1}{3}Q^2\phi_{0x}{}^2=\left(\frac{Q^2}{H_4{}^2}-g\phi_0\right)(\phi_0-H_4)^2. \tag{5.1.9}$$

$$\frac{P_0}{\rho}=\phi_0\left[R_2-\frac{1}{2}g\phi_0-\frac{1}{2}\frac{Q^2}{\phi_0^2}-\frac{1}{6}Q^2\frac{\phi_{0x}^2}{\phi_0^2}\right], \tag{5.1.10}$$

$$\frac{\overline{p}}{\rho}=g\phi_0-\frac{Q^2\phi_{0x}^2}{2\phi_0^2}+\frac{Q^2\phi_{0xx}}{2\phi_0}. \tag{5.1.11}$$

where, R_2 is a constant of integration to determined as part of the solution.

5.1.2 Jump conditions

Now that we have obtained the governing equations of region I and II. However, due to the unknown constants of integration involved in the equations, we cannot solve them until the constants are determined and boundary conditions are specified. Thus the jump conditions become crucial to determine the solution, since they can not only determine the constants, but also provide the necessary boundary conditions. Different from the free waterfall problems discussed in the previous chapter, the sluice gate problem involves a dramatic jump in the variables due to the existence of the sluice gate. For instance, the free surface is discontinuous at the location of the sluice gate, x=0. Before turning to the jump conditions associated with physical laws, we investigate the geometric relation between the sides of the sluice gate. Limited by the sluice gate, the free surface at $x=0^-$ is equal to the distance of the low end of the sluice gate from the flat bottom, that is,

$$\beta|_{x=0^-}=d. \tag{5.1.12}$$

At the same time, the bottom surface is unchanged across the sluice gate. Then we can have

$$\alpha|_{x=0^-} = \alpha|_{x=0^+} = 0. \tag{5.1.13}$$

$$\alpha_x|_{x=0^-} = \alpha_x|_{x=0^+} = 0. \tag{5.1.14}$$

Now we consider the jump conditions associated with the laws of conservation of mass and momentum. Recall that the general jump conditions are

$$\| Q \|_{x=0} = 0, \tag{5.1.15}$$

$$\| \rho Q u_0 + P_0 \|_{x=0} = \lim_{\delta \to 0} \int_{-\delta}^{+\delta} (\hat{p}\,\beta_x - \bar{p}\,\alpha_x) dx. \tag{5.1.16}$$

$$\| \rho Q u_0 \psi_x \|_{x=0} = \lim_{\delta \to 0} \int_{-\delta}^{+\delta} [-\hat{p} + \bar{p} - \rho g \phi_0] dx. \tag{5.1.17}$$

$$\lim_{\delta \to 0} \int_{-\delta}^{+\delta} \left[\rho Q \psi (u_0 \psi_x)_x + \frac{1}{12} \rho Q^2 \phi_0 \left(\frac{\phi_{0x}}{\phi_0} \right)_x \right] dx = \lim_{\delta \to 0} \int_{-\delta}^{+\delta} [P_0 - \rho g \phi_0 \psi - \hat{p}\beta + \bar{p}\alpha] dx. \tag{5.1.18}$$

Due to the approximate nature of the theory utilized here, from (5.1.9) we anticipate that at the right side of sluice gate the slope of the top surface may be finite, instead of being infinite as would be the case in the exact treatment. Then we expect that there is a finite jump in the slope of the thickness at x=0 in addition to a discontinuity of the thickness of the fluid there. In the event that ϕ_{0x} is discontinuous at x=0, an examination of (5.1.10) and (5.1.11) reveals that the bottom pressure $\bar{p}$ may be unbounded there, while the integral pressure P_0 will remain bounded. Keeping this background in mind, in conjunction with the jump conditions (5.1.16), (5.1.17) and (5.1.18), we introduce the following definitions:

$$\lim_{\delta\to 0}\int_{-\delta}^{+\delta}(\hat{p}\,\beta_x-\bar{p}\,\alpha_x)dx=F_1, \tag{5.1.19}$$

$$\lim_{\delta\to 0}\int_{-\delta}^{+\delta}[-\hat{p}+\bar{p}-\rho g\phi_0]dx=F_3. \tag{5.1.20}$$

$$\lim_{\delta\to 0}\int_{-\delta}^{+\delta}[P_0-\rho g\phi_0\psi-\hat{p}\beta+\bar{p}\alpha]dx=L. \tag{5.1.21}$$

where F_1, F_3 and L represent the total horizontal force on the sluice gate, the additional vertical force on the bottom near the sluice gate and arising from its disturbance of the flow, and the z-moment on the sluice gate, respectively. The jump conditions (5.1.15)-(5.1.18) become

$$\| Q \|_{x=0}=0, \tag{5.1.22}$$

$$\| \rho Q u_0+P_0 \|_{x=0}=F_1, \tag{5.1.23}$$

$$\| \rho Q u_0 \psi_x \|_{x=0}=F_3, \tag{5.1.24}$$

$$\lim_{\delta\to 0}\int_{-\delta}^{+\delta}\left[\rho Q\psi(u_0\psi_x)_x+\frac{1}{12}\rho Q^2\varphi\left(\frac{\varphi_x}{\varphi}\right)_x\right]dx=L. \tag{5.1.25}$$

Up to this point, we have obtained the geometric relations (5.1.12), (5.1.13) and (5.1.14), and the jump conditions (5.1.22)-(5.1.25). However, F_1, F_3 and L are all unknown and can be determined only after the solutions have been obtained. Thus (5.1.23)-(5.1.25) are provide no additional information to solve the problem. An additional jump condition is needed. Recall that the momentum equations are identical to the energy equations for the incompressible, inviscid fluid. However, in the sluice gate problem, due to the existence a force on of the sluice gate (F_1), the x-momentum across

the juncture x=0 will change. But according to the conservation law of energy, the mechanical energy across x = 0 are still equal, since the fluid is assumed to be inviscid and incompressible and no work is done on the sluice gate. Thus it is desirable to apply the jump condition associated with the energy equation. The general form of this jump condition is described as

$$\left\| \frac{1}{2}\rho u_0 \phi_0 \left(u_0^{\,2} + u_0^{\,2}\psi_x^{\,2} + \frac{1}{12}u_0^{\,2}\phi_{0x}^{\,2} + 2g\psi \right) + u_0 P_0 \right\|_{x=0} = 0. \qquad (5.1.26)$$

Since the bottom is flat everywhere, then we have

$$\psi = \frac{1}{2}\phi_0, \text{ and } \psi_x = \frac{1}{2}\phi_{0x}. \qquad (5.1.27a, b)$$

Inserting (5.1.27a, b) into (5.1.26), we arrive at

$$\left\| \frac{1}{2}\rho u_0 \phi_0 \left(u_0^{\,2} + \frac{1}{3}u_0^{\,2}\phi_{0x}^{\,2} + g\phi_0 \right) + u_0 P_0 \right\|_{x=0} = 0. \qquad (5.1.28)$$

Now with help of (5.1.28), we have sufficient conditions to link the solutions of region I and II.

5.1.3 Solutions

Before solving this problem, we compare these equations and jump conditions with those of Caulk (1976). In order to make a comparison, we first non-dimensionalize the

governing equations (5.1.9) and (5.1.3) and introduce the definition of the Froude number far downstream:

$$Fr_2 = \frac{U_4}{\sqrt{g H_4}}. \tag{5.1.29}$$

Introducing the notation

$$\eta = \eta(\bar{x}) = \frac{\phi_0}{H_4}, \ \bar{x} = \frac{x}{H_4}, \tag{5.1.30}$$

then (5.1.9) can be non-dimensionalized as

$$\frac{1}{3} Fr_2^2 (\eta')^2 = (Fr_2^2 - \eta)(\eta - 1)^2. \tag{5.1.31}$$

In the same way, by defining the Froude number at far upstream

$$Fr_1 = \frac{U_1}{\sqrt{g H_1}}, \tag{5.1.32}$$

the governing equation of region I (5.1.3) can be written as

$$\frac{1}{3} Fr_1^2 (\theta')^2 = (Fr_1^2 - \theta)(\theta - 1)^2, \tag{5.1.33}$$

where,

$$\theta = \theta(\tilde{x}) = \frac{\phi_0}{H_1}, \ \tilde{x} = \frac{x}{H_1}. \tag{5.1.34}$$

We find that (5.1.31) and (5.1.33) are exactly same as (4.22) and (4.31), respectively, in the paper of Caulk (1976). In addition, the jump conditions (5.1.22) and (5.1.28) are equivalent to (3.7a) and (3.15) respectively in Caulk's paper. It is clear then that our

method is equivalent to the directed theory employed by Caulk, although our theory is based on the Eulerian frame. Due to the equivalent equations and jump conditions we obtained, we will not repeat in detail the calculation of the flow under a vertical sluice gate, as Caulk did. Instead, we make a comparison between our results and the numerical results of Isaacs (1977) using finite element technique. In addition, we compare both solutions with the experimental results of Smetana (1948). Here the experimental results of Smetana are obtained from Figure 5-64 in *Hydraulics of Open Channel Flow* by Montes (1998). Fig. 5.1.2 depicts these results for the vertical sluice gate problem, where, the flow flux Q = 1.3 ft^2/s, the gate opening d = 0.3 ft, and H_1 =1.0 ft. Superimposed on the experimental data is the theoretical profile obtained from the classical gravity-free inviscid theory of Kirchoff (Montes, 1998), and the theoretical profile is slightly adjusted to take into account the empirical contraction ratio of 0.64. The comparison shows that our analysical solution is in good agreement with the numberical results of Isaacs (1977). When compared with the experimental results of Smetana (1948), there exists some difference for both theoretical solutions when x > 0.15. These difference between theoretical and experimental results may be explained by the existence of a boundary layer near the bottom, where the viscocity of the fluid plays an important role in reality. However, both our solution and that of Isaacs neglect the effect the viscocity by assuming that the fluid is inviscid. However, same as the waterfall problem, in reality the uniform flows in far upstream and downstream do not exist for invicid flows, because the gravity will be balanced with the friction.

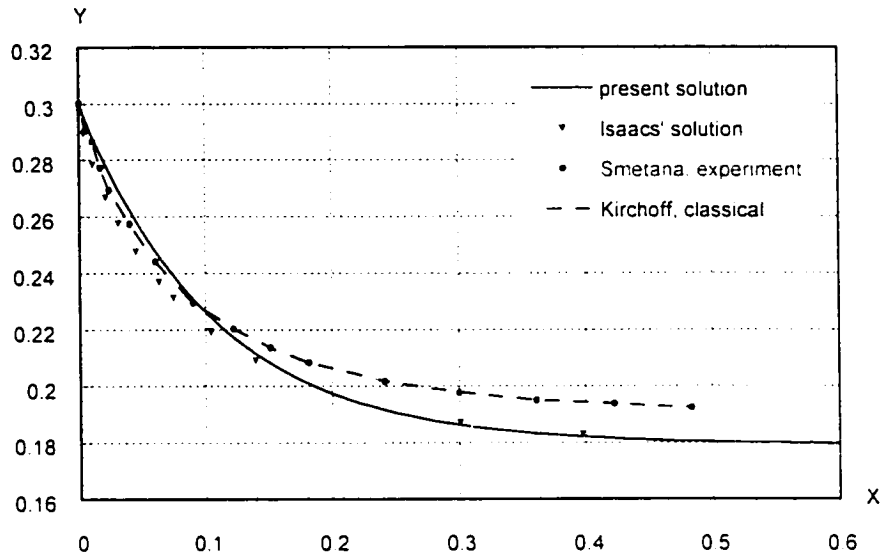

Fig. 5.1.2 Profile of the water surface below a vertical gate, comparison of present solution, numerical results of Isaacs and the experimental results of Smetana (1948).

In the following sections we will consider a few particular problems related to the sluice gate problem. The first problem we consider is the flow through a horizontal sluice gate. In other word, we consider the flow departing from confined parallel flat surfaces.

§5.2 Flow departing from confined parallel flat surfaces

In this section we consider a relatively simple problem, that is, the flow departs from the confined parallel top and bottom surfaces. As we said in above section, this problem can be regarded as a particular case of the sluice gate problem, that is, when the sluice gate is horizontal. Before further proceeding, it is expedient to explicitly state the problem for later convenience.

Consider the steady, two-dimensional flow of an inviscid, incompressible fluid departing from two confined parallel surfaces (as shown in Fig. 5.2.1). Here the effect of surface tension is assumed negligible. From Fig. 5.2.1, we can find that two distinct regions of flow are associated with this problem. The upstream region is characterized by two fixed flat surfaces. In the downstream the top surface is free and the bottom is flat. Far upstream the fluid is assumed to flow as uniform stream. Of particular interest in analyzing this problem is the prediction of the location of the free surface downstream. Here it is assumed that a hydraulic jump does not occur. We expect that the fluid departs smoothly from the upstream region, and the free surface remains smooth in the downstream region. Contrary to the vertical sluice gate problem, we do not adopt the assumption that the far downstream flow is uniform. As a result, waves may occur in the downstream region.

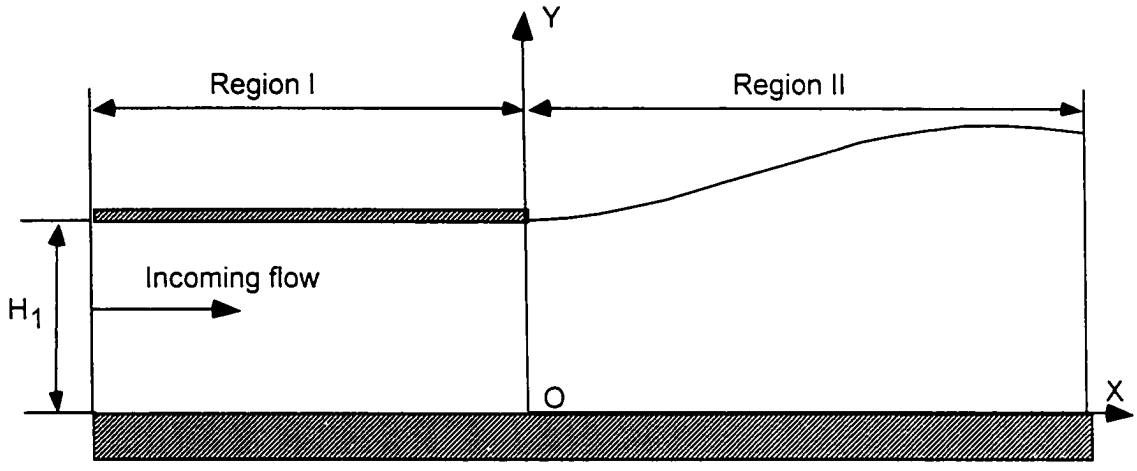

Fig. 5.2.1 Schematic of the flow departing from confined parallel flat surfaces

5.2.1 Governing equations for region I

The upstream is an interesting region, where the fluid is bounded by two confined parallel surfaces. We set up a coordinate system such that the bottom surface $\alpha = 0$ and the joint interface is located at x = 0. Since the top and bottom surfaces are confined and flat, and the far upstream is uniform, then according to the classical hydrodynamic method, that is, Euler equation, we expect that the flow in region I will keep uniform. Consequently, everything is determined, i.e., unchanged from the far downstream. However here we would like to solve this problem by means of Green-Naghdi Level I theory. We will derive the governing equations strictly following the method to see what results.

Recall that for Green-Naghdi Level-I theory, we have obtained in chapter 2 the governing equations for kinematic boundary conditions on material surfaces, continuity

equations and the conservation law for momentum. For two-dimensional, steady flow, the kinematic boundary conditions on top and bottom surfaces are

$$v_0 + v_1\alpha = u_0\alpha_x;$$
$$v_0 + v_1\beta = u_0\beta_x. \qquad (5.2.1a, b)$$

The continuity equations are

$$u_1 = 0.$$

$$u_{0x} + v_1 = 0 \qquad (5.2.2a, b)$$

The conservation law of momentum states:

$$u_{0t}\phi_0 + \phi_0 u_0 u_{0x} = \frac{1}{\rho}(-P_{0x} + \hat{p}\beta_x - \bar{p}\alpha_x)$$

$$\phi_1 u_0 u_{0x} = \frac{1}{\rho}(-P_{1x} + \hat{p}\beta\beta_x - \bar{p}\alpha\alpha_x)$$

$$\phi_0 u_0 v_{0x} + \phi_0 v_0 v_1 + \phi_1 u_0 v_{1x} + \phi_1 v_1 v_1 = \frac{1}{\rho}(-\rho g\phi_0 - \hat{p} + \bar{p}).$$

$$\phi_1 u_0 v_{0x} + \phi_1 v_0 v_1 + \phi_2 u_0 v_{1x} + \phi_2 v_1 v_1 = \frac{1}{\rho}(P_0 - \rho g\phi_1 - \hat{p}\beta + \bar{p}\alpha). \qquad (5.2.3a\text{-}d)$$

In region I, both the top and bottom surfaces are flat, and we have set up the coordinate system such that $\alpha = 0$ everywhere, and $\beta = H_1$ everywhere in region I. H_1 denotes the distance between the top and bottom surfaces in region I. Then with the help of these conditions, from (5.2.1a, b) we have

$$v_0 = 0, \text{ and} \qquad (5.2.4)$$

$$v_1 = 0. \tag{5.2.5}$$

(5.2.4) and (5.2.5) demonstrate that the vertical velocity of the fluid in region I is zero everywhere.

And from (5.2.2b) we have

$$u_{0,x} = 0. \tag{5.2.6}$$

which means that the horizontal velocity of the fluid in region I remains constant.

With the use of (5.2.4), (5.2.5) and (5.2.6), and taking into account that $\alpha = 0$ and $\beta = H_1$, we can obtain the conservation law of momentum as follows:

$$-\frac{P_{0x}}{\rho} = 0. \tag{5.2.7}$$

$$-\frac{P_{1x}}{\rho} = 0. \tag{5.2.8}$$

$$-\rho g \phi_0 - \hat{p} + \bar{p} = 0. \tag{5.2.9}$$

$$P_0 - \rho g \phi_1 - \hat{p} H_1 = 0. \tag{5.2.10}$$

By means of these equations we can obtain the distribution of $\bar{p}$, $\hat{p}$ and P_0 in region I. Actually, from (5.2.7) and (5.2.8), we can easily conclude that the integral pressure P_0 and P_1 remains constant throughout region I. Then by means of (5.2.9) and (5.2.10), we can find that the bottom pressure $\bar{p}$ and the top pressure $\hat{p}$ keep constant in region I. Thus, these results are consistent with those obtained from the classical method.

5.2.2 Governing equations for region II

Region II is characterized with a flat bottom and a free top surface. Because we did not adopt the assumption that the flow far downstream is uniform, we cannot use the governing equations obtained in above section. Thus we derive briefly the governing equations of region II. As usual, we set the atmospheric pressure be equal to zero, then from Chapter 2, we can obtain the Green-Naghdi governing equations as follows:

$$u_1 = 0, \tag{5.2.11}$$

$$u_{0,x} + v_1 = 0, \tag{5.2.12}$$

$$v_0 = 0, \tag{5.2.13}$$

$$v_0 + v_1\beta = u_0\beta_x, \tag{5.2.14}$$

$$\phi_0 u_0 u_{0x} = -\frac{1}{\rho} P_{0x}, \tag{5.2.15}$$

$$\phi_0 u_0 v_{0x} + \phi_0 v_0 v_1 + \phi_1 u_0 v_{1x} + \phi_1 v_1 v_1 = \frac{1}{\rho}(-\rho g \phi_0 + \bar{p}), \tag{5.2.16}$$

$$\phi_1 u_0 v_{0x} + \phi_1 v_0 v_1 + \phi_2 u_0 v_{1x} + \phi_2 v_1 v_1 = \frac{1}{\rho}(P_0 - \rho g \phi_1). \tag{5.2.17}$$

Here (5.2.11) is the restricted theory, and (5.2.12) is the continuity equation. (5.2.13) and (5.2.14) are the kinematic boundary conditions on the flat bottom and the free surface respectively. (5.2.15)-(5.2.17) are the conservation law of momentum.

Inserting (5.2.13) into (5.2.16) and (5.2.17), we can have

$$\phi_1 u_0 v_{1x} + \phi_1 v_1 v_1 = \frac{1}{\rho}(-\rho g \phi_0 + \bar{p}), \tag{5.2.18}$$

$$\phi_2 u_0 v_{1x} + \phi_2 v_1 v_1 = \frac{1}{\rho}(P_0 - \rho g \phi_1), \tag{5.2.19}$$

respectively.

Substituting (5.2.12) into (5.2.14), and integrating and replacing β with ϕ_0, we can obtain the familiar equation:

$$u_0 \phi_0 = Q, \tag{5.2.20}$$

where, Q is a constant of integration, and denotes the constant flux rate of the fluid.

Then with the help of (5.2.20), (5.2.15) can be integrated and a decent equation can be obtained:

$$\frac{P_0}{\rho} = -\frac{Q^2}{\phi_0} + S_2, \tag{5.2.21}$$

where S_2 is another constant of integration to be determined. This equation can be obtained due to the flat bottom in region II.

Substituting (5.2.21) into (5.2.19), and with the help of (5.2.12), finally we obtain a second-order differential equation with regards to ϕ_0 only:

$$\frac{Q^2}{3}\phi_0\phi_{0xx} - \frac{Q^2}{3}\phi_{0x}^2 + \frac{1}{2}g\phi_0^3 - S_2\phi_0 + Q^2 = 0. \tag{5.2.22}$$

This equation is different from (5.1.9), and is a second-order differential equation. We cannot integrate (5.2.22) because no assumption is made concerning the behavior far downstream.

At the same time, with the use of (5.2.12) and (5.2.20), from (5.2.18) we can obtain the bottom pressure in region II:

$$\frac{\bar{p}}{\rho} = g\phi_0 - \frac{Q^2\phi_{0x}{}^2}{2\phi_0^2} + \frac{Q^2\phi_{0xx}}{2\phi_0} . \tag{5.2.23}$$

Thus once the distribution of the thickness of the fluid in region II is obtained, the bottom pressure can be calculated through (5.2.23).

(5.2.21), (5.2.22) and (5.2.23) form the basic governing system for region II. Note that we derived the governing equation with a different strategy from that used in the previous chapter. Here we make full use of the assumption that the is flat bottom when we derive these equations, while in previous chapter we derived the governing equations from the general point of view, making the derivation much more complex.

5.2.3 Jump conditions

Up to this point we have obtained the governing equations for region I and II. Then jump conditions are necessary to match the solutions at the juncture point x=0. Recall that for Green-Naghdi Level-I theory, the jump conditions are as follows:

$$\| Q \|_{x=0} = 0 , \tag{5.2.24}$$

$$\| \rho Q u_0 + P_0 \|_{x=0} = \lim_{\delta \to 0} \int_{-\delta}^{+\delta} \hat{p}\, \beta_x \, dx , \tag{5.2.25}$$

$$\| \rho Q u_0 \psi_x \|_{x=0} = \lim_{\delta \to 0} \int_{-\delta}^{+\delta} [-\hat{p} + \bar{p} - \rho g \varphi] dx , \tag{5.2.26}$$

$$\lim_{\delta\to 0}\int_{-\delta}^{+\delta}[\rho Q u_{0,x}\,\psi]dx+\|P_1\|_{x=0}=\lim_{\delta\to 0}\int_{-\delta}^{+\delta}\hat{p}\beta\beta_x\,dx, \tag{5.2.27}$$

$$\lim_{\delta\to 0}\int_{-\delta}^{+\delta}\left[\rho Q\psi(u_0\psi_x)_x+\frac{1}{12}\rho Q^2\varphi\left(\frac{\varphi_x}{\varphi}\right)_x\right]dx=\lim_{\delta\to 0}\int_{-\delta}^{+\delta}[P_0-\rho g\varphi\psi-\hat{p}\beta]dx. \tag{5.2.28}$$

Here the condition that the bottom is flat has been used. In addition, we expect that the fluid departs from the flat top surface smoothly. As a result, in addition to the physical jump conditions listed above, we have the geometric relations at the juncture point x = 0, namely,

$$\|\beta\|_{x=0}=0, \tag{5.2.29}$$

$$\|\beta_x\|_{x=0}=0. \tag{5.2.30}$$

From the governing equation, we know that pressure on the top surface on the left side of x = 0 is bounded. The pressure on the free surface in region II is equal to zero. Meanwhile, because of the smooth departure of the fluid at x = 0, from (5.2.23) we can conclude that the bottom pressures are bounded. Therefore, the limits in (5.2.25- 28) are equal to zero even if there are finite jumps on $\hat{p}$ and $\bar{p}$ between sides of x = 0. Thus, we have the following jump conditions:

$$\|u_0\phi_0\|_{x=0}=0, \tag{5.2.31}$$

$$\|\rho Q u_0+P_0\|_{x=0}=0, \tag{5.2.32}$$

$$\|\rho Q u_0\,\psi_x\|_{x=0}=0. \tag{5.2.33}$$

Since the bottom is flat throughout the flow region, then the equivalent jump conditions to (5.2.29)-(5.2.33) are:

$$\begin{aligned} &\| \phi_0 \|_{x=0} = 0; \qquad \| \phi_{0x} \|_{x=0} = 0; \\ &\| Q \|_{x=0} = 0; \qquad \| P_0 \|_{x=0} = 0. \end{aligned} \tag{5.2.34}$$

These jump conditions imply that at the joint point x=0,

$$\begin{aligned} &\beta^+ = \beta^- = H_1; \quad \beta_x^+ = \beta_x^- = 0; \\ &Q^+ = Q^-; \qquad P_0^+ = P_0^-. \end{aligned} \tag{5.2.35}$$

These jump conditions provide enough information to solve the governing equations (5.2.21), (5.2.22) and (5.2.23). With the help of (5.2.35a) and (5.2.35d), the constant of integration S_2 can be determined through (5.2.21). Jump condition (5.2.35c) assures that the flux rate Q is constant throughout the region. Then (5.2.35a) and (5.2.35b) act as the boundary conditions at x = 0 for the governing equation (5.2.22). Thus the distribution of the fluid thickness in region II is obtained, and the integral pressure and bottom pressure in region II are determined through (5.2.21) and (5.2.23). Therefore, the solution of this problem is obtained.

5.2.4 Results and discussion

Before we discuss the result, we introduce the definition of the Froude number in this problem as:

$$Fr = \frac{U_1}{\sqrt{g H_1}}, \tag{5.2.36}$$

where, U_1 denotes the velocity of the fluid at far upstream, and H_1 the thickness of the fluid at far upstream and also the distance between the flat top and bottom surfaces.

In order to solve the problem, the pressure at far upstream must be specified beforehand. According to the governing equations in region I, once the top pressure far upstream is given, other pressures, such as the integral pressure P_0 and P_1, and the bottom pressure $\bar{p}$, are determined. Thus we denote the top pressure far upstream by $\hat{p}_0$, and we will discuss the results using the value of $\hat{p}_0$ as an input variable, in addition to the Froude number.

First of all, we consider the case $\hat{p}_0 = 0$, that is, the top pressure far upstream is equal to the atmospheric pressure. In this case, the results are very interesting. After calculation of the governing equations in region II, we find that only one solution exists, no matter the flow far upstream is supercritical, critical, or subcritical. This solution is that the flow throughout the region is uniform. In other words, the flow keeps unchanged throughout the whole region. This result is obviously consistent with practical experiments and common sense.

Then we discuss the case $\hat{p}_0 > 0$, that is, the top pressure at far upstream is greater than the atmospheric pressure. Then according to governing equations in region I, the top pressure is constant in region I, that is, $\hat{p} \equiv \hat{p}_0$. However, in region II the top pressure on

the free surface is equal to the atmospheric pressure, that is, $\hat{p} \equiv 0$. Consequently, in our computation model, there will be a discontinuity of the top pressure across x = 0. By way of illustration, Fig. 5.2.2 depicts the obtained solutions for three values of the Froude number Fr = 0.5, 1.0 and 1.5. Here the distance between the parallel confined plates is 1m, and the top pressure far upstream is $\hat{p}_0/(\rho g H_1) = 0.051\text{m}$. Inspection of Fig. 5.2.2 indicates that waves always appear in the downstream, no matter the flow in the upstream is supercritical, critical or subcritical. And given same conditions, the higher the Froude number, the larger the magnitude and the length of the wave in the downstream. For the supercritical flow, the magnitude of the wave downstream is so high that we may expect that hydraulic jump will occur.

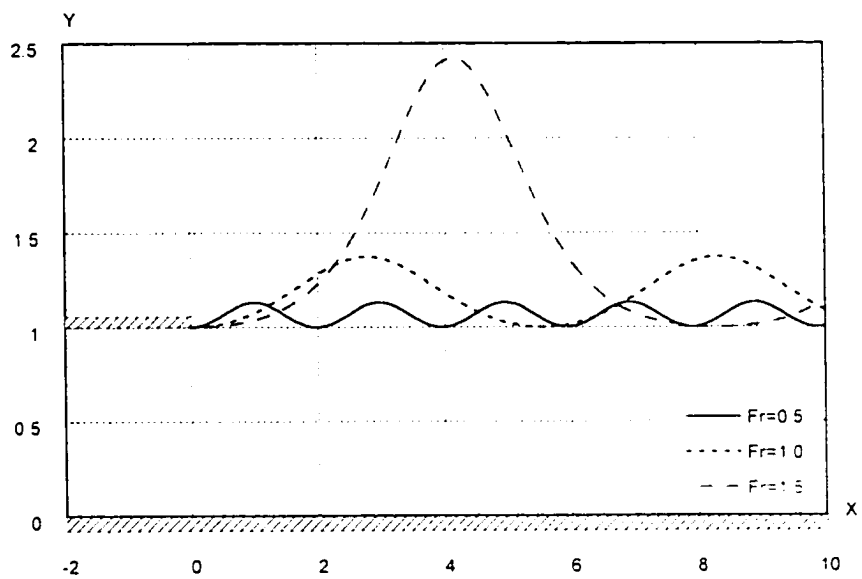

Fig. 5.2.2 Plot of the free surface in the downstream when $\hat{p}_0 > 0$

Finally we consider the case when $\hat{p}_0 < 0$, that is, the top pressure far upstream is less than the atmospheric pressure. Similar to the case $\hat{p}_0 > 0$, there is a jump on the value of the top pressure across x = 0. After calculation for different Froude numbers at far upstream, we found that there are no solutions for the supercritical and critical flows. Under certain conditions, the solution for subcritical flows can be obtained. Two solutions are illustrated in Fig. 5.2.3, where the Froude number Fr = 0.3 and 0.5, and the top pressure far upstream is $\hat{p}_0/(\rho g H_1) = -0.051\text{m}$. The distance between two flat plates is still 1m. In the practical problems, due to the negative pressure on the top surface in region I (compared to the atmospheric pressure), the flow will become unstable and probably will not stay attached to the top plate in region I. Consequently, in this case may not reflect a practical situation.

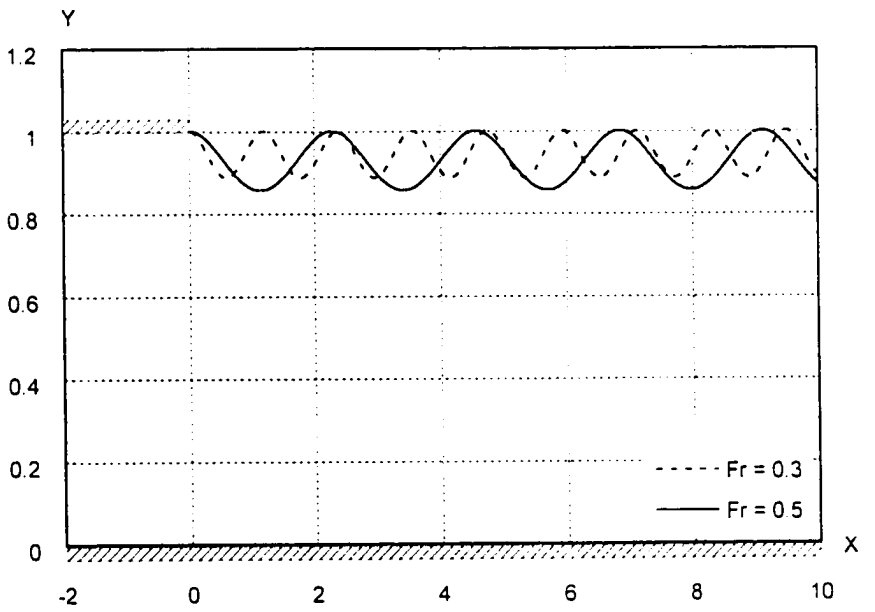

Fig. 5.2.3 Plot of the free surface in the downstream when $\hat{p}_0 < 0$

Comparing these results with Fig. 5.2.2, we found that when $\hat{p}_0 < 0$, the mean water level in the waves in the downstream is below the top surface in region I, that is, y = 1.0m, whereas when $\hat{p}_0 > 0$, the mean water level in the waves is above y = 1m. When $\hat{p}_0 = 0$, the free surface in the downstream is flat and is equal to y = 1m. This implies that the top pressure far upstream determines the pattern of the free surface in the downstream.

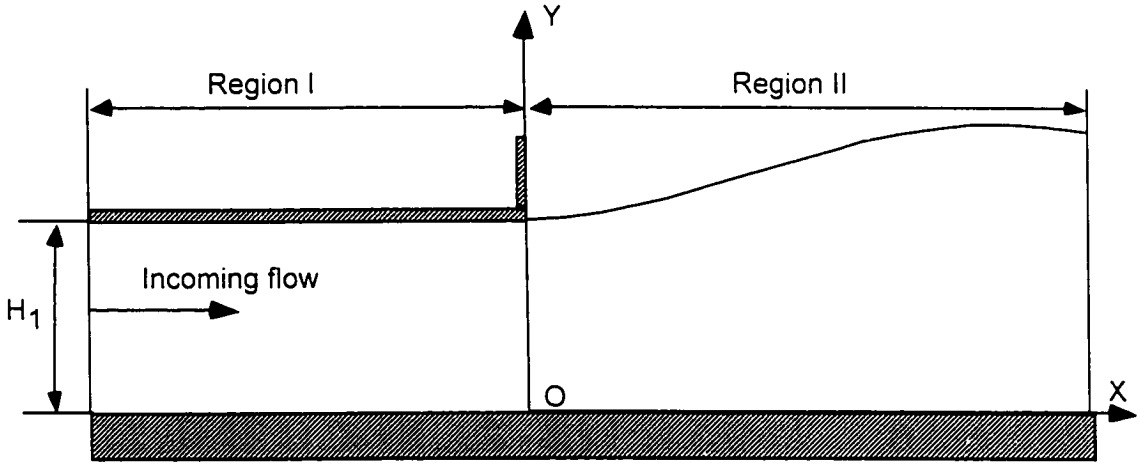

Fig. 5.2.4 Steady, two-dimensional flow past a semi-infinte flat-bottomed body in finite-depth water

Actually, this problem can also be regarded as the steady, two-dimensional flow past a semi-infinite flat-bottomed body in finite-depth water, as shown in Fig. 5.2.4. Vanden-Broeck (1977, 1980) studied the steady two-dimensional flow past a semi-infinite flat-bottomed body in infinite-depth water. As he pointed out, there are two possible solutions for this problem. By using the conformal mapping, Vanden-Broeck (1980) obtained a

solution similar to our solutions illustrated in Fig. 5.2.2, that is, the flow departing smoothly from the corner bottom. Based on an expansion in powers of the Froude number $F = U/(gH)^{\frac{1}{2}}$ (H is the draft of the body in his paper), Vanden-Broeck (1977) obtained another kind of solutions with a stagnation point on the side of the body (as shown in Figure 8 in Vanden-Broeck (1977). This solution was confirmed by Yeung (1991). However, the latter solutions are only physically satisfactory for small values of the Froude number, and become physically unreasonable since the ratio of the elevation of the stagnation point to the draft tends to infinity as $F \to \infty$. For instance, when he calculated the profile of the free surface for F = 6.3, the elevation of the stagnation point is 20 times of the draft of the body.

In both papers, Vanden-Broeck did not consider the effect of the bottom by assuming the water depth is infinite. Here we obtained the solutions in finite-depth water. Note that here the stern waves are noticeably nonlinear with sharp peaks and broad troughs (see Fig. 5.2.2), which is consistent with the first kind of solutions of Vanden-Broeck (1980). The second kind of solutions with a stagnation point (Vanden-Broeck 1977) yield stern waves very close to sine waves, as point out by Vanden-Broeck (1980). Both of the present solutions and those of Vanden-Broeck do not take into consideration the viscosity and surface-tension effects. Yeung (1991) studied both stern and bow waves taking into consideration the effect of viscosity. Recently, Yeung & Ananthakrishnan (1997) studied the viscosity and surface-tension effects on wave generation by a translating body in infinite-depth water. Nevertheless, the problem is very complicated and beyond the discussion in present dissertation.

§5.3 Flow departing from confined non-smooth top surface

Now with the results obtained in the above section, we can deal with much more complicated problems. On the basis of the problem solved above, we expand the flat top surface with a confined inclined part, as shown in Fig. 5.3.1. This problem was mentioned by Benjamin (1956) when he studied the flow under a sluice gate. Before proceeding further, we state the problem explicitly in the following for later convenience.

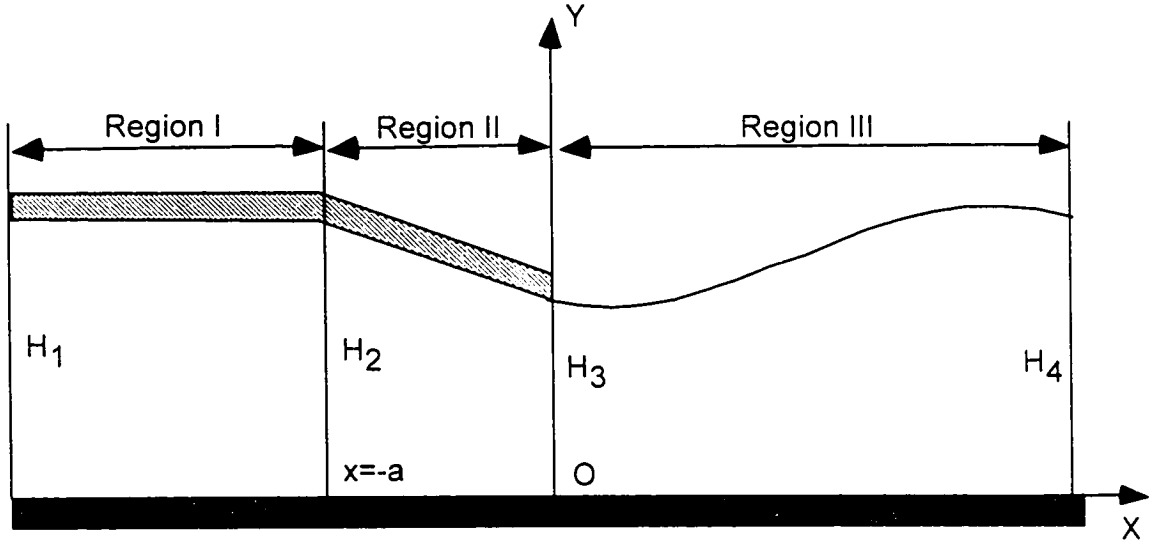

Fig. 5.3.1 Schematic of the flow departing from a non-smooth top surface

Consider the steady, two-dimensional flow of an inviscid, incompressible fluid departing from two confined surfaces (as shown in Fig. 5.3.1). The bottom surface is flat, while the confined top surface becomes inclined some distance from the departure point. Here the effect of surface tension is assumed negligible. Far upstream the fluid is assumed to flow as uniform stream. Of particular interest in analyzing this problem is the prediction of the location of the free surface in the downstream.

With the experience of solving the waterfall problem with a non-smooth bottom, we will divide the whole flow region into three distinct regions since the confined top surface is not smooth. As shown in Fig. 5.3.1, region I is characterized by two confined parallel flat surfaces, and region II is bounded by an inclined top surface and a flat bottom surface, while region III is characterized with a free surface and a flat bottom. In the following the governing equations for each region will be derived.

5.3.1 Governing equations for three regions

Comparing with the problem in the above section, we know that region I and region III here are just same as region I and region II of above problem respectively. Thus we can use these governing equations for these regions. We summarize them in the following without further explanation.

In region I, the Green-Naghdi Level-I governing equations are:

$$v_0 = 0, \tag{5.3.1}$$

$$v_1 = 0, \tag{5.3.2}$$

$$u_{0,x} = 0, \tag{5.3.3}$$

$$-\frac{P_{0x}}{\rho} = 0, \tag{5.3.4}$$

$$-\frac{P_{1x}}{\rho} = 0, \tag{5.3.5}$$

$$-\rho g\beta - \hat{p} + \bar{p} = 0, \tag{5.3.6}$$

$$P_0 - \frac{1}{2}\rho g\beta^2 - \hat{p}\beta = 0. \tag{5.3.7}$$

In region III, the governing equations are

$$\frac{Q^2}{3}\phi_0\phi_{0xx} - \frac{Q^2}{3}\phi_{0x}^2 + \frac{1}{2}g\phi_0^3 - S_2\phi_0 + Q^2 = 0, \tag{5.3.8}$$

$$\frac{P_0}{\rho} = -\frac{Q^2}{\phi_0} + S_2. \tag{5.3.9}$$

$$\frac{\bar{p}}{\rho} = g\phi_0 - \frac{Q^2\phi_{0x}^2}{2\phi_0^2} + \frac{Q^2\phi_{0xx}}{2\phi_0}. \tag{5.3.10}$$

Now we need to derive the governing equations for region II, which is bounded by a flat bottom and an inclined top surface. Since the bottom surface is flat, then from the kinematic boundary conditions, we obtain

$$v_0 = 0, \tag{5.3.11}$$

$$v_1\beta = u_0\beta. \tag{5.3.12}$$

The continuity equations state that

$$u_1 = 0, \tag{5.3.13}$$

$$u_{0x} + v_1 = 0. \tag{5.3.14}$$

From the conservation law of momentum, and taking (5.3.11) into account, we can obtain

$$\beta u_0 u_{0x} = -\frac{1}{\rho} P_{0x} + \frac{\hat{p}}{\rho}\beta_x , \tag{5.3.15}$$

$$\frac{1}{2}\beta^2 u_0 v_{1x} + \frac{1}{2}\beta^2 v_1 v_1 = \frac{1}{\rho}(-\rho g\beta - \hat{p} + \bar{p}) . \tag{5.3.16}$$

$$\frac{1}{3}\beta^3 u_0 v_{1x} + \frac{1}{3}\beta^3 v_1 v_1 = \frac{1}{\rho}(P_0 - \frac{1}{2}\rho g\beta^2 - \frac{\hat{p}}{\rho}\beta) . \tag{5.3.17}$$

Substituting (5.3.14) into (5.3.12), and integrating, we obtain

$$u_0 \beta = Q . \tag{5.3.18}$$

where Q is a constant of integration, and denotes the constant flux rate of the fluid.

With the help of (5.3.18), (5.3.15), (5.3.15) and (5.3.17) become

$$\rho Q^2 \left(\frac{1}{\beta}\right)_x = \hat{p}\beta_x - P_{0x} , \tag{5.3.19}$$

$$\frac{1}{2}\rho Q^2 \left(\frac{\beta_x}{\beta}\right)_x = -\rho g\beta - \hat{p} + \bar{p} , \tag{5.3.20}$$

$$\frac{1}{3}\rho Q^2 \beta \left(\frac{\beta_x}{\beta}\right)_x = P_0 - \frac{1}{2}\rho g\beta^2 - \hat{p}\beta , \tag{5.3.21}$$

respectively.

From (5.3.20), we have

$$\bar{p} = \hat{p} + \rho g\beta + \frac{1}{2}\rho Q^2 \left(\frac{\beta_x}{\beta}\right)_x . \tag{5.3.22}$$

And from (5.3.21) we get

$$P_0 = \hat{p}\beta + \frac{1}{2}\rho g\beta^2 + \frac{1}{3}\rho Q^2\beta\left(\frac{\beta_x}{\beta}\right)_x . \qquad (5.3.23)$$

Inserting (5.3.23) into (5.3.19), and integrating, we obtain

$$\frac{\hat{p}}{\rho} = B - g\beta - \frac{1}{2}Q^2\frac{1}{\beta^2} + \frac{1}{6}Q^2\frac{\beta_x^2}{\beta^2} - \frac{1}{3}Q^2\frac{\beta_{xx}}{\beta}. \qquad (5.3.24)$$

where, B is a constant of integration, and to be determined as part of solution.

Inserting (5.3.24) into (5.3.23), we obtain

$$\frac{P_0}{\rho} = B\beta - \frac{1}{2}g\beta^2 - \frac{Q^2}{2\beta} - \frac{Q^2\beta_x^2}{6\beta}. \qquad (5.3.25)$$

In the same way, substituting (5.3.24) into (5.3.22), we have

$$\frac{\bar{p}}{\rho} = B - \frac{1}{2}\frac{Q^2}{\beta^2} - \frac{1}{3}Q^2\left(\frac{\beta_x}{\beta}\right)^2 + \frac{1}{6}Q^2\frac{\beta_{xx}}{\beta}. \qquad (5.3.26)$$

Since the top surface is given, then only thing needed to be determined is the constant of integration B. Once the constant of integration B is determined, we can calculate the top pressure through (5.3.24). At the same time, the integral pressure and the bottom pressure can be obtained from (5.3.25) and (5.3.26), respectively. The determination of B depends on the application of jump conditions at the junction point x = -a discussed in the following section.

5.3.2 Boundary conditions and jump conditions

Now that we have obtained the governing equations in three regions, we need to consider appropriate boundary conditions to solve these equations. As before, we assume that the stream is uniform at far left boundary. Besides, we need to specify the integral pressure, or the top pressure at far left boundary because the top surface is confined instead of being free. Therefore the boundary conditions at far left boundary are

$$\beta = H_1;\ u_0 = U_1; P_0 = P_{0-\infty}, \text{as } x \to -\infty. \tag{5.3.27}$$

Since the fluid flux Q remains constant throughout the whole flow region, Q is determined as

$$Q = U_1 H_1. \tag{5.3.28}$$

Recall that the fluid is bounded by two confined parallel flat surfaces. Then in region I the thickness of the fluid keeps constant, that is,

$$\beta \equiv H_1. \tag{5.3.29}$$

Thus the distribution of the integral pressure, top pressure and bottom pressure can be determined through (5.3.4), (5.3.7) and (5.3.6), respectively. Then we have obtained the solution for region I. Actually, all of these variables are constant in region I according to our computational model.

Now we consider region II and III, which are much more complex than region I. However, in order to solve the governing equations in region II and III, we must apply jump conditions at x = -a and x = 0 to determine the constants of integration in these equations. In addition, the jump conditions will yield the boundary conditions needed for the calculation of the differential equations. We first consider the jump conditions at the junction point between region I and II, say x = -a, where a jump on the slope of the top surface occurs. This means that the top surface is continuous at x=-a, while the slope of the top surface is discontinuous there. Thus the second order derivative of the top surface may be unbounded. After observing (5.3.24) and (5.3.26), we find that the top pressure $\hat{p}$ and bottom pressure $\bar{p}$ may be unbounded as well. However, from (5.3.25) we know that the integral pressure P_0 is bounded across the joint interface x = -a.

As before, we first consider the geometric relations at x = -a. Obviously, the thickness and the central line of the fluid is continuous across x = -a, that is,

$$\| \phi_0 \|_{x=-a} = 0, \text{ and} \tag{5.3.30}$$

$$\| \psi \|_{x=-a} = 0. \tag{5.3.31}$$

Since the bottom is flat, we can just use one equivalent jump condition, that is,

$$\| \beta \|_{x=-a} = 0. \tag{5.3.32}$$

Another geometric jump condition at x = -a is the discontinuity of the slope of the top surface, that is,

$$\| \beta_x \|_{x=-a} = K, \tag{5.3.33}$$

where. K denotes the slope of the top surface in region II. and is specified beforehand.

Next we consider the jump conditions associated with physical laws. Before further proceeding, we define as before

$$\lim_{\delta \to 0} \int_{-a-\delta}^{-a+\delta} (\hat{p}\, \beta_x - \bar{p}\, \alpha_x) dx = F_1. \tag{5.3.34}$$

$$\lim_{\delta \to 0} \int_{-a-\delta}^{-a+\delta} [-\hat{p} + \bar{p} - \rho g \varphi] dx = F_3. \tag{5.3.35}$$

$$\lim_{\delta \to 0} \int_{-a-\delta}^{-a+\delta} [P_0 - \rho g \varphi \psi - \hat{p}\beta + \bar{p}\alpha] dx = L. \tag{5.3.36}$$

Recall that we have obtained the general jump conditions for Green-Naghdi Level I method in chapter 3. Now we apply them to this particular problem. Making use of the above definition. we can obtain

$$\| Q \|_{x=-a} = 0. \tag{5.3.37}$$

$$\| \rho Q u_0 + P_0 \|_{x=-a} = F_1. \tag{5.3.38}$$

$$\| \rho Q u_0 \psi_x \|_{x=-a} = F_3. \tag{5.3.39}$$

$$\lim_{\delta \to 0} \int_{-a-\delta}^{-a+\delta} \left[\rho Q \psi (u_0 \psi_x)_x + \frac{1}{12} \rho Q^2 \varphi \left(\frac{\varphi_x}{\varphi} \right)_x \right] dx = L. \tag{5.3.40}$$

However, since F_1, F_3 and L are unknown beforehand, we need another jump condition, that is, the energy equation. Recall that the general energy jump condition for Green-Naghdi Level-I theory is:

$$\left\| \frac{1}{2}\rho u_0 \phi_0 \left(u_0^2 + u_0^2 \psi_x^2 + \frac{1}{12} u_0^2 \phi_{0x}^2 + 2g\psi \right) + u_0 P_0 \right\|_{x=-a} = 0. \qquad (5.3.41)$$

This jump condition can be simplified. From (5.3.37) and (5.3.32), we can deduce that u_0 is continuous across x = -a. At the same time, since the bottom is flat throughout the flow region, then (5.3.41) can be simplified as

$$\left\| \frac{1}{6} Q u_0^2 \beta_x^2 + u_0 \frac{P_0}{\rho} \right\|_{x=-a} = 0. \qquad (5.3.42)$$

Now with the jump conditions (5.3.28) and (5.3.33), together with the geometric jump conditions at x =-a, that is, (5.3.32) and (5.3.33), we can determine the constant of integration B in the governing equations (5.3.24), (5.3.25) and (5.3.26). Therefore the solution for region II can be obtained through these equations.

Finally we consider region III, where the governing equations have been obtained, that is, (5.3.8), (5.3.9) and (5.3.10). To solve these equations, the crucial point is to solve (5.3.8) to obtain the distribution of the thickness of the fluid. Equation (5.3.8) is a second-order differential equation, which requires appropriate boundary conditions to be solved. In addition, there exist two constants of integration (5.3.8), which need to be determined before the solution of (5.3.8) is obtained. In other words, four conditions are needed to

determine the solution in region III. All of these conditions can be obtained by the application of jump conditions at the joint point between region II and III, say x = 0. Then let us focus on the jump conditions at x = 0. We suppose that the stream departs smoothly from the joint interface, which requires that the top surface and the slope of the top surface are continuous, that is,

$$\|\beta\|_{x=0} = 0. \tag{5.3.43}$$

$$\|\beta_x\|_{x=0} = 0. \tag{5.3.44}$$

As before, from the general jump conditions obtained before, we have

$$\| Q \|_{x=0} = 0. \tag{5.3.45}$$

$$\| \rho Q u_0 + P_0 \|_{x=0} = 0. \tag{5.3.46}$$

$$\| \rho Q u_0 \psi_x \|_{x=0} = 0. \tag{5.3.47}$$

The equivalent jump conditions at x = 0 are as follows:

$$\begin{aligned} &\beta^+ = \beta^-; \quad \beta_x^+ = \beta_x^-; \\ &Q^+ = Q^-; \quad P_0^+ = P_0^-. \end{aligned} \tag{5.3.48a-d}$$

By means of (5.3.48c) and (5.3.48d), the constants of integration Q and S_2 in (5.3.9) can be determined. Then (5.3.48a, b) will act as the boundary conditions at x = 0 for (5.3.8), and thus the location of free surface in region III is obtained. Consequently, the integral pressure P_0 and the bottom pressure $\bar{p}$ are obtained through (5.3.9) and (5.3.10)

respectively, and thus the solution for region III can be obtained. This means the solution throughout the flow region is obtained.

5.3.3 Results and discussion

Same as in the above section, we define the Froude number far upstream as

$$Fr = \frac{U_1}{\sqrt{g H_1}}, \tag{5.3.49}$$

where, U_1 denotes the velocity of the fluid at far upstream, and H_1 the thickness of the fluid far upstream, i.e., the distance between the flat top and bottom surfaces in region I. Then given the top pressure at far upstream, H_1 and U_1 (or the Froude number Fr), we can determine the solution for the whole region through the equations and jump conditions obtained above.

Fig. 5.3.2 depicted the free surface in region III for different Froude numbers while other conditions are same. Here the top pressure at far upstream $\hat{p}_0$ is equal to zero. The thickness of the fluid far upstream H_1 = 1.0m and the thickness of the fluid at departure point (x =0) H_3 = 0.6m. The length of region II is a = 1m. Once H_1, H_3 and a are specified, the slope of the top surface in region II, say K, is determined. Inspection of Fig. 5.3.2 indicates that the higher the Froude number, the longer the wave length. The magnitude of the wave appears not to change much with the Froude number up to Fr = 0.5. But Fig. 5.3.3 indicates that the Height (magnitude) of the waves will increase rapidly when the Froude number is greater that 0.4.

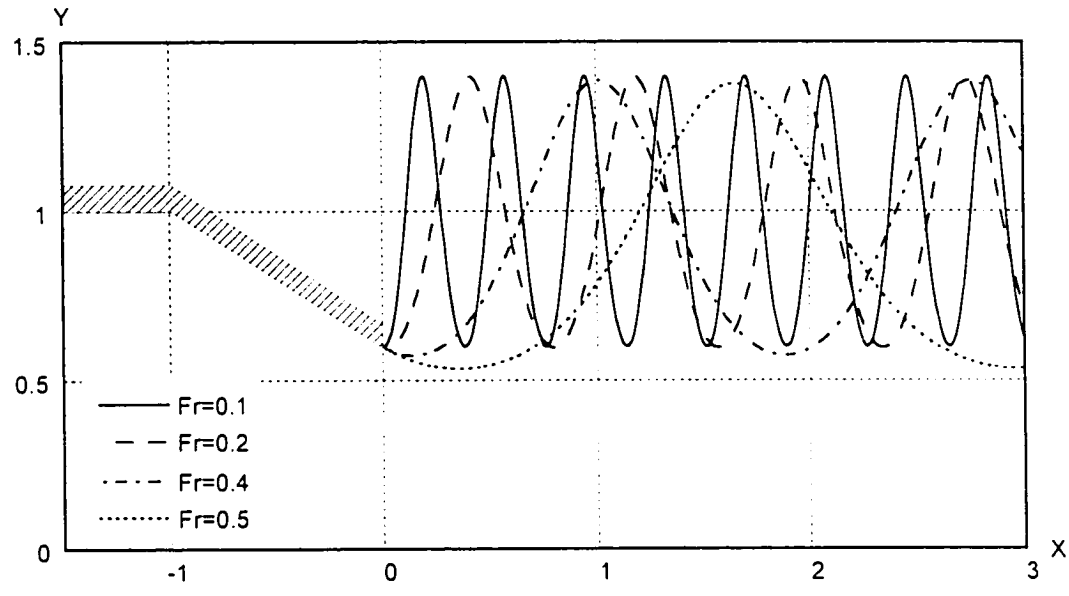

Fig. 5.3.2 Plot of waves in region III for different Froude numbers

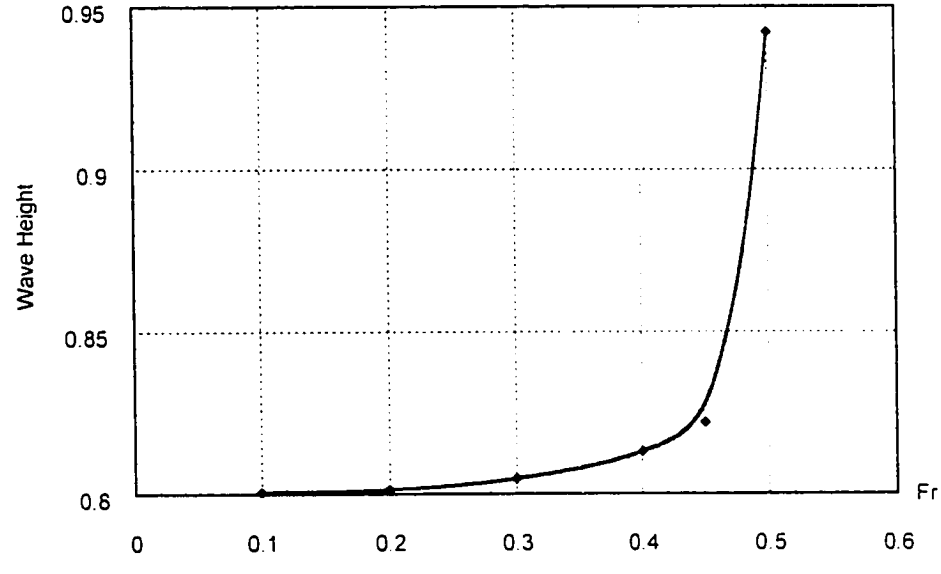

Fig. 5.3.3 Plot of the wave height in region III as a function of Froude number

Fig. 5.3.4 shows the effect of the top pressure far upstream on the waves in region III. Here the given data are: H_1=1.0m; H_3=0.6m; a = 1.0m; and Fr = 0.5. The results indicates that the higher the top pressure far upstream $\hat{p}_0$, the larger the magnitude of the waves and the smaller the wave length.

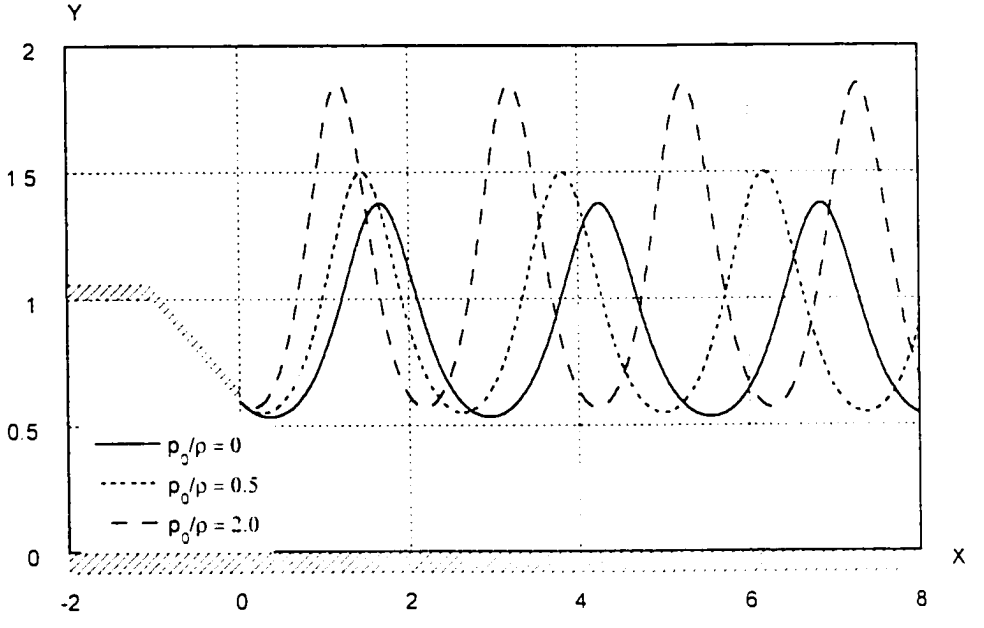

Fig. 5.3.4 Plot of waves in region III for different top pressures far upstream

Next we consider effect of the slope of the top surface in region II on the waves appearing in region III. Fig. 5.3.5 and Fig. 5.3.6 show the effects on the wave length and height in region III, respectively. From these results, we found that the wave length and height of waves in region III increase with the slope of the top surface in region II.

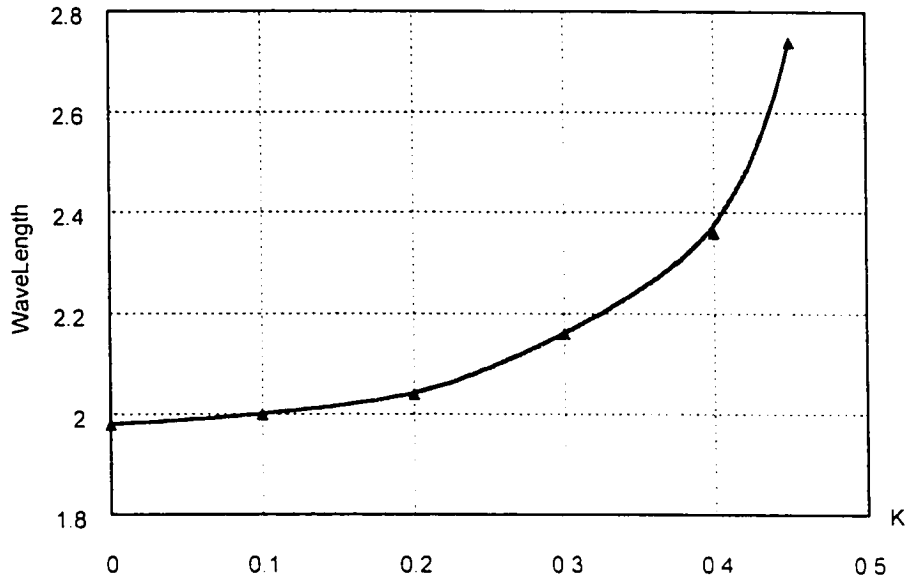

Fig. 5.3.5 Plot of the wave length in region III as a function of the slope K of the top surface

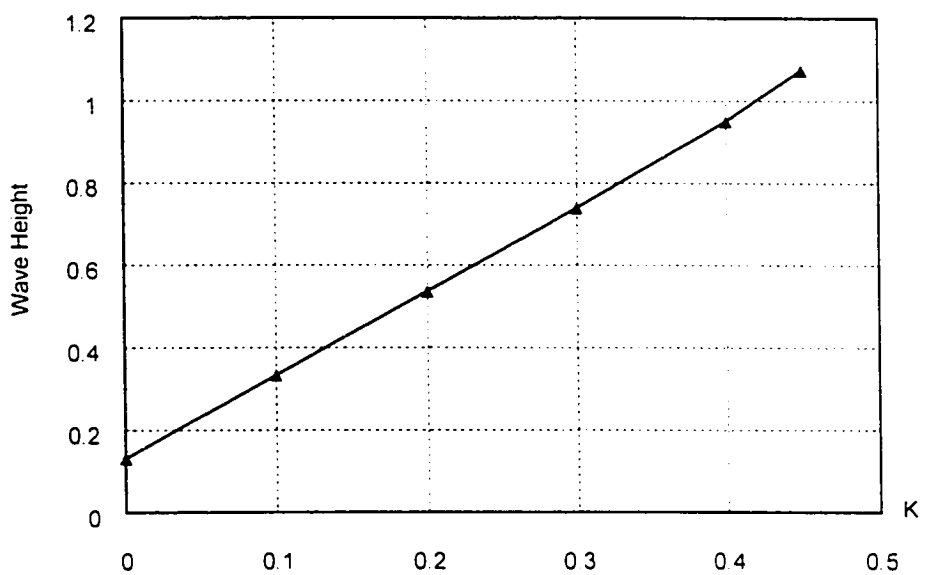

Fig. 5.3.6 Plot of the wave height in region III for different slopes K of top surface

To date, all of the results show that waves always occur in region III. However, further study found that solutions other than waves are possible if particular conditions are sought. An interesting solution is one where the flow in region III will approach uniform flow at far downstream. We now discuss the possibility of this solution. Recall that when we solved this problem above, we did not assume that the flow far downstream is uniform. If so, we would find that this problem is over-determined. But, on the other hand, this also means that more than enough conditions have been given.

With the assumption that the flow in region III becomes uniform at far downstream, we can integrate the governing equation (5.3.8). After the integration as we did before, we can obtain the familiar equation

$$\frac{1}{3}Q^2\phi_{0x}{}^2=\left(\frac{Q^2}{H_4{}^2}-g\phi_0\right)(\phi_0-H_4)^2, \tag{5.3.50}$$

where, H_4 denotes the constant thickness in region III at far downstream. Thus the second-order differential equation is simplified to first-order differential equation. The integral pressure can be obtained through

$$\frac{P_0}{\rho}=-\frac{Q^2}{\phi_0}+S_2, \tag{5.3.51}$$

where, S_2 is a constant of integration. Due to the uniform flow far downstream, we can deduce the relation between S_2 and H_4, that is,

$$S_2=\frac{Q^2}{H_4}+\frac{1}{2}gH_4{}^2. \tag{5.3.52}$$

After observing (5.3.50)-(5.3.52), we find that three conditions are needed to determine the solution in region III. In detail, two are needed to determine Q and H_4, and another one is needed to act as the boundary condition to solve (5.3.50). However, there are four jump conditions at x = 0, say (5.3.48a-d). As discussed above, two possibilities are associated with this case, that is, this problem is over-determined, or more than enough conditions are given. In other words, some given conditions are related, rather than independent. For instance, if we specify H_1, H_3, the slope K, and the Froude number far upstream, then unlike what we did before, we cannot specify the value of the top pressure at far upstream.

Fig. 5.3.7 illustrates the result of one case, where H_1=1.0m, H_3 = 0.5m, Fr = 0.5 and the inclined angle is equal to $30°$. Once these data are given, the corresponding top pressure far upstream is determined and thus a unique solution, if exists, can be obtained. More results are given in Fig. 5.3.8 for different values of Froude number while other conditions are same. After observing Fig. 5.3.8, we find that the constant thickness of the fluid far downstream increases with the Froude number. However, H_4 varies little with the Froude number after Fr is greater than 0.7. Note that the vertical coordinate is enlarged to see clearly the solutions for different Froude numbers.

To date, we have obtained both solutions with waves and without waves for this flow problem. Usually, waves occur after the fluid departs from the confined top surface. However under certain circumstances, we are able to obtain the solution that the flow in region III approaches uniform at far downstream.

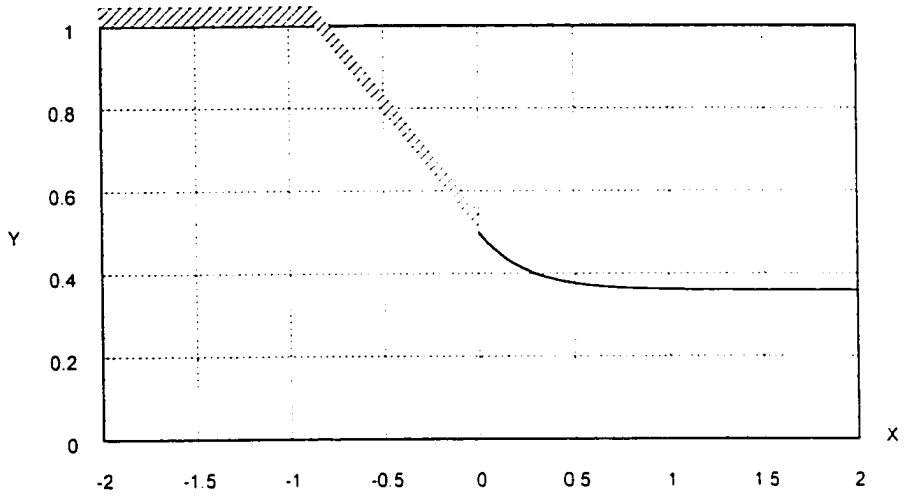

Fig. 5.3.7 Illustration of a solution of region III when the far downstream is uniform

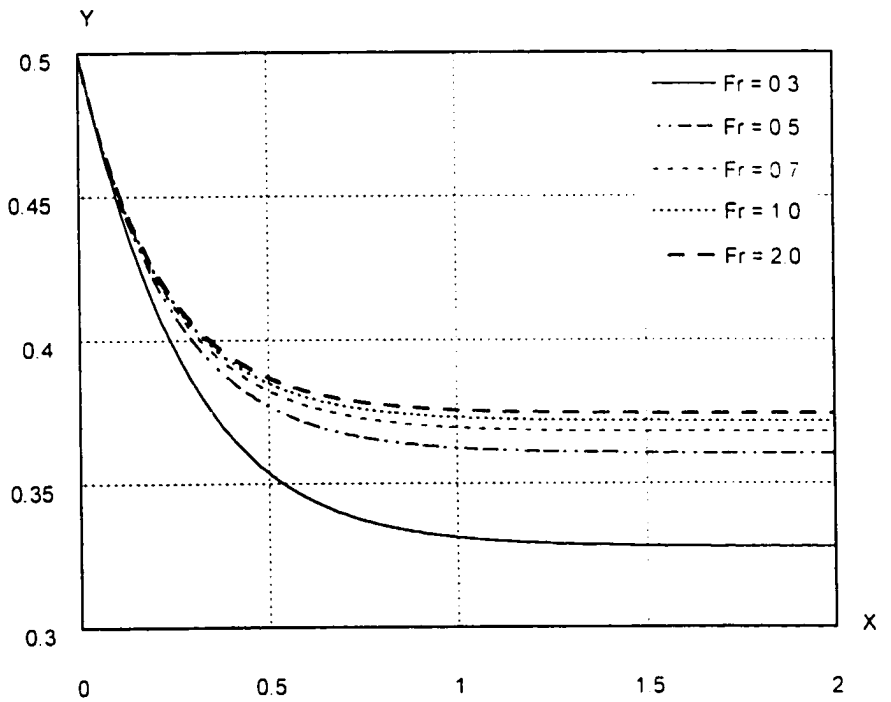

Fig. 5.3.8 Plot of the free surface in region III for different Froude numbers

Chapter 6

Steady Inviscid Flow over a Weir

In Chapter 4 we have solved the waterfall problem over a slanted bottom, that is, the flow over an inclined weir. When the inclined weir becomes vertical, this problem becomes a classical thin weir problem, which is the main concern of this chapter. More precisely, we consider a flow in a channel of finite depth that is uniform far upstream and ends with a vertical weir. There are usually two types of weirs: thin weirs (sharp crested weirs) and broad crested weirs. Both of them will be considered in this chapter.

The use of weirs as flow control devices in dams and open channels can be traced back to 325 BC from the archeological studies of the remaining portions of some dams in the Middle East, Smith (1971). Large numbers of experiments, both at laboratory and in the field, have been made during last several centuries. However, theoretical results are rare. The first theoretical prediction of the flow over a rectangular sharp crested weir appears to have been made by Boussinesq (1907). The weir problem, same as the free waterfall problem, is complex due to one or more unknown free surfaces, whose shape must be found as part of the solution and on which the boundary conditions to be satisfied is highly nonlinear. What differentiates the weir problem from the waterfall problem is the presence of the vertical weir, which causes a jump in the thickness of the fluid and this makes it more difficult to solve. In the following sections, we will discuss both sharp crested weirs and broad crested weirs.

§6.1 Thin weirs

The thin weirs have remained one of the simplest, most accurate and useful gauging structures under laboratory and controlled field conditions. The interesting characteristic of weir flows is that given the height of the weir, the Froude number and the height of the fluid far upstream are not independent. Although a large number of experiments have been made, analytical solutions are rare and even numerical solutions are difficult to obtain due to the complex nature of weir flows. By means of conformal mapping method, Vanden-Broeck & Kell (1987) obtained numerical thin-weir solutions for small Froude numbers. Dias & Tuck (1991) extended their calculation to larger Froude numbers with limited success. However, to our knowledge, the study of weir flows with Green-Naghdi theory has not been done yet. Before further processing, it is desirable for later reference to provide here the following statement of the thin weir problem.

The steady two-dimensional flow of an incompressible, inviscid fluid over a thin weir is considered. The flow is uniform far upstream in a channel of finite depth, which ends with a thin weir. After the thin weir, the flow forms a jet bounded by two free surfaces, which falls under the effect of gravity. From Fig. 6.1.1 we can find that two distinct regions of flow are associated with this problem. The upstream region ahead of the weir is characterized by a free top surface and a flat bottom. In the downstream behind the weir a jet is bounded by two unknown free surfaces. Of particular interest in analyzing this problem is to compute the relation between the upstream flow, the geometry of the weir, and the location of two free surfaces of the free jet after the weir.

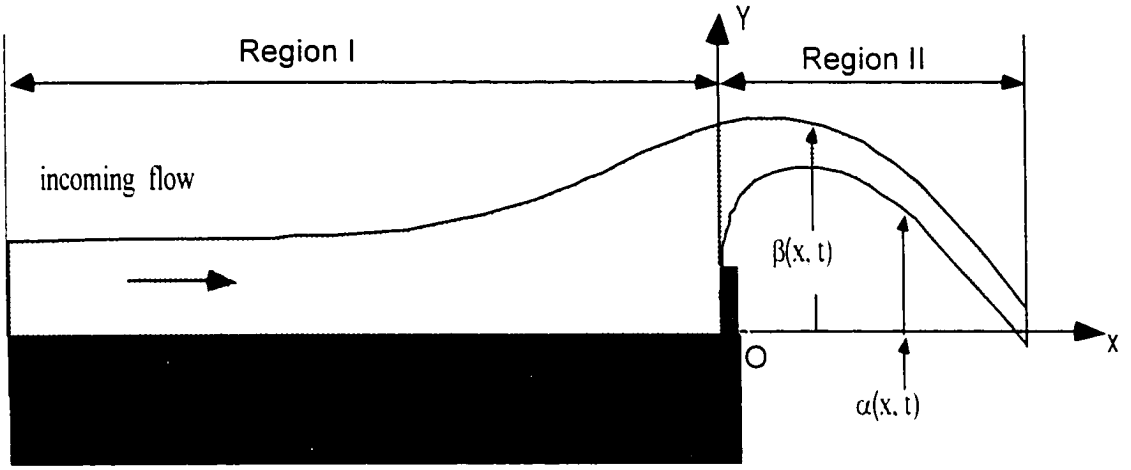

Fig. 6.1.1 Schematic of flow over a thin weir

6.1.1 Formulation of the problem

We choose a coordinate system with the x-axis along the bottom of the channel and y-axis up the vertical weir. Then the y-axis divides the flow into two parts: Region I (upstream) is bounded by a free surface and a flat bottom; while Region II (downstream) is bounded by two free surfaces. As in the waterfall problem, we assume that the flow is uniform in the horizontal direction and the horizontal component of the velocity approaches constant far downstream. Then the far downstream boundary conditions are, as in Chapter 4 for the waterfall problem,

$$\text{as } x \to +\infty,$$
$$\phi_0 \to H_\infty,\ \phi_{0x} \to 0,\ u_0 \to U_\infty,\ P_0 \to 0. \qquad (6.1.1)$$

Since the flow is uniform far upstream and the bottom is flat in region I, then the far upstream boundary conditions are

$$\text{as } x \to -\infty,$$
$$\phi_0 \to H_1,\ \ \phi_{0x} \to 0,\ \ u_0 \to U_1,\ \ P_0 \to \tfrac{1}{2}\rho g H_1^2. \tag{6.1.2}$$

With these boundary conditions and the characteristics of the flow, the governing equations obtained in Chapter 4 are valid here. Thus in Region I the governing equations of Green-Naghdi Level I theory are:

$$\frac{1}{3}Q^2\phi_{0x}^{\ 2} = \left(\frac{Q^2}{H_1^{\ 2}} - g\phi_0\right)(\phi_0 - H_1)^2. \tag{6.1.4}$$

$$\frac{P_0}{\rho} = -\frac{Q^2}{\phi_0} + S_1; \tag{6.1.5}$$

$$\frac{\overline{p}}{\rho} = g\phi_0 - \frac{Q^2\phi_{0x}^{\ 2}}{2\phi_0^2} + \frac{Q^2\phi_{0xx}}{2\phi_0}. \tag{6.1.6}$$

where,

$$Q = Fr\sqrt{gH_1}\,H_1. \tag{6.1.7}$$

$$S_1 = \frac{1}{2}gH_1^{\ 2} + \frac{Q^2}{H_1}. \tag{6.1.8}$$

Here we adopt the same notation as in previous chapters. And in region II the governing equations are

$$\phi_0 = H_4 + Ae^{-Bx}; \tag{6.1.9}$$

$$\frac{P_0}{\rho} = -\frac{Q^2}{\phi_0} + S_3; \tag{6.1.10}$$

$$\psi = -\frac{gH_4^2}{2Q^2}x^2 + CH_4 x + \frac{gAH_4}{Q^2B}xe^{-Bx} - \frac{gA^2}{2Q^2B^2}e^{-2Bx} - \frac{AC}{B}e^{-Bx} + D. \quad (6.1.11)$$

where

$$A = H_3 - H_4. \quad (6.1.12)$$

$$B = \frac{2\sqrt{3}}{H_4}. \quad (6.1.13)$$

$$S_3 = \frac{Q^2}{H_4}. \quad (6.1.14)$$

C and D are constants of integration to be determined.

6.1.2 Jump conditions

Now that the governing equations for Region I and II have been obtained, which are same as those in the waterfall problem, then the jump conditions become the crucial part of the solution. What differentiates the weir flow from the waterfall problem is the presence of the vertical weir, which results in a jump in the thickness of the fluid at x = 0. Before considering the jump conditions associated with physical laws, we analyze the jump conditions from the geometric point of view. We expect that the top surface across the weir is smooth, although hydraulic jumps are possible due to the existence of the weir. Then we have the geometric relations across the weir x = 0:

$$\|\beta\|_{x=0} = 0. \quad (6.1.15)$$

$$\|\beta_x\|_{x=0} = 0. \quad (6.1.16)$$

$$\| \alpha \|_{x=0} = W, \qquad \text{or, } \| \phi_0 \|_{x=0} = -W, \tag{6.1.17}$$

where W denotes the height of the weir.

With the help of these geometric jump conditions, we can handle the physical jump conditions much easier. Recall that the jump conditions for Green-Naghdi Level I theory are:

$$\| Q \|_{x=0} = 0, \tag{6.1.18}$$

$$\| \rho Q u_0 + P_0 \|_{x=0} = \lim_{\delta \to 0} \int_{-\delta}^{+\delta} \hat{p}\, \beta_x \, dx, \tag{6.1.19}$$

$$\| \rho Q u_0 \psi_x \|_{x=0} = \lim_{\delta \to 0} \int_{-\delta}^{+\delta} [-\hat{p} + \bar{p} - \rho g \varphi] dx, \tag{6.1.20}$$

$$\lim_{\delta \to 0} \int_{-\delta}^{+\delta} [\rho Q u_{0,x} \psi] dx + \| P_1 \|_{x=0} = \lim_{\delta \to 0} \int_{-\delta}^{+\delta} \hat{p} \beta \beta_x \, dx, \tag{6.1.21}$$

$$\lim_{\delta \to 0} \int_{-\delta}^{+\delta} \left[\rho Q \psi (u_0 \psi_x)_x + \frac{1}{12} \rho Q^2 \varphi \left(\frac{\varphi_x}{\varphi} \right)_x \right] dx = \lim_{\delta \to 0} \int_{-\delta}^{+\delta} [P_0 - \rho g \varphi \psi - \hat{p} \beta] dx. \tag{6.1.22}$$

As a result of the discontinuity of the thickness of the fluid, the first and second order derivatives of ϕ_0 may be unbounded at the left side of the weir. According to (6.1.5) and (6.1.6), the integral pressure P_0 is bounded while the bottom pressure $\bar{p}$ may be unbounded as well at the left side of the weir. So we define that

$$\lim_{\delta \to 0} \int_{-\delta}^{+\delta} (\hat{p}\, \beta_x - \bar{p}\, \alpha_x) dx = F_1, \tag{6.1.23}$$

$$\lim_{\delta\to 0}\int_{-\delta}^{+\delta}\left[-\hat{p}+\bar{p}-\rho g\varphi\right]dx = F_3, \tag{6.1.24}$$

$$\lim_{\delta\to 0}\int_{-\delta}^{+\delta}\left[P_0-\rho g\varphi\psi-\hat{p}\beta+\bar{p}\alpha\right]dx = L. \tag{6.1.25}$$

Then the jump conditions (6.1.18)-(6.1.21) becomes

$$\| Q \|_{x=0} = 0, \tag{6.1.26}$$

$$\| \rho Q u_0 + P_0 \|_{x=0} = F_1, \tag{6.1.27}$$

$$\| \rho Q u_0 \psi_x \|_{x=0} = F_3, \tag{6.1.28}$$

$$\lim_{\delta\to 0}\int_{-\delta}^{+\delta}\left[\rho Q\psi(u_0\psi_x)_x+\frac{1}{12}\rho Q^2\varphi\left(\frac{\varphi_x}{\varphi}\right)_x\right]dx = L. \tag{6.1.29}$$

Here F_1, F_3 and L have real physical meanings. That is, F_1 is clearly the horizontal force on the face of the weir in the x direction, F_3 is the vertical force on the bottom of the channel, and L is the moment on the face of the weir and bottom of the channel. Due to the presence of the weir, some part of momentum has been transferred to the forces on the weir. The challenge is that F_1, F_3 and L are part of the solution and not known beforehand. Thus, these jump conditions introduce three new variables and, as such, these jump conditions cannot be used to determine the solution. We need alternative jump conditions that do not involve any unknown variables. Obviously, the jump condition associated with the energy equation meets this requirement. Recall that the general energy jump condition for Green-Naghdi Level-I theory is:

$$\left\| \frac{1}{2}\rho u_0\phi_0\left(u_0^2+u_0^2\psi_x^2+\frac{1}{12}u_0^2\phi_{0x}^2+2g\psi\right)+u_0P_0\right\|_{x=0}=0. \qquad (6.1.30)$$

Unfortunately, due to two unknown free surfaces in region II, (6.1.30) cannot be simplified as we did in Chapter 4. To date, we have obtained all of the jump conditions associated with physical laws. After observing these jump conditions, however, we find that only the geometric jump conditions (6.1.15)-(6.1.17) and physical jump conditions (6.1.26) and (6.1.30) are helpful to seek the solution. Thus, at this point we do not have enough jump conditions to complete the solution. The following sections then are aimed at determining an additional condition needed for obtaining the solution.

6.1.3 Solutions

Now we have obtained the governing equations and jump conditions for the weir flow. First let us consider the region I, where the governing equation about the thickness of the fluid is:

$$\frac{1}{3}Q^2\phi_{0x}^2=\left(\frac{Q^2}{H_1^2}-g\phi_0\right)(\phi_0-H_1)^2. \qquad (6.1.4)$$

Before solving (6.1.4), we non-dimensionalize it. Recall that we have defined the Froude number as

$$Fr=\frac{V_0}{\sqrt{gH_1}}, \qquad (6.1.3)$$

where V_0 denotes the uniform velocity at far upstream.

Introducing the notation

$$\eta=\eta(\tilde{x})=\frac{\phi_0}{H_1},\quad \tilde{x}=\frac{x}{H_1}. \tag{6.1.31}$$

and making use of (6.1.3), (6.1.4) may be written as

$$\frac{1}{3}\mathrm{Fr}^2(\eta')^2=(\mathrm{Fr}^2-\eta)(\eta-1)^2. \tag{6.1.32}$$

The responding boundary conditions become

$$\eta\to 1,\eta'\to 0 \text{ as } \tilde{x}\to-\infty. \tag{6.1.33}$$

After observing (6.1.32), we find that two kinds of solutions exist depending on the value of the Froude number. One of the possibilities is that the Froude number Fr is less than $\sqrt{\eta}$. Under this condition, the term $(\mathrm{Fr}^2-\eta)$ is negative while the other terms in (6.1.32) are all positive or zero. As a result, the only solution of (6.1.32) when Fr < 1 is $\eta=1$ identically.

Clearly, if η is not identically equal to 1, since all of the terms in (6.1.32) are positive, it is required that

$$\mathrm{Fr}^2\geq\eta. \tag{6.1.34}$$

Taking (6.1.33) into consideration, we can find that if we want η to be different from 1, then we must require that

$$Fr \geq 1. \tag{6.1.35}$$

Up to this point, we can conclude that the solution of (6.1.4) depends on the Froude number far upstream. If $Fr < 1$, the only possible solution is $\eta = 1$, or

$$\phi_0 = H_1, \tag{6.1.36}$$

in the upstream region. If $Fr \geq 1$, solutions other than uniform flows are possible.

Now we consider the governing equations for region II. The solutions for the downstream can be easily obtained if we can determine the constants of integration in (6.1.11). Through the jump conditions the solution for region II must match the solution of region I at their junction. As a result, the solution for downstream depends on the Froude number far upstream too. Thus we will treat the two cases $Fr \geq 1$ and $Fr < 1$ separately.

First we consider the case when the Froude number $Fr > 1$, that is, the flow in upstream region is supercritical. Under this condition, solutions other than the uniform flow in region I are possible. The solution can only be determined with the help of jump conditions. Recall that only the geometric jump conditions (6.1.15)-(6.1.17) and physical jump conditions (6.1.26) and (6.1.30) are helpful to seek the solution. Upon inspection of the governing equations in region I and II, we find that there are five unknowns to be determined, that is, $\beta|_{x=0^-}$, and the constants of integration A, B, C and D. However, we have only four jump conditions to apply, that is, (6.1.15)-(6.1.17) and (6.1.30). (Remember that the jump condition (6.1.26) has been used in deriving the governing equations.) Obviously, one more conditions is needed to close the system. Recall that the

fluid is assumed to be incompressible and inviscid and the flow is two-dimensional and steady. Then Bernoulli's equation is valid along any streamline in the entire fluid, that is,

$$\frac{1}{2}(u^2+v^2)+g\,y+\frac{p}{\rho}=\frac{1}{2}V_0^2+g\,H_1. \tag{6.1.37}$$

Here the uniform flow far upstream has been taken into account. (6.1.37) can also be regarded as the dynamic boundary condition on the bottom free surface in region II.

Then we can apply Bernoulli's equation along the bottom line, and at the departure point of the weir we have

$$\frac{1}{2}\frac{Q^2}{\left(\beta|_{x=0}-W\right)^2}+\frac{1}{2}v^2+g\,W=\frac{1}{2}\frac{Q^2}{H_1^2}+g\,H_1. \tag{6.1.38}$$

That is, the solution must satisfy (6.1.38) at the departure point of the weir. Now we have enough conditions to determine the unknowns. Given the Froude number and the thickness of the fluid at far upstream, and the height of the weir, the solution for the whole region is determined.

Now we consider the case when the Froude number Fr < 1, that is, the flow in upstream region is subcritical. As we discussed above, when Fr < 1, the only possible solution in region I is the uniform flow, that is, $\phi_0=H_1$ ($\eta=1$). Then we only need to seek the solution for region II with the help of jump conditions. Due to the limitation of uniform flow in region I, then the thickness at the left side of the weir is known, that is,

$$\beta|_{x=0^-}=H_1. \tag{6.1.39}$$

Thus, we have only four unknowns to be determined, that is, A, B, C and D. As discussed above, we have already obtained four jump conditions (6.1.15)-(6.1.17) and (6.1.30).

However, the dynamic boundary condition, Bernoulli's equation, (6.1.38) should be still valid. So now we have five conditions. This implies that the Froude number and the thickness of the fluid at far upstream, and the height of the weir are not independent. This result is consistent with the experimental results and numerical study of many others. By numerical calculation, results can be obtained for small Froude numbers.

6.1.4 Results and discussions

Now we have sufficient conditions to determine the solutions for both regions. As pointed out in above section, two possibilities of the solutions exist depending on the Froude number. First we consider the case where the Froude number is less than 1.

By way of illustration, Fig. 6.1.2 depicts a flow over a thin weir for the value of the Froude number Fr = 0.1 and the thickness of the fluid at far upstream $H_1 = 1.0$ m. The numerical results show that a unique value of the height of the weir is determined, and the corresponding ratio H/W is equal to 0.79. Therefore, with this method, we can find a unique subcritical flow for a thin weir of height W in a channel of finite depth H_1, which is equal to H + W. However, the ratio H/W is different from the result of Vanden-Broeck & Keller (1987), whose responding result is H/W = 0.42. It is not surprising because the method here requires that the flow upstream of the weir be uniform and the free surface elevation flat. In Vanden-Broeck & Keller's solution the free surface elevation decreases as it approaches the weir. Another reason for the difference is the application of

Bernoulli's equation, which is not compatible with Green-Naghdi theory, as we will discuss later.

Our calculation also shows that solutions can be obtained only for small Froude numbers. Fig. 6.1.2 through Fig. 6.1.5 show the numerical results at the values of the Froude number Fr = 0.1, 0.2, 0.3 and 0.4 respectively. From these figures we find that the corresponding height of the thin weir decreases rapidly with the increase of the Froude number. When the Froude number is equal to 0.4, the weir height W is equal to 0.0098, very close to zero. In other words, the ratio H/W will increase rapidly with the Froude number. Fig. 6.1.6 depicts the ratio H/W varies with the Froude number. Our calculation shows that the H/W will approach infinity for some value of Fr greater than 0.4, and the calculation will break down. Once the weir height W is equal to zero, the weir problem becomes the free waterfall over a flat bottom. Recall that there are no subcritical solutions for free waterfalls, as we obtained in Chapter 4. Fig. 6.1.7 depicts the distribution of the integral pressure P_0 in the downstream for Fr = 0.1 and H_1 = 1.0m. We find that P_0 decreases to zero rapidly. Due to the uniform flow in the upstream, the integral pressure P_0 and the bottom pressure $\overline{p}$ are constant in the upstream region. Therefore, jumps on both P_0 and $\overline{p}$ occur across the location of the thin weir.

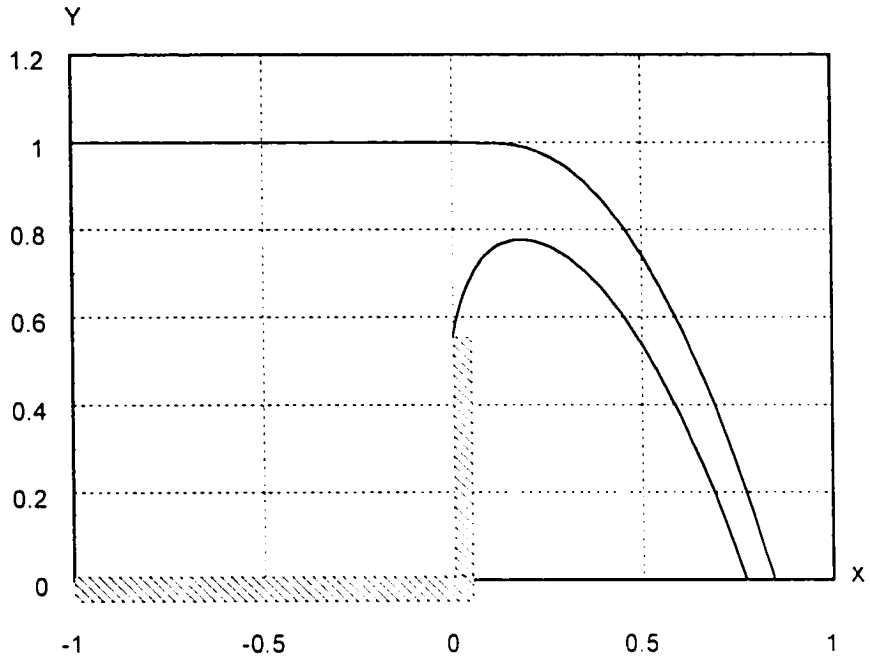

Fig. 6.1.2 Computed free surface profile for the flow over a thin weir, here the Froude number Fr =0.1, and the thickness of fluid far upstream H_1 = 1.0m.

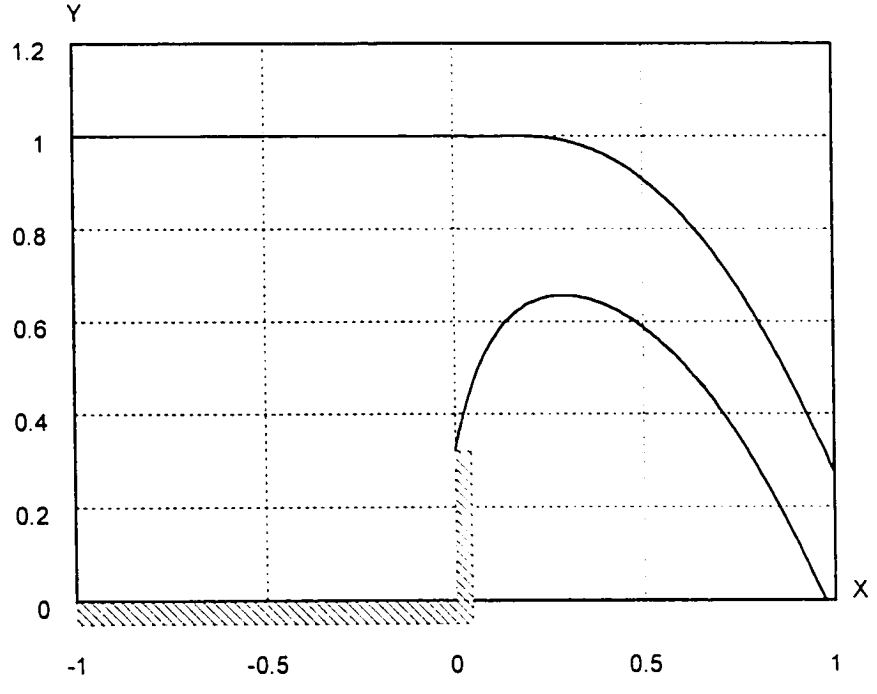

Fig. 6.1.3 Computed free surface profile at Fr = 0.2

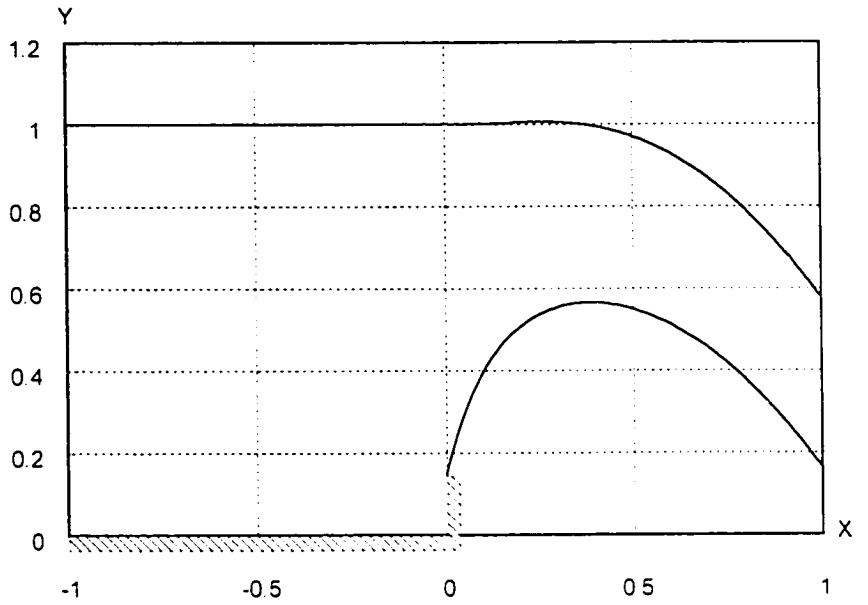

Fig. 6.1.4 Computed free surface profile at Fr = 0.3

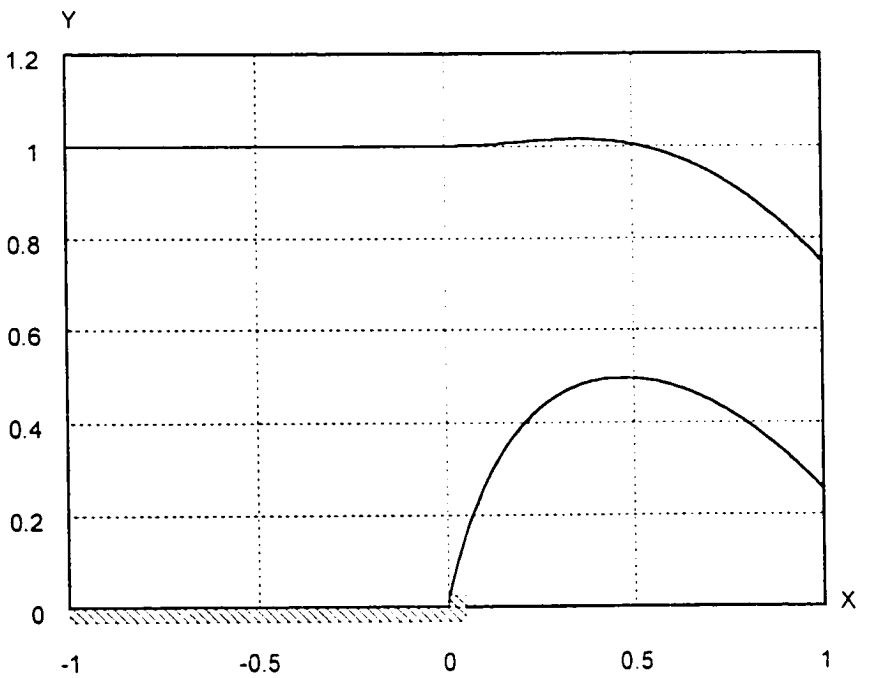

Fig. 6.1.5 Computed free surface profile at Fr = 0.4

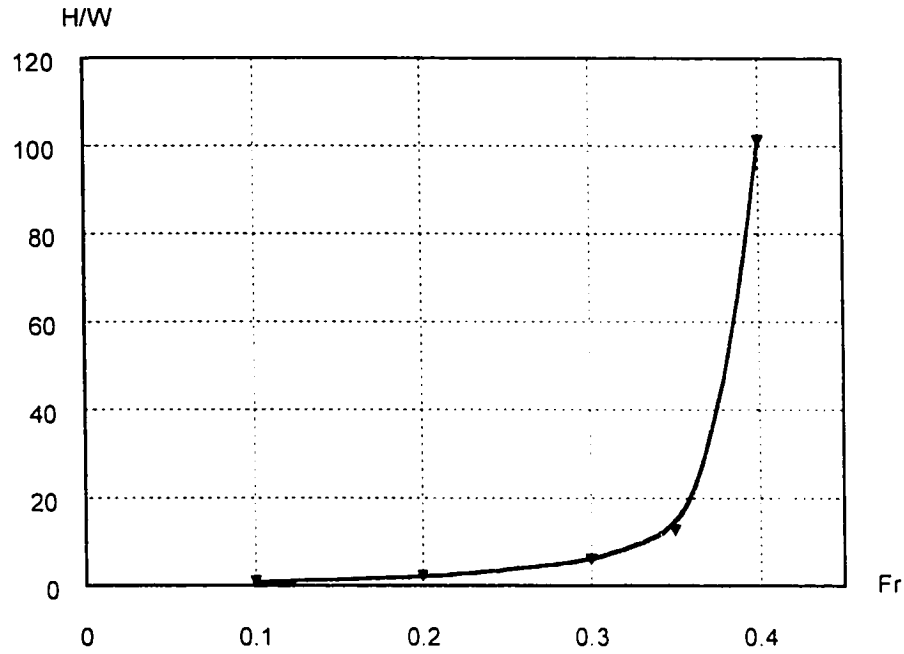

Fig. 6.1.6 Plot of the ratio H/W as a function of the Froude number

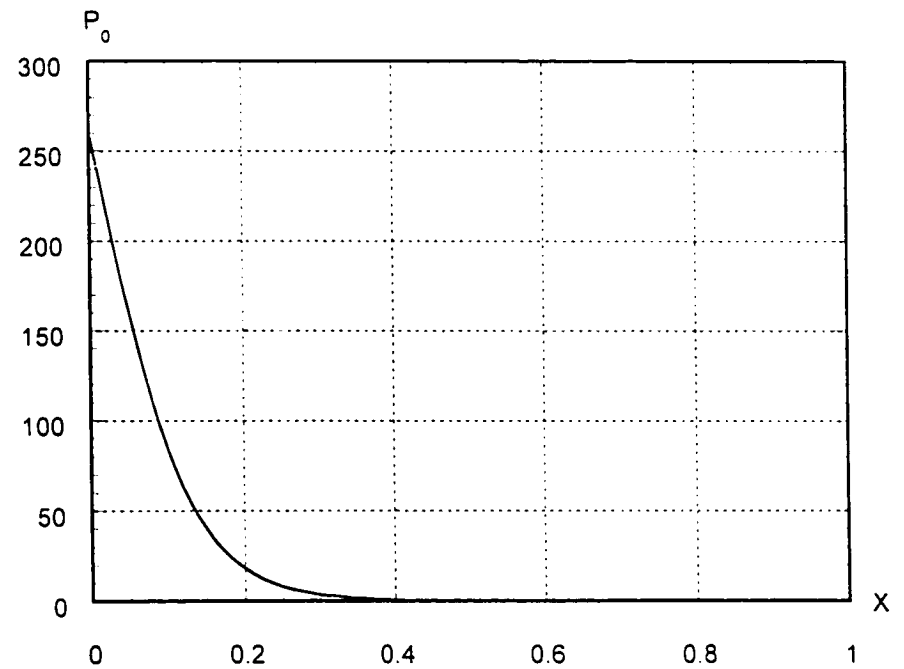

Fig. 6.1.7 The distribution of the integral pressure P_0 in the downstream when Fr = 0.1 and H_1 =1.0 m

Now we turn to the case when Fr > 1. Based on the governing equations and jump conditions obtained in above section, our numerical calculation shows that there are no solutions for supercritical flows. This result is not surprising, although theoretically, there is a family of supercritical flows over a thin weir in a channel of finite depth. When Vanden-Broeck & Keller (1987) studied the weir flow, they did not give out any solutions for the Froude numbers larger than 0.3, as pointed out by Dias & Tuck (1991). Later on, although Dias & Tuck (1991) extended their calculation, they could only obtain supercritical flows up to Fr = 1.6. On the other hand, experimental data are only available for small Froude numbers. Hydraulic jumps will occur at large Froude numbers.

Note that in Fig. 6.1.2 the slope of the bottom free surface at the right side of the weir is not vertical, in contrast to a three-dimensional analysis of this problem that takes into consideration the exact kinematic boundary on the face of the weir. Recall that when we derived the jump conditions at the location of the weir, we could not obtain enough conditions to determine the solution. Only after the application of Bernoulli's equation at the top of the weir, we could determine the slope of the bottom surface and thus obtain a unique solution throughout the whole region. Here we fully realize that it is not appropriate to apply Bernoulli's equation at a particular point in the region. Bernoulli's equation is associated with the Euler integral equation, and is valid along a streamline. On the contrary, although Green-Naghdi governing equations are derived from the Euler equations, they are valid in the sense of the integration of variables along the vertical coordinate. In other words, the Green-Naghdi theory is associated with the integral

properties of physical laws, and the integral properties are refer to the integral values of variables along the vertical coordinate, say y here. Thus, from Green-Naghdi method's point of view, there really is no concept of streamlines as would exist in a full, three-dimensional fluid. The fluid is considered as the "sheet-like" model bounded by two material surfaces, on which exact kinematic boundary conditions are imposed. The dynamic boundary conditions have been taken into consideration in the governing equations.

We also need to point out that there does exist a kinematic condition at the joint point, that is, the slope of the fluid bottom surface at the top edge of the weir should be vertical. This condition implies that the horizontal component of the velocity of fluid at the top of the weir is zero. Recall the assumed profile of velocity in Green-Naghdi Level I theory. From this we can deduce that u_0 is equal to zero at x=0. Thus the flux of the fluid would be zero, which would violate the conservation law of mass. As a result, we cannot make use of this kinematic condition. Due to lack of the jump conditions, we "borrowed" Bernoulli's equation and applied it at the top of the weir to determine the slope of the bottom surface, which was unknown and free. From the classical theory's point of view, Bernoulli's equation is valid in the entire fluid because the two-dimensional flow is steady and is assumed to be uniform far upstream. Thus the shape of the bottom surface at x=0 is actually restricted by this condition, which is the motivation to use Bernoulli's equation.

Recall that our purpose to study weir flows is to make theoretical preparation for the study of breaking waves. Fortunately, the horizontal component of the velocity of the fluid at the dividing location is not zero, as in the weir flow. Moreover, the variables at the joint interface are expected to be continuous. This will simplify the derivation and application of jump conditions. Thus, as far as jump conditions are considered, the weir flow is more complicated than the breaking wave. As a result, the study of weir flows is a challenge to the versatility of Green-Naghdi theory and its associated jump conditions, and thus is worthy of study in its own right.

§6.2 Broad crested weirs

Thin weirs have proved to be too fragile to be considered reliable gauging structures in open channels, especially in irrigation channels. Thus broad-crested weirs have been developed. These are referred to horizontal broad-crested weirs, ones whose cross sections along the flow direction are rectangular. Considering the cases of flood flow over embankments and levees, then the study of broad crested weirs has practical importance. Experiments have shown that the water surface profile over broad-crested weirs is surprisingly complex. In the following we describe the statement of problem for later reference.

Consider a two-dimensional steady flow over a broad-crested weir in a channel with a finite depth. The fluid is assumed to be incompressible and inviscid. The flow far upstream is uniform, and after passing over the broad crested weir, the fluid forms a jet falling down freely forever under the effect of gravity. As shown in Fig. 6.2.1, the broad crested weir divided the flow into three parts: the upstream before the weir, say region I, is bounded by a flat bottom and a free surface; the central stream on top of the weir, say region II, is also characterized by a flat bottom and a free surface; and the downstream after the weir, called region III, is distinct from the other regions by the jet bounded by two free surfaces.

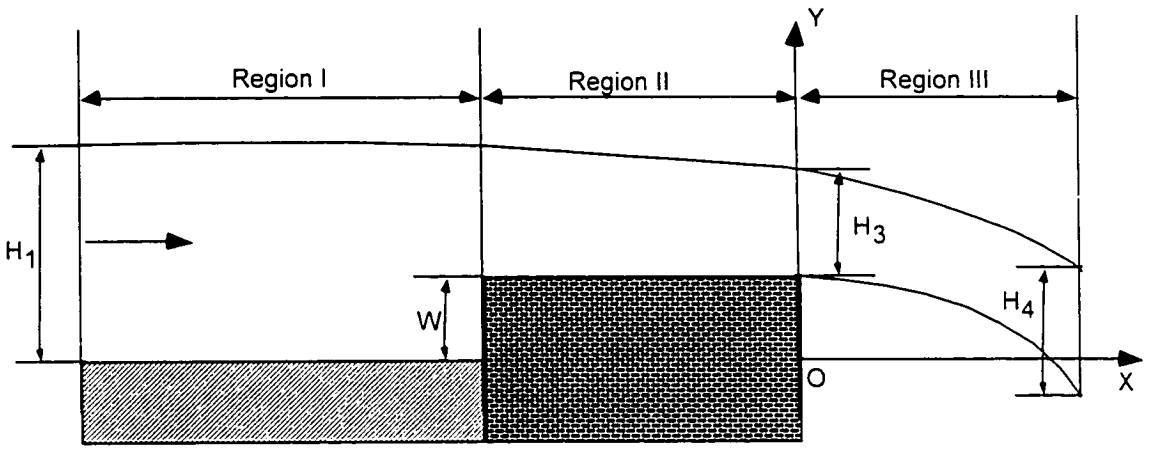

Fig. 6.2.1 Schematic of the flow over a broad crested weir

6.2.1 Formulation of the problem

Before further processing, we choose a system such that the x-axis is along the bottom of the channel and y-axis points upward along the right side of the broad-crested weir, as shown in Fig. 6.2.1. The width of the weir is assumed to be L and the height W. In the chosen system, the channel ends at x = -L. There are three regions associated with this problem, but regions I and II are qualitatively the same. As before, we assume that the flow at far upstream is uniform and far downstream the flow is uniform in the horizontal direction and the horizontal component of the velocity approaches constant. Thus based on previous results, we can list the governing equations in region I and region III.

In Region I the governing equations of Green-Naghdi Level I theory are:

$$\frac{1}{3}Q^2\phi_{0x}{}^2=\left(\frac{Q^2}{H_1{}^2}-g\phi_0\right)(\phi_0-H_1)^2. \tag{6.2.1}$$

$$\frac{P_0}{\rho}=-\frac{Q^2}{\phi_0}+S_1; \tag{6.2.2}$$

$$\frac{\overline{p}}{\rho}=g\phi_0-\frac{Q^2\phi_{0x}{}^2}{2\phi_0^2}+\frac{Q^2\phi_{0xx}}{2\phi_0}. \tag{6.2.3}$$

where,

$$Q=Fr\sqrt{gH_1}\,H_1. \tag{6.2.4}$$

$$S_1=\frac{1}{2}gH_1{}^2+\frac{Q^2}{H_1}. \tag{6.2.5}$$

Here we adopt the same notations as in previous chapters. And in region II the governing equations are

$$\phi_0=H_4+Ae^{-Bx}; \tag{6.2.6}$$

$$\frac{P_0}{\rho}=-\frac{Q^2}{\phi_0}+S_3; \tag{6.2.7}$$

$$\psi=-\frac{gH_4{}^2}{2Q^2}x^2+CH_4x+\frac{gAH_4}{Q^2B}xe^{-Bx}-\frac{gA^2}{2Q^2B^2}e^{-2Bx}-\frac{AC}{B}e^{-Bx}+D. \tag{6.2.8}$$

where

$$A=H_3-H_4. \tag{6.2.9}$$

$$B=\frac{2\sqrt{3}}{H_4}, \tag{6.2.10}$$

$$S_3=\frac{Q^2}{H_4}, \tag{6.2.11}$$

C and D are constants of integration to be determined.

Although region II and I are same in principle, because the flow at the left boundary in region II is not uniform, the governing equations cannot be integrated. Thus the governing equations in region II are:

$$\frac{Q^2}{3}\phi_0\phi_{0xx} - \frac{Q^2}{3}\phi_{0x}^{\ 2} + \frac{1}{2}g\phi_0^{\ 3} - S_2\phi_0 + Q^2 = 0. \tag{6.2.12}$$

$$\frac{P_0}{\rho} = -\frac{Q^2}{\phi_0} + S_2. \tag{6.2.13}$$

$$\frac{\bar{p}}{\rho} = g\phi_0 - \frac{Q^2\phi_{0x}^{\ 2}}{2\phi_0^2} + \frac{Q^2\phi_{0xx}}{2\phi_0}. \tag{6.2.14}$$

Here S_2 is a constant of integration.

6.2.2 Jump conditions

There are two points to apply the jump conditions, that is, x = -L and x = 0. First we consider the jump conditions at x = -L, where the existence of the weir results in the jump of the thickness of the fluid between region I and II. Again we expect that the top surface at x =-L is smooth, although hydraulic jumps are possible due to the existence of the weir. Thus the geometric jump conditions are:

$$\|\beta\|_{x=-L} = 0, \tag{6.2.15}$$

$$\|\beta_x\|_{x=-L} = 0. \tag{6.2.16}$$

$$\| \alpha \|_{x=-L} = W, \qquad \text{or, } \| \phi_0 \|_{x=-L} = -W \tag{6.2.17}$$

Making use of the definition of (6.1.23)-(6.1.25), we can obtain the jump conditions associated with the conservation law of the momentum:

$$\| Q \|_{x=-L} = 0, \tag{6.2.18}$$

$$\| \rho Q u_0 + P_0 \|_{x=-L} = F_1. \tag{6.2.19}$$

$$\| \rho Q u_0 \psi_x \|_{x=-L} = F_3, \tag{6.2.20}$$

$$\lim_{\delta \to 0} \int_{-L-\delta}^{-L+\delta} \left[\rho Q \psi (u_0 \psi_x)_x + \frac{1}{12} \rho Q^2 \varphi \left(\frac{\varphi_x}{\varphi} \right)_x \right] dx = L. \tag{6.2.21}$$

Here we still need the jump condition associated with the energy equation. Recall that the general energy jump condition for Green-Naghdi Level-I theory is:

$$\left\| \frac{1}{2} \rho u_0 \phi_0 \left(u_0^2 + u_0^2 \psi_x^2 + \frac{1}{12} u_0^2 \phi_{0x}^2 + 2g\psi \right) + u_0 P_0 \right\|_{x=-L} = 0. \tag{6.2.22}$$

This expression can be simplified since the bottoms at both sides of x =-L are flat. Then after simplification, (6.2.22) becomes

$$\left\| \frac{1}{2} \rho u_0 \phi_0 \left(u_0^2 + \frac{1}{3} u_0^2 \phi_{0x}^2 + 2g\psi \right) + u_0 P_0 \right\|_{x=-L} = 0. \tag{6.2.22a}$$

Now that we have obtained the jump conditions at x =-L, we consider the jump conditions at x=0, where the fluid departs from the broad crested weir. We expect that the departure is smooth so that both the top and bottom surfaces are smooth at x =0. Thus the geometric jump conditions at x = 0 are the same as the waterfall problem in Section 4.

$$\|\beta\|_{x=0} = 0, \tag{6.2.23}$$

$$\|\beta_x\|_{x=0} = 0, \tag{6.2.24}$$

$$\|\alpha\|_{x=0} = 0, \tag{6.2.25}$$

$$\|\alpha_x\|_{x=0} = 0. \tag{6.2.26}$$

With the help of above jump conditions, we can derive the jump conditions associated with the physical laws. After observing the governing equations in region II and III, and taking the jump conditions (6.2.23)-(6.2.26) into account, we can deduce that the integral pressure and bottom pressure at both sides of x =0 are bounded. Then the limits in the physical jump conditions are equal to zero and we obtain

$$\|Q\|_{x=0} = 0, \tag{6.2.27}$$

$$\|\rho Q u_0 + P_0\|_{x=0} = 0, \tag{6.2.28}$$

$$\|\rho Q u_0 \psi_x\|_{x=0} = 0, \tag{6.2.29}$$

$$\lim_{\delta\to 0}\int_{-\delta}^{+\delta}\left[\rho Q\psi(u_0\psi_x)_x + \frac{1}{12}\rho Q^2\varphi\left(\frac{\varphi_x}{\varphi}\right)_x\right]dx = 0. \tag{6.2.30}$$

We can express the jump conditions at x = 0 succinctly as their equivalent

$$\begin{aligned} &\|u_0\phi_0\|_{x=0} = 0; \quad \|\beta\|_{x=0} = 0; \quad \|\beta_x\|_{x=0} = 0; \\ &\|\alpha\|_{x=0} = 0; \quad \|\alpha_x\|_{x=0} = 0; \quad \|P_0\|_{x=0} = 0. \end{aligned} \tag{6.2.31}$$

Because of the smoothness of the top and bottom surface, the jump condition associated with the energy equation are equivalent to the jump conditions associated with

the conservation law of momentum. Thus in this case there is no need to consider the energy equation.

To date we have obtained sufficient conditions at two joint point x = -L and x = 0 respectively. With the help of these jump conditions, we can solve the governing equations in three regions to obtain a uniform solution throughout the flow.

6.2.3 Solutions

Before processing further, we recall the definition of the Froude number.

$$Fr = \frac{V_0}{\sqrt{g H_1}}. \tag{6.2.32}$$

where V_0 denotes the uniform velocity at far upstream. We also non-dimensionalize (6.2.1) as before

$$\frac{1}{3} Fr^2 (\eta')^2 = (Fr^2 - \eta)(\eta - 1)^2. \tag{6.2.33}$$

where

$$\eta = \eta(\tilde{x}) = \frac{\phi_0}{H_1}, \tilde{x} = \frac{x}{H_1}. \tag{6.2.34}$$

The responding boundary conditions far upstream become

$$\eta \to 1, \eta' \to 0 \text{ as } \tilde{x} \to -\infty. \tag{6.2.35}$$

Clearly, if η is not identically equal to 1, it is required that

$$Fr \geq \eta . \tag{6.2.36}$$

Taking (6.1.35) into consideration, we find that if we want η not to be identically 1, then we must require that

$$Fr \geq 1 . \tag{6.2.37}$$

Up to this point, we can conclude that the solution of (6.2.1) depends on the Froude number far upstream. If Fr < 1, the only possible solution is $\eta = 1$, or

$$\phi_0 = H_1 \tag{6.2.38}$$

in the upstream region. If $Fr \geq 1$, solutions other than uniform flow are possible. Obviously, the final solution depends on the value of the Froude number at far upstream.

First we consider the case when the Froude number Fr > 1, that is, the flow in the upstream region is supercritical. Under this condition, solutions other than the uniform flow in region I are possible. The solution can only be determined with the help of jump conditions, and the governing equations in all of three regions must be considered together. We define that the Froude number in region II as

$$Fr = \frac{u}{\sqrt{g H_2^+}} , \tag{6.2.39}$$

where u denotes the horizontal component of the velocity, and H_2^+ the thickness of the fluid at $x = -L^+$. From the geometric jump conditions at x=-L, we know that

$$H_2^+ = H_2^- - W . \tag{6.2.40}$$

The flow in region I is supercritical, that is, Fr > 1, then with the help of (6.2.40) and the continuity equation, we can deduce that the flow in region II is supercritical as well. Recall that in the free waterfall problem it is required that the flow in upstream region be supercritical. Here region II and III also form a free waterfall problem. Therefore this condition is necessary to obtain a solution.

Then we consider the case when the Froude number Fr < 1. According to (6.2.23), the flow in region I is uniform, which is the only solution of (6.2.23). At the same time, the Froude number defined in (6.2.39) must be larger than 1 in order to obtain a solution. This condition will restrict the range of the Froude number far upstream and the ratio H/W, where H is equal to H_1 - W. Due to the flow in region I is uniform, with help of the jump conditions at x = -L, both the thickness of the fluid and the slope of the free surface at $x = -L^-$ are determined. That is,

$$H_2 = H_2^* = H_1 - W, \tag{6.2.41}$$

$$\beta_x\big|_{x=-L^-} = 0. \tag{6.2.42}$$

Then by means of the jump condition (6.2.22), we can obtain the constant of integration S_2 in (6.2.12) and (6.2.13). Consequently, the governing equation (6.2.12) in region II can be solved, given the boundary conditions (6.2.41) and (6.2.42). Once the solution in region II is obtained, by means of the jump conditions at x = 0, we can easily obtain the solution in region III, as we did in free waterfall problems.

6.2.4 Results and discussion

First we consider the supercritical flow over a broad crested weir. In our knowledge, supercritical solutions with a broad crested weir have not been computed in the past. Here both the Froude number and the height of the fluid far upstream must be specified for a given broad crested weir, that is, the height and length of the weir are given. For the sake of illustration, Fig. 6.2.2 shows a steady, two-dimensional flow over a broad crested weir for the value of the Froude number Fr = 1.5 far upstream and the thickness of fluid H_1 = 1.0m, and the width and height of the weir L = 5.0m and W = 0.1m respectively.

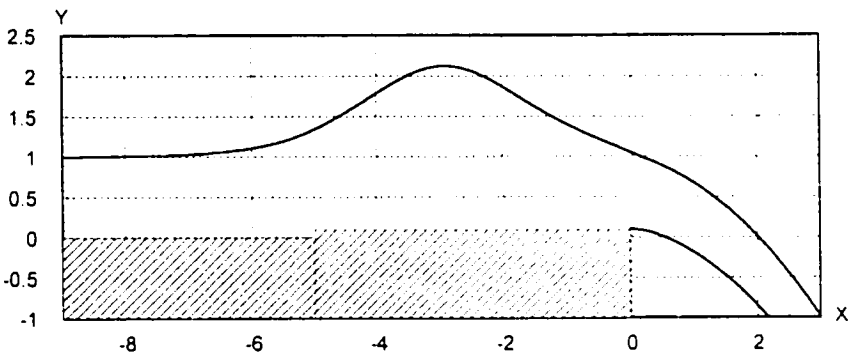

Fig. 6.2.2 Illustration of the supercritical flow over a broad crested weir

From Fig. 6.2.2, we find that the free surface is "lifted up" due to the existence of the weir, and approaches to the top point and then is "pulled down" by the gravity because of the sudden end of the weir. When Dias and Tuck (1991) studied the supercritical flow over a thin weir, they obtained a so-called "solitary-wave-type" solution. When

comparing with their results, we find our results are similar in principle, although the weirs are different. However, we have not obtained the so-called "waterfall-type" solutions as they did in dealing with the thin weir flow.

Fig. 6.2.3 depicts the solutions of the flow over the same broad crested weir for different values of the Froude number, i.e., Fr = 1.5, 2.0 and 2.5, while H_1 = 1.0m, and the width and height of the weir L = 5.0m and W = 0.1m respectively. From Fig. 6.2.3, we find that the elevation of the top free surface increases extremely with the Froude number.

Fig. 6.2.4 shows the effect of the height of the weir on the elevation of the top free surface. Here the conditions upstream keep unchanged, i.e., H_1 = 1.0m and Fr = 2.0, and the length of the weir is L = 5.0m. Three values of the height of the broad crested weir are considered, i.e., W = 0.2, 0.4 and 0.6 respectively. From Fig. 6.2.4, we find that the highest elevation of the free surface above the weir decreases with the weir height W. Fig. 6.2.5 shows the thickness of the fluid at the end of the weir, i.e., H_3, as a function of the weir height, while Fig. 6.2.6 depicts the thickness of the fluid at positive infinity, i.e., H_4, as a function of the weir height. The conditions are Fr = 2.0, H_1 = 1.0m and L = 5.0m. After observing these figures, we find that both H_3 and H_4 increase with the weir height, and H_4 seems to increase linearly with W. In other words, the velocity will decrease with the increase of the weir height, as shown in Fig. 6.2.7.

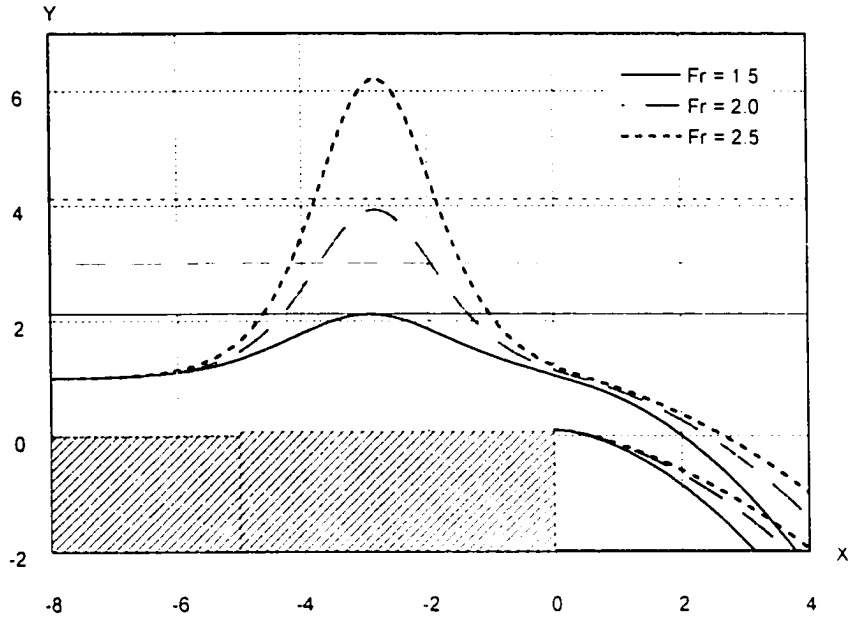

Fig. 6.2.3 Plot of solutions for different Froude numbers for W = 0.1 m

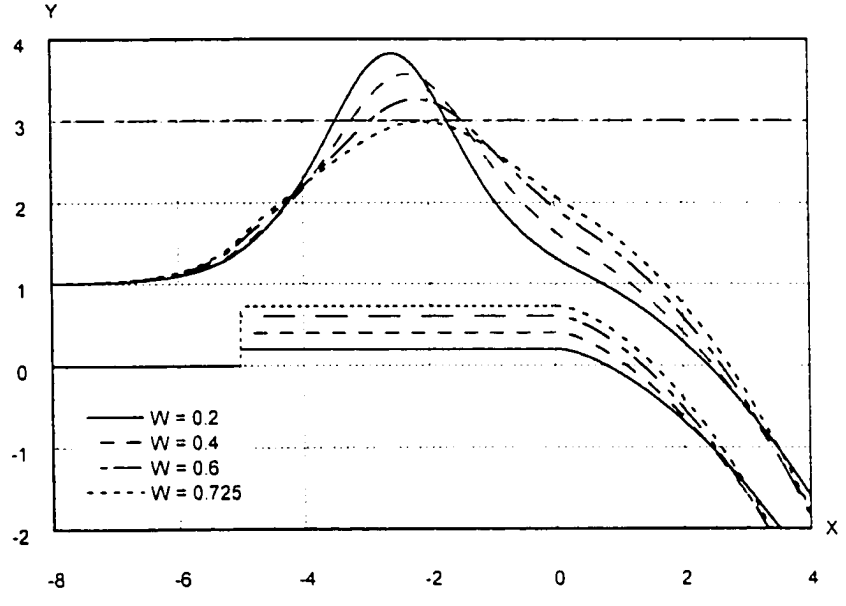

Fig. 6.2.4 Plot of solutions for different heights of the weir at Fr = 2.0

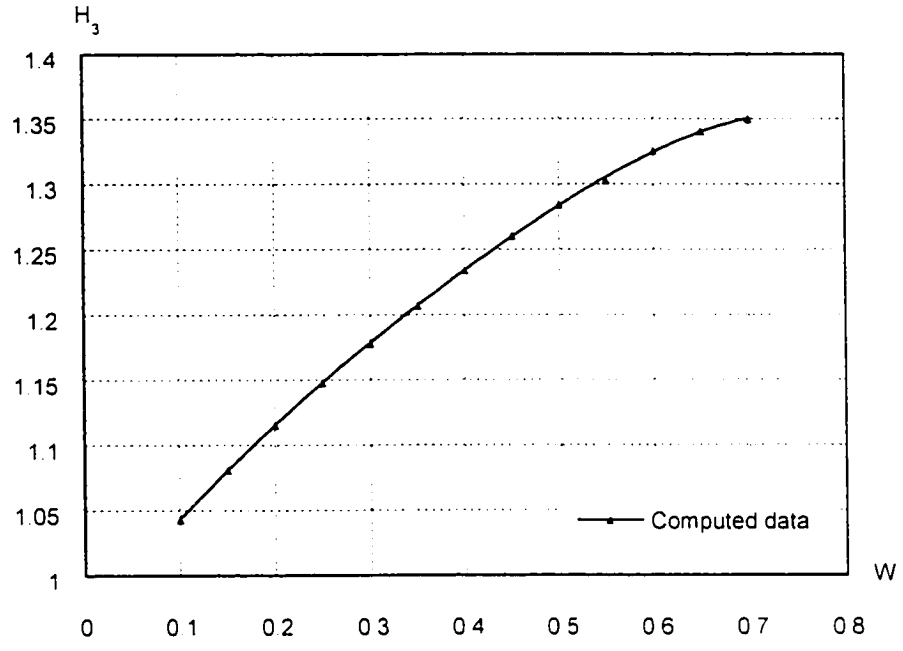

Fig. 6.2.5 Plot of H_3 as a function of the weir height W at Fr = 2.0 and H_1 = 1.0m

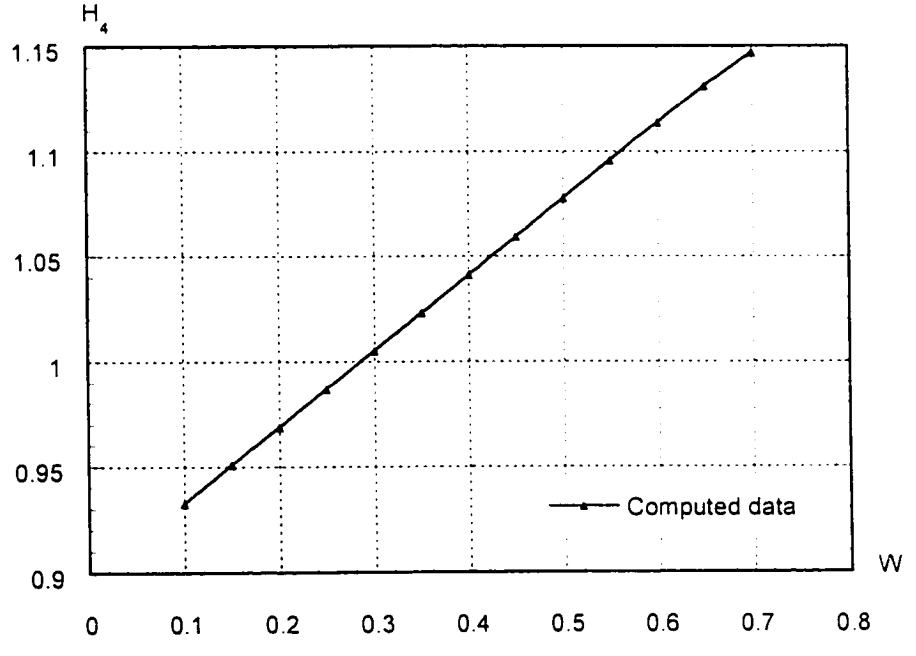

Fig. 6.2.6 Plot of H_4 as a function of the weir height W at Fr = 2.0 and H_1 = 1.0m

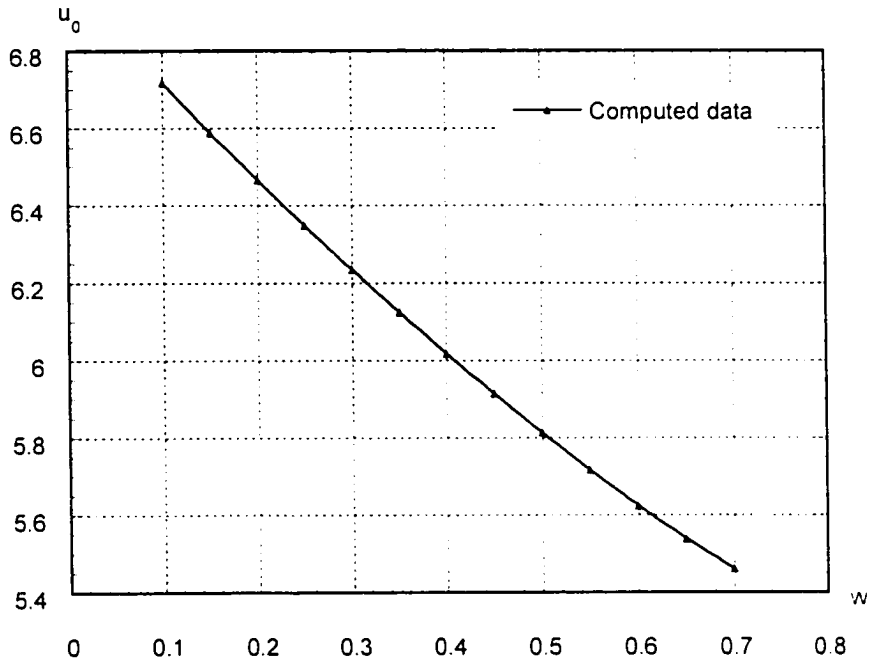

Fig. 6.2.7 Plot of u_0 at infinity as a function of the weir height W

The observation of Fig. 6.2.3 indicates the elevations of the free surface above the broad weir are very high. For instance, when Fr = 2.5, the highest elevation of the top surface is slightly over 6.0m. This value is larger than the corresponding total head of this flow, i.e., h_0 = 4.125m here for Fr = 2.5. The straight lines in Fig. 6.2.3 denotes the total heads for different Froude numbers. From Fig. 6.2.3 we find that when Fr = 1.5, the highest elevation of the free surface is slightly less than the total head, i.e. h_0 = 2.125m for Fr = 1.5 and H_1 = 1.0m. However, when Fr = 2.0 and 2.5, the highest elevations of the free surface are greater than the corresponding total heads, as shown in Fig. 6.2.3. This is physically impossible. On the other hand, we find from Fig. 6.2.4 that the highest elevation of the free surface above the weir decreases with the height of the weir.

Actually, when the height of the weir W reaches 0.725, the highest elevation of the free surface drops slightly below the total head, say $h_0 = 3.0$m. This shows that the method used here is not appropriate, or at least the level the Green-Naghdi theory is too low. That is, the assumption that the horizontal velocity is uniform in the vertical direction is not valid due to the sudden change of the bottom. More complicated profile of the velocity should be imposed.

Then we consider the subcritical flow over a broad crested weir. As discussed in above section, the only solution for subcritical flows in region I is the uniform flow. Then we only need to consider the solutions for region II and III. At x =-L, the joint point between region I and II, taking into account the solution in region I, application of jump conditions (6.2.15) and (6.2.16) yields

$$\beta|_{x=-L^-} = H_1, \text{or } \phi_0|_{x=-L^-} = H_1 - W, \tag{6.2.43}$$

$$\beta_x|_{x=-L^-} = \phi_{0x}|_{x=-L^-} = 0. \tag{6.2.44}$$

With these boundary conditions, together with the condition that the flow in region I is uniform, the broad crested weir problem becomes the free waterfall problem. The only difference is that it is required that the Froude number in region I be less than 1 and the corresponding Froude number in region II should be larger than 1. Since we have studied the waterfall problem in Chapter 4, it is no need discussing this problem again. However, we need to point out that this solution is reasonable for those broad crested weirs satisfying the requirement $L/H >> 1$, although we did not use this requirement during the

process of solving the broad crested weir problem. Actually, when L/H <<1, the weir becomes a thin weir, which we have discussed in the above section.

In summary, with the help of the jump conditions, we have obtained both subcritical and supercritical solutions for the flow over a broad crested weir by means of Green-Naghdi theory. In our knowledge, it is the first time that the supercritical solution for broad-crested weir flow is obtained theoretically, although the existence of the steady supercritical flow is doubtful.

Chapter 7

Summary and Conclusion

Based on the Green-Naghdi theory derived by Shields & Webster (1988), we developed the general form of the jump conditions associated with an arbitrary level of Green-Naghdi theory. These jump conditions are different from what Green & Naghdi obtained, but they are equivalent to each other in principle. In addition, particular form of jump conditions for Green-Naghdi Level-I theory is derived, including the jump condition associated with the energy equation.

A variety of problems are studied in order to demonstrate the validation of the jump conditions associated with the Green-Naghdi theory. In Chapter 4, we studied free waterfall problems, which involve double free surfaces. Two regions with distinct characteristic are associated with this problem, and the jump conditions are applied at the departure point. The bottom surface in upstream can be flat, or arbitrary as long as it is smooth. When the bottom is flat, analytic solution has been obtained and the results are same as what Naghdi & Rubin (1981) obtained and are in good agreement with the experimental data reported by Rouse (1936). At the same time, numerical solutions were obtained for an arbitrary smooth bottom. Furthermore, the free waterfall over a non-smooth bottom was studied with the help of the jump conditions, in particular, the jump condition associated with the energy equation. Our results confirmed that only supercritical solutions exist for free waterfalls over a flat bottom. Furthermore, it is found

for the first time that the local Froude number can be less than 1 for waterfalls over a non-flat smooth bottom or non-smooth bottom.

In Chapter 5, we considered the flow under a sluice gate, where a dramatic jump on the thickness of the fluid occurs. Our results are equivalent to what Caulk (1976) obtained, although our method is based on Eulerian frame while the method Caulk employed is in Lagrangian frame. The analytical solutions are in good agreement with the numerical results of Isaacs (1977). The case of a horizontal sluice gate was also studied. In addition, the flow departing from a confined non-smooth top surface was studied. Our results showed that solutions with waves and without waves are possible in the downstream. In Chapter 6, we studied the flow over a weir, and both a thin weir and a broad crested weir were considered. For the flow over a thin weir, the solutions for small Froude numbers are obtained. For the flow over a broad crested weir, both subcritical solutions and supercritical solutions are obtained. Under the subcritical case, the solution is similar to those of free waterfall problem. Under the supercritical case, the solutions are similar to the so-called "solitary-wave-type" solution by Dias and Tuck (1991), who studied the supercritical flow over a thin weir by means of conformal mapping. In our knowledge, supercritical solutions with a broad crested weir have not been computed in the past.

In conclusion, the Green-Naghdi theory has proved to be a very powerful approximate method for shallow-water problems. With the development of the jump conditions associated with the Green-Naghdi theory, the application of this theory has

been largely expanded. That is, the problems including rapid or discontinuous changes in rigid boundaries can now be solved with the help of the jump conditions. Unlike the classical methods such as conformal mapping, the application of the jump conditions involves clear physical meaning and sticks to the concepts of hydrodynamics.

By solving the free waterfall problems, and the flows under a sluice gate and over a weir, the jump conditions have demonstrated their versatility and power in solving problems involving rapid or discontinuous changes. Furthermore, these studies have built a solid theoretical foundation for more complicated problems, such as the breaking wave. Due to the limitation of the Green-Naghdi Level-I theory, application of higher levels of Green-Naghdi method to these problems appears an appropriate next step.

References:

Ahrens, John P 1970 "The influence of breaker type on riprap stability" Coastal Engineering Conference Proceedings, Vol. III, pp. 1557-1566.

Airy, G. B., 1845, "Tides and waves," Section 392. In Encyc. Metropolitana, 5:241-396.

Baba, E., "Study of separation of ship resistance components," Mitsubishi Technical Bulletin, No. 59, 1969, pp. 1-16.

Banner, M.L., Phillips, O.M. 1974, "On the incipient breaking of small scale waves", Journal of Fluid Mechanics, Vol. 65, pp647-656.

Benjamin, T. B. 1956 "On the flow in channels when rigid obstacles are placed in the stream", Journal of Fluid Mechanics, v1, pp. 227-248.

Biesel, F. 1952 "Study of wave propagation in water of gradually varying depth", Natl. Bur. Of Stand. Circ. 521, pp. 243.

Birkhoff, G., Zarantonello, E. H., 1957 *Jets, Wakes and Cavities*, Academic Press, New York.

Bonmarin, P., 1989 "Geometric properties of deep-water breaking waves", Journal of Fluid Mechanics, Vol. 209, pp405-433.

Boussinesq, J.V., 1907 "Theorie approchee de l'dcoulement de l'eau sur un deversoir en mince paroi et sans contractions laterales", Memoires de l'Academie des Sciences, 50, pp.1-118 and 121-134.

Caulk, D. A. 1976 "On the problem of fluid flow under a sluice gate", Int. J. Engng. Sci., Vol. 14, pp. 1115-1125.

Challis, J. 1848 "On the velocity of sound", Philosophical Magazine, 32, pp. 494-499.

Chow, W. L., Han, T. 1979 "Inviscid solution for the problem of free overfall", J. Appl. Mech. 46, pp. 1-5.

Clarke, N. S. 1965 "On two-dimensional inviscid flow in a waterfall", Journal of Fluid Mechanics, Vol. 22, pp. 359-369.

Cokelet, E. D. 1978 "Breaking waves – the plunging jet and interior flow field", In *Mechanics of Wave-Induced Forces on Cylinders*, ed. T. L. Shaw, pp. 287-301. London: Pitman. xiv + 752 pp.

Chesnutt, C. B., 1971 "Scour of simulated gulf coast and beaches due to wave action in front of sea walls and dune barriers" MS Thesis in Civil Engineering, Texas A & M University.

Dagan, G., and Tulin, M. 1970 "Non-linear free surface effects in the vicinity of blunt ship bows," Proceeding of Eighth Symposium Naval Hydrodynamics, Pasadena, National Academy Press, Washington, DC, pp. 607-626.

Dagan, G., and Tulin, M. 1972 "Two-dimensional free-surface gravity flow past blunt bodies," Journal of Fluid Mechanics, Vol. 51, pp. 529-543.

Demirbilek, Z., Webster, W.C. 1992 "Application of the Green-Naghdi theory of fluid sheets to shallow-water wave problems", U.S. Army Corps of Engineers, Vicksburg, Mississippi, Technical Report CERC-92-11, pp. 45.

Dias, F., Keller, J. B., and Vanden-Broeck, J. M., 1988 "Flows over rectangular weirs." Phys. Fluids. v31(8), pp. 2071-2076.

Dias, F. and Tuck, E. O., 1991 "Weir flows and waterfalls." J. Fluid Mech., v230, pp. 525-539.

Duncan, J. H. 1981 "An experimental investigation of breaking waves produced by a towed hydrofoil", Proc. R. Soc. Lond. A 377, pp. 331-348.

Duncan, J. H. 1983 "The breaking and non-breaking wave resistance of a two-dimensional hydrofoil", Journal of Fluid Mechanics, Vol. 126, pp. 507-520.

Duncan, J. H., 1999, "Gentle spilling breakers: crest profile evolution.", Journal of Fluid Mechanics, Vol. 379, pp191-222.

Earnshaw, S. 1860 "On the mathematical theory of sound", Transactions of the Royal Society of London 150, pp. 133-148.

Flick, R.E., Guza, R.T., Inman, R.L., 1981 "Elevation and velocity measurements of laboratory shoaling waves", Journal of Geophysical Research, Vol. 86, pp. 4149-60.

Galvin, C. J., "Breaker type classification on three laboratory beaches," Journal of Geophysics. Res. 73: 3651-59, 1968.

Galvin, C. J., "Wave breaking in shallow water." Waves on Beaches and resulting Sediment Transport, ed. R. E. Meyer. 1972, pp. 413-56. New York: Academic.

Green, A. E., Laws, N. & Naghdi, P. M. 1974 "On the theory of water waves", Proc. Roy. Soc. A338, pp. 43.

Green, A. E., Naghdi, P. M. 1976 "A derivation of equations for wave propogation in water of variable depth", Journal of Fluid Mechanics, V78.2, pp. 237-246.

Green, A. E., Naghdi, P. M. 1976 "Directed fluid sheets", Proc. R. Soc. Lond. A. 347, pp. 447-473.

Green, A. E., Naghdi, P. M. 1986 "A non-linear theory of water waves for finite and infinite depths", Phil. Tran. R. Soc. Lond. A. 320, pp. 37-70.

Green, A. E., Naghdi, P. M. 1987 "Further developments in a nonlinear theory of water waves for finite and infinite depths", Phil. Tran. R. Soc. A. 324, pp. 47-72.

Grosenbaugh, M. A. and Yeung, R. W. 1989 "Nonlinear free-surface flows at a two-dimensional bow", Journal of Fluid Mechanics, vol. 209, pp. 57-75.

Hedges, T.S., Kirkgoz, M.S. 1981 "An experimental study of the transformation zone of plunging breakers", Coastal Egn. 4:319-33.

Hudson, R. Y. 1959 "Laboratory investigations of Rubble-Mound breakwaters" Proceedings, Journal of the Waterways and Harbors Division, ASCE, 85, No. WW3, Proceeding Paper 2171, pp. 93-119.

Hugoniot, H. 1889 "Sur la propagation du mouvement dans les corps et specialement dans les gaz parfaits", Journal de l'ecole polytechnique 58, pp. 1-125.

Inui, T. 1981 "From bulbous bow to free-surface shock waves – trends of 20 years' research on ship waves at the Tokyo University Tank," Journal of Ship Research, Vol. 25, pp. 147-180.

Isaacs, L. T. 1977 "Numerical solution for flow under sluice gates", Journal of the Hydraulics Division, ASCE, HY5, pp. 473-485.

Iversen, H. W., 1953. "Waves and breakers in shoaling water," Proc. 3rd Conf. On Coastal Eng., Council on wave research Berkeley, Chap. 1, pp. 1-12.

Kadib, Abdel-Latif. 1963 "Beach profile as affected by vertical walls" Tech. Mem. No. 134, U.S. Army Beach Erosion Board, Washington, D. C.

Keller, J. B., Geer, J. 1973 " ", Journal of Fluid Mechanics, vol. 59, pp. 417.

Keller, J. B., Weitz, M. L. 1957 " ", Proc. 9th Int. Congr. Appl. Mech. Brussels, Belgium, vol. 1, pp316.

Keulegan, Garbis H. 1948 "An experimental study of submarine sand bars" Beach Erosion Board, Tech. Rep. No. 3.

Kjeldsen, S.P. Myrhaug, D. 1980 "Wave-wave interactions, current-wave interactions and resulting extreme waves and breaking waves", Proc. Conf. Coastal Eng., 17th, pp. 2277-303.

Klassen, V. J. 1967, J. Math. Ann. Appl. V19, pp. 253.

Longuet-Higgins, M. S. 1978a "The instabilities of gravity waves of finite amplitude in deep water, I. Super-harmonics", Proc. R. Soc. London Ser. A 360:471-88.

Longuet-Higgins, M. S. 1978b "The instabilities of gravity waves of finite amplitude in deep water, II. Sub-harmonics", Proc. R. Soc. London Ser. A 360:479-505.

Longuet-Higgins, M. S. 1980a "The unsolved problem of breaking waves", Proceedings of the 17th Coastal Engineering Conference, v1:1-28.

Longuet-Higgins, M. S. 1980b "On the forming of sharp corners at a free surface", Proc. R. Soc. London Ser. A 371:453-78.

Longuet-Higgins, M. S. 1981 "On the overturning of gravity waves", Proc. R. Soc. London Ser. A 376:377-400.

Longuet-Higgins, M. S., & Cleaver, R. P. 1994 "Crest instabilities of gravity waves. Part 1. The almost-highest wave", Journal of Fluid Mechanics, 258, pp115-129.

Longuet-Higgins, M. S., Cleaver, R. P., & Fox, M. J. 1994 "Crest instabilities of gravity waves. Part 2. Matching and asymptotic analysis", Journal of Fluid Mechanics, 259, pp333-344.

Longuet-Higgins, M. S., Cokelet, E. D. 1976 "The deformation f steep surface waves on water. I. A numerical method of computation", Proc. R. Soc. London Ser. A 350:1-26.

Longuet-Higgins, M. S., Cokelet, E. D. 1978 "The deformation f steep surface waves on water. II. Growth of normal-mode instabilities", Proc. R. Soc. London Ser. A 364:1-28.

Longuet-Higgins, M. S. & Dommermuth, D. G. 1997 "Crest instabilities of gravity waves. Part 3. Nonlinear development and breaking", Journal of Fluid Mechanics, 336, pp33-50.

Markland, E. 1965 "Calculation of flow at a free overfall by relaxation methods", Proceedings. Institution of Civil Engineers 31, pp. 71-78.

Marchi, E. 1953 Annali Mat. Pura ed Appl. 35, pp. 327.

Mason, M. A., 1952. "Some observations of breaking waves," Gravity Waves, U.S. Nat. Bur. Standards, Circular No. 521, pp. 215-220.

McIver, P., Peregrine, D. H. 1981 "Comparison of numerical and analytical results for waves that are starting to break", Int. Symp. Hydrodyn. Ocean Eng., Trodheim, Norway, pp. 203-15.

Melville, 1996, "The role of surface-wave breaking in air-sea interaction", Annual Review of Fluid Mechanics, vol. 28, pp. 279-321.

Milne-Thompson, L. M. 1968 "*Theoretical Hydrodynamics*", Mc Millan, London.

Montes, S. 1998 *Hydraulics of Open Channel Flow*, ASCE Press, Reston.

Naghdi, P. M., Rubin, M. B., 1981 "On the transition to planning of a boat", Journal of Fluid Mechanics, Vol. 103, pp. 345-374.

Naghdi, P. M., Rubin, M. B., 1981 "On inviscid flow in a waterfall", Journal of Fluid Mechanics, Vol. 103, pp. 375-387.

New, A. L., McIver, P. and Peregrine, D. H. 1985 "Computations of overturning waves", Journal of Fluid Mechanics, Vol. 150, pp. 233-251.

Pajer, g. 1937 "Uber der stromungsvergang an einer unterstromten scharfskantigen planschutze", Zeitschrift fur Angewandte Mathematik und Mechanik, 17, pp. 259-269.

Peregrine, D.H. 1983 "Breaking waves on beaches", Annual Reviews of Fluid Mechanics, v15, pp. 149-78.

Peregrine, D. H., Cokelet, E. D., McIver, P. 1980 "The fluid mechanics of waves approaching breaking", Proc. Conf. Coastal Eng., 17th, pp. 512-28.

Peregrine, D.H., Svendsen, I.A. 1978, "Spilling breakers, bores and hydraulic jumps", Proc. Conf. Coastal Eng., 16th, pp.540-550.

Poison, S. D. 1808 "Menoire sur la theorie du son", Journal de l'dcole polytechnique, 14th, Cahier, 7, pp. 319-392.

Price, R. K. 1971 "The breaking of water waves", Journal of Geophysical Research, v76, pp. 1576.

Rankine, W. J. M. 1870 "On the thermodynamic theory of waves of finite longitudinal disturbance", Transactions of the Royal Society of London 160, pp. 277-288.

Rayleigh, J. 1910 "Aerial plane waves of finite amplitude", Proceedings of the Royal Society 84, pp. 247-284.

Riemann, B. 1860 "Uber die Fortpflanzung ebener Luftwellen von endlicher Schwingungsweite", Abhandlungen der Gesellschaft der Wissenschafoten zu Gottingen, Mathematisch- physikalische Klasse 8, pp. 43, or Gesammelte Werke, 1876, pp. 144.

Rubin, M. B., 1997 "Relationship of critical flow in waterfall to minimum energy head." Journal of Hydraulic Engineering, v123, pp.82-84.

Saville, T. Jr. 1957 "Scale effects in two dimensional beach studies" Proc. Conf. IAHR, Lisbon, paper A-3.

Shields, J. J., Webster, W. C. 1988 "On direct methods in water-wave theory", Journal of Fluid Mechanics, Vol. 197, pp. 171-199.

Shields, J. J., Webster, W. C. 1989 "Conservation of mechanical energy and circulation in the theory of inviscid fluid sheets", J. Engng. Math. Vol. 23, pp. 1-15.

Smith, A. C. and Abd-El-Malek, M. B., 1983 "Hilbert's method for numerical solution of flow from a uniform channel over a shelf." J. Engrg. Math., 17(1), pp. 27-39.

Smith, N., 1971 "A history of dams", Peter Davies, London.

Southwell, R. V., Vaisey, G. 1946 Phil. Trans. Roy. Soc. A 240, 117.

Stoker, J. J., 1957. "Water waves." New York: Interscience. pp. 567.

Stokes, E. E. 1848 "On a difficulty in the theory of sound", Philosophical Magazine, 33, pp349-356.

Stokes, G.G. 1880 "Considerations relative to the greatest height of oscillatory irrotatoinal waves which can be propagated without change of form. Math. Phys. Pap.1:225-28.

Tanaka, M. 1983 "The stability of steep gravity waves" Journal of Physical Society, Japan. 52, pp.3047-3055.

Tanaka, M. 1986 "The stability of solitary waves" Physics of Fluids, 29, pp.650-655.

Tanaka, M. 1995 "On the 'crest instabilities' of steep gravity waves", Proceeding of Workshop on Mathematical Problems in the Theory of Nonlinear Water Waves, CIRC, Luminy, France, pp.15-19.

Tulin, M. P. 1979 "Ship wave resistance – a survey." Proceedings, U.S. National Congress on Applied Mechanics, UCLA.

Van Dorn, W.G. 1978 "Breaking invariants in shoaling waves", Journal of Geophysical Research, Vol. 83, pp.2981-88.

Vanden-Broeck, J. M. 1977 "Computation of near-bow or stern flows, using series expansion in the Froude number", Proceedings of 2nd International Conference on Numerical Ship Hydrodynamics, Berkeley, pp. 371-381.

Vanden-Broeck, J. M. 1980 "Nonlinear stern waves", Journal of Fluid Mechanics, vol. 96, pp. 603-611.

Vanden-Broeck, J. M. and Keller, J. B., 1987 "Weir flows." Journal of Fluid Mechanics, vol. 176, pp.283-293.

Webster, W. C., Wehausen, J. V. 1995 "Bragg scattering of water waves by Green-Naghdi theory", ZAMP, 1995.

Yeung, R. W. 1982 "Numerical methods in free-surface flows", Annual Review of Fluid Mechanics, vol. 14, pp. 395-442.

Yeung, R. W. 1991 "Nonlinear Bow and Stern Waves – Inviscid and Viscous Solutions", Chapter 26, in Mathematical Aproaches in Hydrodynamics, SIAM Publisher, Philadelphia, PA.

Yeung, R. W. and P. Ananthakrishnan 1997 "Viscosity and surface-tension effects on wave generation by translating bodies", Journal of Engineering Mathematics, vol. 32, pp. 257-280.

Appendix A

Derivation of the Jump Condition Associated with the Energy Equation

First let us consider the general form of the conservation law of energy for inviscid fluid. It can be written in the following form:

$$\frac{D}{Dt}\iiint_{\Omega}\frac{1}{2}\rho\vec{v}^{2}d\sigma=-\oiint_{\partial\Omega}(p\vec{n})\cdot\vec{v}ds+\iiint_{\Omega}\vec{f}\cdot\vec{v}d\sigma \qquad (A.1)$$

We apply it into the very narrow region near the joint point x=-a, as shown in the following figure.

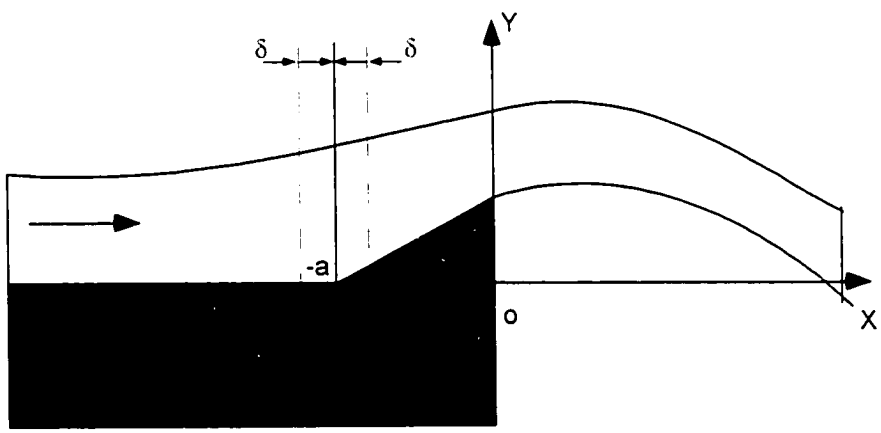

Fig. A.1 Schematic for derivation of jump condition associated with the energy equation at x = -a.

For steady problems, the energy equation (A.1) becomes:

$$\frac{D}{Dt}\iiint_{\Omega}\frac{1}{2}\rho\vec{v}^{2}d\sigma=\iiint_{\Omega}\frac{\partial}{\partial t}(\frac{1}{2}\rho\vec{v}^{2})d\sigma+\oiint_{\partial\Omega}(\vec{v}\cdot\vec{n})(\frac{1}{2}\rho\vec{v}^{2})ds=\oiint_{\partial\Omega}(\vec{v}\cdot\vec{n})(\frac{1}{2}\rho\vec{v}^{2})ds$$
$$=-\oiint_{\partial\Omega}(p\vec{n})\cdot\vec{v}ds+\iiint_{\Omega}\vec{f}\cdot\vec{v}d\sigma \qquad (A.2)$$

Considering our present two-dimensional problems and the assumed profile of fluid velocity in Green-Naghdi Level I theory, applying the above expression to the small region $-a-\delta \le x \le -a+\delta$ as shown in Fig. 4.6, we can obtain the left hand side of (A.2) as follows:

$$\begin{aligned} \oiint_{\partial\Omega} (\bar{v}\cdot\bar{n})\left(\frac{1}{2}\rho\bar{v}^2\right) ds &= \int_{\alpha}^{\beta} u_0 \cdot (-1)\left(\frac{1}{2}\rho\bar{v}^2\right) dy + \int_{\alpha}^{\beta} u_0 \left(\frac{1}{2}\rho\bar{v}^2\right) dy \\ &= \left\| \int_{\alpha}^{\beta} u_0 \left(\frac{1}{2}\rho\bar{v}^2\right) dy \right\|_{x=-a} \end{aligned} \qquad (A.3)$$

where we have taken the limit as $\delta \to 0$.

Keeping the assumed velocity profile in mind, we can integrate the above expression. Then the left hand side of (A.2) becomes:

$$\begin{aligned} \left\| \int_{\alpha}^{\beta} u_0 \left(\frac{1}{2}\rho\bar{v}^2\right) dy \right\|_{x=-a} &= \left\| \int_{\alpha}^{\beta} \frac{1}{2}\rho u_0 \left[u_0^2 + (v_0 + v_1 y)^2\right] dy \right\|_{x=-a} \\ &= \left\| \frac{1}{2}\rho u_0 \phi_0 \left(u_0^2 + v_0^2 + 2 v_0 v_1 \phi_0 \psi + v_1^2 \phi_0 \psi^2 + \frac{1}{12} v_1^2 \phi_0^2 \right) \right\|_{x=-a} \end{aligned} \qquad (A.4)$$

In the same way, the first term of the right hand side of the energy equation becomes

$$\begin{aligned} -\oiint_{\partial\Omega} (p\,\bar{n})\cdot\bar{v} ds &= -\int_{\alpha}^{\beta} p(-1) u_0 \, dy - \int_{\alpha}^{\beta} p \, u_0 \, dy \\ &= -\| u_0 P_0 \|_{x=-a} \end{aligned} \qquad (A.5)$$

and the second term is

$$\iiint_{\Omega} \bar{f} \cdot \bar{v} d\sigma = -\int_{x^-}^{x^+} dx \int_{\alpha}^{\beta} \rho g (v_0 + v_1 y) dy$$
$$= -\int_{x^-}^{x^+} \rho g v_0 \phi_0 dx - \int_{x^-}^{x^+} \rho g v_1 \phi_0 \psi dx \qquad (A.6)$$

Both (A.4) and (A.5) are simple functions, but (A.6) is difficult to apply since it still involves integral items, which prevent direct application. We have to integrate these items for application of this jump condition. Before proceeding further, we collect the results obtained so far

$$\left\| \frac{1}{2} \rho u_0 \phi_0 \left(u_0^2 + v_0^2 + 2 v_0 v_1 \psi + v_1^2 \psi^2 + \frac{1}{12} v_1^2 \phi_0^2 \right) + u_0 P_0 \right\|_{x=-a}$$
$$+ \int_{x^-}^{x^+} \rho g v_0 \phi_0 dx \Big|_{x=-a} + \int_{x^-}^{x^+} \rho g v_1 \phi_0 \psi dx \Big|_{x=-a} = 0 \qquad (A.7)$$

Now we try to eliminate these troublesome integral terms in equation (A.7). Recall that in Green-Naghdi Level I theory, for steady, two-dimensional problems, the kinematic boundary conditions on the top and bottom surfaces are

$$v_0 + v_1 \alpha = u_0 \alpha_x ;$$
$$v_0 + v_1 \beta = u_0 \beta_x . \qquad (A.8a, b)$$

where both surfaces are supposed to be material surfaces.

Adding two equations together, and replacing α and β with ϕ_0 and ψ, then we can obtain:

$$v_0 = -v_1 \psi + u_0 \psi_x . \qquad (A.9)$$

Substituting (A.9) into these integral items in (A.7), we have

$$\int \rho g v_0 \phi_0 \, dx \Big|_{x=-a} + \int \rho g v_1 \phi_0 \psi \, dx \Big|_{x=-a} = \rho g \int \phi_0 (-v_1 \psi + u_0 \psi_x + v_1 \psi) dx$$

$$= \rho g \int \phi_0 u_0 \psi_x \, dx \qquad (A.10)$$

Recall that the conservation law of mass requires that

$$\phi_0 u_0 \equiv Q. \qquad (A.11)$$

And thus with the help of (A.11), we can integrate these integral items as:

$$\int \rho g v_0 \phi_0 \, dx \Big|_{x=-a} + \int \rho g v_1 \phi_0 \psi \, dx \Big|_{x=-a} = \rho g \int Q \psi_x \, dx$$

$$= \| \rho g Q \psi \|_{x=-a} \qquad (A.12)$$

Inserting (A.12) into (A.7), we finally obtain an elegant formula for the jump condition associated with the energy equation:

$$\left\| \frac{1}{2} \rho u_0 \phi_0 \left(u_0^2 + v_0^2 + 2 v_0 v_1 \psi + v_1^2 \psi^2 + \frac{1}{12} v_1^2 \phi_0^2 + 2 g \psi \right) + u_0 P_0 \right\|_{x=-a} = 0 . \qquad (A.13)$$

When we apply the Green-Naghdi Level I theory, we usually get rid of the variables v_0 and v_1 from the governing equations. Then we would rather obtain the jump

condition which does not involve v_0 and v_1. Recall that in Chapter 2 from the continuity equation we have obtained

$$v_1 = -u_{0x}. \tag{A.14}$$

Substituting (A.14) and (A.9) into (A.13), we can obtain an alternate statement of (A.13)

$$\left\| \frac{1}{2}\rho u_0 \phi_0 \left(u_0^2 + u_0^2 \psi_x^2 + \frac{1}{12} u_0^2 \phi_{0x}^2 + 2g\psi \right) + u_0 P_0 \right\|_{x=-d} = 0. \tag{A.15a}$$

or

$$\left\| \frac{1}{2}\rho Q \left(u_0^2 + u_0^2 \psi_x^2 + \frac{1}{12} u_0^2 \phi_{0x}^2 + 2g\psi \right) + u_0 P_0 \right\|_{x=-d} = 0. \tag{A.15b}$$

Thus, we have obtained the jump condition from the conservation law of energy for Green-Naghdi Level I theory. We need to point out that (A.15) is the general form of the jump condition for Green-Naghdi Level I theory since no approximation is introduced and no simplification is made during the derivation. Moreover, (A.15) is valid no matter whether there exist discontinuities or not, as long as there is no loss of energy. This demand is always met since we assume the fluid is incompressible and inviscid. We note that when Green & Naghdi applied the directed sheet method to many problems the jump condition associated with the energy equation was necessary for some of those problems. However, this general form of the jump condition was not obtained. Rather, they only presented particular forms of this jump condition for problems with a flat bottom. In contrast, (A.15) can be applied to problems with any kind of top and bottom surface, no

matter whether they are smooth or not, continuous or not. As we will discuss later, when the flat bottom is taken into account, the jump condition (A.15) can be reduced to the form Naghdi & Rubin obtained.